HORMONAL REGULATION, HISTONE REGULATION, AND TRANSCRIPTIONAL PROFILING OF STEM CELLS IN THE DROSOPHILA TESTIS

by

Yijie Li

A dissertation submitted to Johns Hopkins University in conformity with the requirements for the degree of Doctor of Philosophy

Baltimore, Maryland

December 2015

ABSTRACT

Stem cells are regulated by local signals, systemic signals and cell-intrinsic epigenetic modulation. Adult stem cells reside in specific microenvironments, called niches, and are found in many different tissues and organs. The *Drosophila* testis and ovary contain well-characterized adult stem cell niches. The functional conservation between *Drosophila* gonadal stem cell niches and mammalian stem cell niches makes the former systems ideal for genetic studies of stem cell maintenance and function. Male germline stem cells (GSCs) reside in a niche generated by somatic hub cells and adjacent cyst stem cells (CySCs). Both types of stem cells can divide asymmetrically to produce differentiated progeny that are displaced from the stem cell niche. Daughters of male GSCs will finally differentiate to produce sperm. In the ovary, quiescent somatic cap cells are the niche cells and provide signals to the surrounding 2-3 GSCs to prevent them from differentiating. Differentiation of germ cells is supported by follicle stem cells (FSCs) and their progeny.

To investigate new mechanisms for how stem cells are maintained, we first looked at the effect of hormonal signals on stem cells. We showed that depletion of free 20E from adult males by overexpressing a dominant negative form of the *Ecdysone receptor* (*EcR*) or its heterodimeric partner *ultraspiracle* (*usp*) causes GSC and CySC loss that is rescued by 20E feeding, uncovering a requirement for 20E in stem cell maintenance. EcR and USP are expressed, activated and autonomously required in the CySC lineage to promote CySC maintenance, as are downstream genes *ftz-f1* and *E75*. In contrast, GSCs non-autonomously require ecdysone signaling. Global inactivation of *EcR* increases cell

death in the testis that is rescued by expression of *EcR-B2* in the CySC lineage, indicating that ecdysone signaling supports stem cell viability primarily through a specific receptor isoform. Finally, *EcR* genetically interacts with the NURF chromatin-remodeling complex, which we previously showed maintains CySCs. Thus, although 20E levels are lower in males than females, ecdysone signaling acts through distinct cell types and effectors to ensure both ovarian and testis stem cell maintenance.

We also examined cell intrinsic mechanisms involved in stem cell regulation. Gene expression can be mediated not only genetically but also epigenetically, which causes heritable changes in gene expression without affecting primary DNA sequences. This causes stem cells and differentiated cells to share the same genome but have different properties. However, little is known about how epigenetic inheritance regulates gene expression, which can impact stem cell regulation. Here we used the CRISPR/Cas9 system to generate flies with the entire histone gene cluster removed and replaced with varying copy numbers of histone genes inserted at the original locus on chromosome 2L. We found that flies with low /numbers of histone genes (< 20 copies) have reduced fertility with deficiencies in both sperm and oocyte development. Using this system, we also systematically mutagenized all modified residues (45 total) on histone H3 and H4. Systematic analysis of flies with histone mutations reveals the importance of certain post-translational modifications of histones. Particularly, we found H4K16 acetylation is required for ovary GSC maintenance and required for male viability due to X-chromosome dosage compensation. Overall, we found the number of histone genes in the genome and certain post-translational modifications on specific histone residues are critical for fly viability, fertility and gonad development.

To gain a deeper insight into the niche regulation of stem cell fate, we used a newly developed technique called TaDa (Targeted DamID - DNA adenine methyltransferase identification), which can identify tissue specific DNA loci that bind DNA- or chromatin-binding proteins. When DNA adenine methyltransferase fused to RNA polymerase II (Pol II) is under spatial and temporal control using the Gal4-UAS system in *Drosophila*, we can obtain cell-type specific transcription profile according to where Pol II binds. Here, we performed TaDa in different cell types in the testis and ovary and were able to identify hundreds of genes specifically expressed in certain cell types. This sets the stage for many future studies of stem cells and their associated niche cells in both the *Drosophila* testis and ovary.

Thesis advisor: Dr. Erika Matunis

Thesis Reader: Dr. Daniela Drummond-Barbosa

ACKNOWLEDGEMENTS

First and foremost, I would like to express my sincere gratitude to my thesis advisor, Prof. Erika Matunis, for her support, encouragement, and immense knowledge. Throughout my six years in the lab, she was always available and willing to help me with anything ranging from solving research problems and mysteries to making great presentations and thinking about my future career. When I told her I wanted to try something different for my future career, she was very supportive and did whatever she could to help me. She is an incredible scientist and I cannot imagine having a better advisor and mentor for my Ph.D. study.

Besides my advisor, I would also like to thank the rest of my thesis committee: Prof. Peter Espenshade, Prof. Daniela Drummond-Barbosa, Prof. Elizabeth Chen, Prof. Jeff Boeke, and Prof. Denise Montell, for their insightful comments and suggestions. Their advice and questions greatly broadened my knowledge and enhanced my research from their various perspectives. My sincere thanks also goes to my collaborators, Prof. Brian Oliver at the NIH, Prof. Andrea Brand and Dr. Owen Marshall at the Gurdon Institute, and Prof. Guanjun Gao and Prof. Junbiao Dai at Tsinghua University, who always have great ideas and suggestions.

I would also like to thank all my labmates, including Dr. Maggie de Cuevas, Dr. Melanie Issigonis, Dr. Xuting (Becca) Sheng, Dr. Christopher Cherry, Dr. Rachel Stine, Dr. Phylis Hétié, Dr. Qing Ma, Salman Hasan, Leah Greenspan, Miriam Akeju and Chuchao Zhu. They made me feel that our lab is a big family and that I can always share my happiness and sadness with them, rather than it just being a workplace. They were

also very helpful during the course of my research. With their help, we were able to dissect more than 20,000 gonads in our special dissection parties. I would like to thank Melanie for giving me lots of training and suggestions at the beginning of my Ph.D. training, Maggie and Leah for spending so much time helping to revise my papers and other documents, and Miriam for helping with finishing the DamID project. I would also like to thank Qing, Phylis, Rachel and Salman for their precious friendship. They really made me enjoy my graduate life here.

Finally, I would like to thank my parents for taking good care of me. They are always very supportive of whatever decisions I make. With their love and encouragement, I feel that I am never alone no matter what difficulties I meet. I would also give my special thanks to my boyfriend, Yunlong Liu. For the two years we have been together, I feel that life has become more colorful. He is like sunshine into my world, helping me with my studies, cooking good food for me, and taking me to lots of places in the world. I am really lucky to have him in my life.

TABLE OF CONTENTS

LIST OF TABLES

LIST OF FIGURES

Chapter 1

General Introduction

Stem cells in the *Drosophila* testis and ovary

Stem cells are undifferentiated cells that can divide asymmetrically to generate both differentiated daughter cells and self-renewing stem cells (Hsu and Fuchs 2012). This process, called asymmetric division, is critical for the maintenance, regeneration and repair of adult tissues. Stem cells reside in niches, or specialized microenvironments, that produce local signals that prevent stem cells from differentiating. Adult stem cells are found in many different tissues and organs, including the brain, intestine, blood, skin and gonads, in a wide variety of organisms (Li and Xie 2005). However, the lack of stem cell markers and complexity of most tissues make it hard to study stem cells in many instances. In contrast, The *Drosophila* testis and ovary contain well-characterized adult stem cell niches that sustain the continuous production of sperm and eggs throughout most of the fly's lifespan (Li and Xie 2005, de Cuevas and Matunis 2011). Moreover, the functional conservation between *Drosophila* gonadal stem cell niches and mammalian stem cell niches makes the former systems ideal for genetic studies of stem cell maintenance and function (Li and Xie 2005).

The *Drosophila* testis stem cell niche is located at the testis apex, where a group of ~10-15 non-dividing somatic cells called the hub (Figure 1.1A, yellow cells) produce signals that maintain the surrounding germline stem cells (GSCs, dark red cells) and cyst stem cells (CySCs, dark green cells) (Hardy, Tokuyasu et al. 1979, Kiger, Jones et al. 2001, Tulina and Matunis 2001, Leatherman and Dinardo 2010). There are around 10 GSCs per testis, which make broad contact with the hub. GSCs divide asymmetrically to generate both GSCs and gonialblast daughter cells (dark red cells). The gonialblast undergoes 4 rounds of synchronous mitotic divisions while further differentiating into 2-,

4-, 8- and 16-cell spermatogonia (light red cells). After mitotic divisions are complete, spermatogonia undergo meiosis and then spermiogenesis, ultimately differentiating into sperm. Each GSC is flanked by approximately two CySCs (dark green cells). Therefore, the number of CySCs is approximately twice the number of GSCs. CySCs generate non-mitotic daughters called cyst cells, two of which envelop each gonialblast and cluster of spermatogonia as they differentiate.

The ovarian germline stem cell niche is located at the tip of each ovariole within the germarium, where 2-3 GSCs are anchored to a group of non-dividing somatic cap cells (Figure 1.1B, grey cells) via adherens junctions (Song, Zhu et al. 2002). As in the testis, GSCs in the ovary continuously self-renew and produce differentiated germ cells. Unlike male germ cells, which all become sperm, one of the sixteen interconnected female germ cells will become an oocyte, and the remaining 15 will become supporting nurse cells. Somatic cells in the ovary also look and behave quite differently from the somatic cells in the testis. Somatic inner germarial sheath cells (sometimes called escort cells, ECs, grey cells) located in the anterior half of the germarium are partners of early germ cells and remain quiescent most of the time (Kirilly, Wang et al. 2011, Morris and Spradling 2011). Midway through the germarium, somatic follicle stem cells (FSCs, dark green cells) produce follicle cells (light grey cells). Unlike quiescent cyst cells in the testis, differentiated follicle cells undergo several rounds of division to form a columnar epithelium that encases the germline cyst, forming an egg chamber. As an egg chamber buds off the germarium, it grows in size. Five to eight follicle cells become stalk cells (dark blue cells) and separate adjacent egg chambers (Dobens and Raftery 2000), and

these chains of interconnected egg chambers are called ovarioles. Each ovary has approximately sixteen ovarioles.

Hormonal regulation of stem cells

Stem cells are regulated and maintained by both local signals and systemic signals, such as nutrition state, stress conditions and hormone levels (Drummond-Barbosa and Spradling 2001, Ito, Hirao et al. 2004, Ables, Laws et al. 2012). Understanding how systemic signals affect stem cells can help us learn how stem cells respond to physiological changes. Hormones are well-studied systemic signals that can regulate development of the organs and the behavior of the whole body. However, their roles in stem cell function are still poorly understood. We are interested in understanding how hormones regulate stem cell function, which might help to reduce the incidence of some cancers.

In *Drosophila*, the steroid hormone 20-hydroxyecdysone (ecdysone, 20E) is the most well-studied hormone, and it is known to coordinate transitions between all the development stages. This includes embryogenesis, larval molting, puparium formation and metamorphosis (Baehrecke 1996, Yamanaka, Rewitz et al. 2013). Ecdysone acts through binding to a heterodimeric receptor composed of the franesoid X receptor/liver X receptor ortholog Ecdysone receptor (EcR) and the Retinoid X receptor ortholog ultraspiracle (usp) (Hayward, Bastiani et al. 1999, King-Jones and Thummel 2005). This ligand/receptor complex binds to a defined promoter sequence element, called the ecdysone response element (EcRE), to activate or repress downstream gene expression in response to the absence or presence of cell type-specific co-activators (Tsai, Kao et al.

1999, Perera, Zheng et al. 2005, Jang, Chang et al. 2009, Francis, Zorzano et al. 2010, Carbonell, Mazo et al. 2013) (Figure 1.2). Detectable titers of ecdysteroid are known to trigger the developmental transitions. However, the level of overall ecdysone is relatively low in adult flies, especially male adult flies, compared to that of larvae and pupae (Hodgetts, Sage et al. 1977, Handler 1982, Bownes, Dubendorfer et al. 1984, Kozlova and Thummel 2000). The significance of ecdysone in the adult flies was undervalued for a long time. Recently, adult ecdysone signaling has been shown to modulate reproduction, sleep, life span and male courtship behavior (Carney and Bender 2000, Ishimoto, Sakai et al. 2009, Tricoire, Battisti et al. 2009, Ishimoto and Kitamoto 2010). The function of ecdysone in modulating stem cell maintenance has been studied in fly ovaries. The EcR/USP heterodimer is required in the ovarian GSCs to promote their proper proliferation and maintenance. *EcR* can interact genetically with components of the Nucleosome remodeling factor (NURF) complex, suggesting that ecdysone signaling regulates GSCs by modulating their epigenetic state (Ables and Drummond-Barbosa 2010). Moreover, somatic ablation of the EcR leads to an increased number of undifferentiated germ cells and elevated levels of the cell adhesion molecule DE-cadherin (Buszczak, Freeman et al. 1999, Konig, Yatsenko et al. 2011, Morris and Spradling 2012). These findings indicate that ecdysone signaling plays a critical role in maintaining stem cells in the ovary.

In contrast to the wealth of knowledge regarding the roles of ecdysone in the ovary, the function of ecdysone in other adult tissues, especially in fly testis, is poorly understood. Titers of ecdysone in adult male flies are much lower than females but there is detectable ecdysone in the testis (Hodgetts, Sage et al. 1977, Handler 1982, Bownes,

Dubendorfer et al. 1984, Parisi, Gupta et al. 2010). In light of our lab's previous finding that the NURF complex is required in stem cell maintenance in the testis (Cherry and Matunis 2010), combined with the fact that NURF and ecdysone pathway components interact with each other genetically and physically during development and oogenesis (Badenhorst, Xiao et al. 2005, Ables and Drummond-Barbosa 2010), we chose to study the role of ecdysone in the testis stem cell niche. We showed that the ecdysone pathway components are expressed, activated and required for CySC maintenance in the adult male testis as described in Chapter 2.

Histone regulation of stem cells

Gene expression can be mediated not only genetically but also epigenetically, which causes heritable changes in gene expression without affecting primary DNA sequences. This allows cells with an identical genome to behave quite differently and turn into distinct cell types. This is also true when it comes to stem cells. Stem cells and differentiated cells share the same genome but have different properties. However, little is known about how epigenetic inheritance regulates gene expression, which includes stem cell regulation (Martin and Zhang 2007, Bonasio, Tu et al. 2010, Dias, Maddox et al. 2015, Xie, Wooten et al. 2015). Nowadays, more and more scientists emphasize understanding how stem cells are regulated epigenetically. In eukaryotes, DNA wraps around histone octamers comprised of two copies of each of histones H2A, H2B, H3 and H4 to form the fundamental building block of chromatin, called the nucleosome (Luger, Rechsteiner et al. 1997, Chandler and Wolffe 1999). Epigenetic gene regulation can be achieved by changing the accessibility of particular regions of the DNA to regulatory proteins. DNA methylation and alterations in chromatin structure caused by post-

translational modifications of histones (e.g. phosphorylation, methylation, acetylation, ubiquitination, etc) (Kouzarides 2007) are well-studied examples of epigenetic regultion.

Recent research has revealed that dynamic regulation of histones and histone modifications is required for GSC maintenance and differentiation in both sexes of *Drosophila melanogaster*. In 2012, Chen's lab reported that in *Drosophila* testes, pre-existing histone H3 is prone to segregate with GSCs, which remain in the niche and retain stem cell identity, while newly synthesized histone H3 molecules are enriched in differentiating daughter cells, or gonialblasts (Tran, Lim et al. 2012, Tran, Feng et al. 2013). Their recent studies further showed that uneven distribution of histone H3 during the asymmetric division of GSCs is regulated by phosphorylation at threonine 3 of H3 (H3T3P) (Xie, Wooten et al. 2015). It is not known if a similar phenomenon occurs in ovarian GSCs. However, the Ubiquitin protease *scrawny* (*scny*) deubiquitylates H2B and is involved in gene silencing in both male and female GSCs. Flies carrying *scny* mutation have elevated levels of H2B ubiquitylation and H3K4 trimethylation, and this causes GSC loss in both the testis and the ovary of adult flies (Buszczak, Paterno et al. 2009). Histone genes, dynamic regulation of histone modifications and their functions are well conserved from yeast to human (Fuchs, Demidov et al. 2006). Thus, learning the functions of histones and their modifications is helpful for better understanding stem cells.

To understand the function of a given histone modification, one can perturb the modification by modulating the activity of the appropriate histone modifying enzymes. However, modifying enzymes often have both histone and non-histone substrates, which can interfere with the interpretations in this type of study. Alternatively, one can mutate particular histone amino acid residues to mimic certain modifications or block the ability

of that histone to be modified. However, extensive mutagenesis studies on histones are limited to *Saccharomyces cerevisiae* (Dai, Hyland et al. 2008, Huang, Maertens et al. 2009) because of the number and distribution of histone genes in more complex eukaryotic genomes. For example, there are 64 histone genes within the human genome, which are distributed at three major loci on different chromosomes (Marzluff and Duronio 2002). In order to supply the cells with histones solely from a mutated version, one would need to inactivate all 64 histone genes in all three loci in the genome, which, if not impossible, is laborious and time-consuming with current gene knockout technologies. Currently, the only multicellular organism in which histone mutagenesis has been performed is the fruit fly. This is possible because all of the canonical histone genes (around 100 copies) are clustered at a single locus (chromosome 2L) (Lifton, Goldberg et al. 1978) (Figure 1.3A). In collaboration with Gao's and Dai's lab in Tsinghua University, we used the CRISPR/Cas9 system to generate flies with the entire histone gene cluster removed and replaced with varying copy numbers of histone genes inserted at the original locus on chromosome 2L (Figure 1.3B). We found that flies with low numbers of histone genes (< 20 copies) have reduced fertility with deficiencies in both sperm and oocyte development. Using this system, we also systematically mutagenized all modified residues (45 total) on histone H3 and H4 (Figure 1.3C), and tested the consequences of these mutations on viability, development, DNA-damage sensitivity and heterochromatic gene silencing as discussed in Chapter 3.

Transcription profiles in different cell types in the ovary and testis

For the past few decades, many pathways have been shown to play roles in maintaining stem cell function or promoting stem cell differentiation in flies and mice. In

order to gain a more comprehensive understanding of stem cell regulation, extensive global gene expression profiling studies, using techniques such as RNA sequencing and microarray analysis, have been applied to identify genes involved in stem cell maintenance and differentiation (Miyazato, Ueno et al. 2001, Yu, Vodyanik et al. 2007, Gan, Chepelev et al. 2010, Tang, Barbacioru et al. 2010). The tissues analyzed in these studies were induced pluripotent stem cell lines and embryonic stem cells. As described above, *Drosophila* gonads are powerful systems to study the molecular mechanisms regulating stem cell maintenance and differentiation. However, a full understanding of stem cell regulation is still limited due to technical barriers. Transcription profiles from gonads with mutations that cause the tissue to accumulate an excess number of undifferentiated cells have been compared to those from wild-type gonads to approximate the gene expression profiles of hub cells, CySCs, GSCs and their early daughters (Kai, Williams et al. 2005, Gan, Chepelev et al. 2010). These studies successfully revealed many new features of the putative stem cell and early progeny transcriptome, including epigenetic, splicing and sex-specific regulation of gene expression. However, these techniques are still restricted in that they reveal the transcriptome of the whole gonad but fail to provide information regarding how the specific cell types are regulated in the system. Identifying hub-enriched genes, CySC-enriched genes, and GSC-enriched genes by studying cell type-specific transcriptional profiles would be helpful to understand how stem cells are maintained.

Cell type-specific transcriptional profiles can be obtained after performing cell isolation using fluorescent activated cell sorting (FACS) or laser capture microdissection (LCM) followed by RNA-seq (Fu, Spence et al. 1999, Neira and Azen 2002). However,

cell isolation can be technically challenging. Sometimes it is hard to separate cells of different cell types because they adhere to each other, which leads to a mixed population of cells. One can also examine transcription profiles using targeted expression of RNA-binding or ribosomal binding proteins to pull down RNA (Roy, Stuart et al. 2002, Miller, Robinson et al. 2009, Thomas, Lee et al. 2012). However, these kinds of approaches are unable to provide the genome-wide binding profile of chromatin binding or transcription factors.

Several years ago, the van Steensel lab invented the technique of DamID (Dam identification) wherein a protein of interest (a chromatin binding protein or transcription factor) is fused to DNA adenine methyltransferase (van Steensel and Henikoff 2000, van Steensel, Delrow et al. 2001). Dam is a prokaryotic protein, which methylates adenines in the sequence GATC. Upon Dam-fusion protein expression in cultured cells or intact organisms, Dam is targeted to where the protein of interest normally binds, which results in local methylation of adenines. The methylation marks can then be identified by specific methylation-sensitive restriction enzyme digestion, followed by PCR amplification and high-throughput sequencing. Based on the methylation profile, one can easily determine the binding profile of the specific DNA-binding or chromatin binding protein.

Recently, the Brand lab developed targeted DamID (TaDa) to study DamID-fusion protein genome-wide binding profiles under both spatial and temporal control. The lab adapted DamID for this purpose by using the GAL4-UAS system to express Dam-fusion proteins in specific cell types, and the inclusion of a temperature sensitive GAL4 repressor enables temporal regulation of fusion protein expression. RNA polymerase II

(Pol II) (Figure 1.4) is a critical enzyme found in eukaryotic cells, which catalyzes the synthesis of RNA from DNA template. By fusing Pol II to Dam (Dam-Pol II), an approximation of gene expression in vivo can be obtained without cell isolation. The method is very sensitive and needs far fewer than 10,000 cells. The Dam-Pol II occupancy profile can be used to predict actively transcribed genes in specific cells (Figure 1.4) (Southall, Gold et al. 2013, Handley, Schauer et al. 2015, Marshall and Brand 2015). Here, we performed TaDa in different cell types in the *Drosophila* ovary and testis, including hub cells and CySC lineage cells in the testis, as described in Chapter 4.

References

Ables, E. T. and D. Drummond-Barbosa (2010). "The steroid hormone ecdysone functions with intrinsic chromatin remodeling factors to control female germline stem cells in Drosophila." Cell Stem Cell **7**(5): 581-592.

Kiger, A. A., D. L. Jones, C. Schulz, M. B. Rogers and M. T. Fuller (2001). "Stem cell self-renewal specified by JAK-STAT activation in response to a support cell cue." Science **294**(5551): 2542-2545.

Badenhorst, P., H. Xiao, L. Cherbas, S. Y. Kwon, M. Voas, I. Rebay, P. Cherbas and C. Wu (2005). "The Drosophila nucleosome remodeling factor NURF is required for Ecdysteroid signaling and metamorphosis." Genes Dev **19**(21): 2540-2545.

Baehrecke, E. H. (1996). "Ecdysone signaling cascade and regulation of Drosophila metamorphosis." Arch Insect Biochem Physiol **33**(3-4): 231-244.

Bonasio, R., S. Tu and D. Reinberg (2010). "Molecular signals of epigenetic states." Science **330**(6004): 612-616.

Bownes, M., A. Dubendorfer and T. Smith (1984). "Ecdysteroids in Adult Males and Females of Drosophila-Melanogaster." Journal of Insect Physiology **30**(10): 823-830.

Buszczak, M., M. R. Freeman, J. R. Carlson, M. Bender, L. Cooley and W. A. Segraves (1999). "Ecdysone response genes govern egg chamber development during mid-oogenesis in Drosophila." Development **126**(20): 4581-4589.

Buszczak, M., S. Paterno and A. C. Spradling (2009). "Drosophila stem cells share a common requirement for the histone H2B ubiquitin protease scrawny." Science **323**(5911): 248-251.

Carbonell, A., A. Mazo, F. Serras and M. Corominas (2013). "Ash2 acts as an ecdysone receptor coactivator by stabilizing the histone methyltransferase Trr." Molecular Biology of the Cell **24**(3): 361-372.

Carney, G. E. and M. Bender (2000). "The Drosophila ecdysone receptor (EcR) gene is required maternally for normal oogenesis." Genetics **154**(3): 1203-1211.

Chandler, S. and A. P. Wolffe (1999). "Analysis of linker histone binding to mono- and dinucleosomes." Methods Mol Biol **119**: 103-112.

Cherry, C. M. and E. L. Matunis (2010). "Epigenetic regulation of stem cell maintenance in the Drosophila testis via the nucleosome-remodeling factor NURF." Cell Stem Cell **6**(6): 557-567.

Dai, J., E. M. Hyland, D. S. Yuan, H. Huang, J. S. Bader and J. D. Boeke (2008). "Probing nucleosome function: a highly versatile library of synthetic histone H3 and H4 mutants." Cell **134**(6): 1066-1078.

de Cuevas, M. and E. L. Matunis (2011). "The stem cell niche: lessons from the Drosophila testis." Development **138**(14): 2861-2869.

Dias, B. G., S. A. Maddox, T. Klengel and K. J. Ressler (2015). "Epigenetic mechanisms underlying learning and the inheritance of learned behaviors." Trends Neurosci **38**(2): 96-107.

Dobens, L. L. and L. A. Raftery (2000). "Integration of epithelial patterning and morphogenesis in Drosophila ovarian follicle cells." Dev Dyn **218**(1): 80-93.

Drummond-Barbosa, D. (2008). "Stem cells, their niches and the systemic environment: an aging network." Genetics **180**(4): 1787-1797.

Drummond-Barbosa, D. and A. C. Spradling (2001). "Stem cells and their progeny respond to nutritional changes during Drosophila oogenesis." Dev Biol **231**(1): 265-278.

Francis, V. A., A. Zorzano and A. A. Teleman (2010). "dDOR Is an EcR Coactivator that Forms a Feed-Forward Loop Connecting Insulin and Ecdysone Signaling." Current Biology **20**(20): 1799-1808.

Fu, A. Y., C. Spence, A. Scherer, F. H. Arnold and S. R. Quake (1999). "A microfabricated fluorescence-activated cell sorter." Nat Biotechnol **17**(11): 1109-1111.

Fuchs, J., D. Demidov, A. Houben and I. Schubert (2006). "Chromosomal histone modification patterns--from conservation to diversity." Trends Plant Sci **11**(4): 199-208.

Gan, Q., I. Chepelev, G. Wei, L. Tarayrah, K. Cui, K. Zhao and X. Chen (2010). "Dynamic regulation of alternative splicing and chromatin structure in Drosophila gonads revealed by RNA-seq." Cell Res **20**(7): 763-783.

Ganter, G. K., A. E. Panaitiu, J. B. Desilets, J. A. Davis-Heim, E. A. Fisher, L. C. Tan, R. Heinrich, E. B. Buchanan, K. M. Brooks, M. T. Kenney, M. G. Verde, J. Downey, A. M. Adams, J. S. Grenier, S. Maddula, P. Shah, K. M. Kincaid and J. R. O'Brien (2011). "Drosophila male courtship behavior is modulated by ecdysteroids." J Insect Physiol **57**(9): 1179-1184.

Handler, A. M. (1982). "Ecdysteroid titers during pupal and adult development in Drosophila melanogaster." Dev Biol **93**(1): 73-82.

Handley, A., T. Schauer, A. G. Ladurner and C. E. Margulies (2015). "Designing Cell-Type-Specific Genome-wide Experiments." Mol Cell **58**(4): 621-631.

Hardy, R. W., K. T. Tokuyasu, D. L. Lindsley and M. Garavito (1979). "The germinal proliferation center in the testis of Drosophila melanogaster." J Ultrastruct Res **69**(2): 180-190.

Hayward, D. C., M. J. Bastiani, J. W. Trueman, J. W. Truman, L. M. Riddiford and E. E. Ball (1999). "The sequence of Locusta RXR, homologous to Drosophila Ultraspiracle, and its evolutionary implications." Dev Genes Evol **209**(9): 564-571.

Hodgetts, R. B., B. Sage and J. D. O'Connor (1977). "Ecdysone titers during postembryonic development of Drosophila melanogaster." Dev Biol **60**(1): 310-317.

Hsu, H. J., L. LaFever and D. Drummond-Barbosa (2008). "Diet controls normal and tumorous germline stem cells via insulin-dependent and -independent mechanisms in Drosophila." Dev Biol **313**(2): 700-712.

Hsu, Y. C. and E. Fuchs (2012). "A family business: stem cell progeny join the niche to regulate homeostasis." Nat Rev Mol Cell Biol **13**(2): 103-114.

Huang, H. L., A. M. Maertens, E. M. Hyland, J. B. A. Dai, A. Norris, J. D. Boeke and J. S. Bader (2009). "HistoneHits: A database for histone mutations and their phenotypes." Genome Research **19**(4): 674-681.

Ishimoto, H. and T. Kitamoto (2010). "The steroid molting hormone Ecdysone regulates sleep in adult Drosophila melanogaster." Genetics **185**(1): 269-281.

Ishimoto, H., T. Sakai and T. Kitamoto (2009). "Ecdysone signaling regulates the formation of long-term courtship memory in adult Drosophila melanogaster." Proc Natl Acad Sci U S A **106**(15): 6381-6386.

Ito, K., A. Hirao, F. Arai, S. Matsuoka, K. Takubo, I. Hamaguchi, K. Nomiyama, K. Hosokawa, K. Sakurada, N. Nakagata, Y. Ikeda, T. W. Mak and T. Suda (2004).

"Regulation of oxidative stress by ATM is required for self-renewal of haematopoietic stem cells." Nature **431**(7011): 997-1002.

Jang, A. C., Y. C. Chang, J. Bai and D. Montell (2009). "Border-cell migration requires integration of spatial and temporal signals by the BTB protein Abrupt." Nat Cell Biol **11**(5): 569-579.

Kai, T., D. Williams and A. C. Spradling (2005). "The expression profile of purified Drosophila germline stem cells." Dev Biol **283**(2): 486-502.

Kiger, A. A., D. L. Jones, C. Schulz, M. B. Rogers and M. T. Fuller (2001). "Stem cell self-renewal specified by JAK-STAT activation in response to a support cell cue." Science **294**(5551): 2542-2545.

King-Jones, K. and C. S. Thummel (2005). "Nuclear receptors--a perspective from Drosophila." Nat Rev Genet **6**(4): 311-323.

Kiger, A. A., D. L. Jones, C. Schulz, M. B. Rogers and M. T. Fuller (2001). "Stem cell self-renewal specified by JAK-STAT activation in response to a support cell cue." Science **294**(5551): 2542-2545.

Konig, A., A. S. Yatsenko, M. Weiss and H. R. Shcherbata (2011). "Ecdysteroids affect Drosophila ovarian stem cell niche formation and early germline differentiation." EMBO J **30**(8): 1549-1562.

Kouzarides, T. (2007). "Chromatin modifications and their function." Cell **128**(4): 693-705.

Kozlova, T. and C. S. Thummel (2000). "Steroid regulation of postembryonic development and reproduction in Drosophila." Trends Endocrinol Metab **11**(7): 276-280.

Leatherman, J. L. and S. Dinardo (2010). "Germline self-renewal requires cyst stem cells and stat regulates niche adhesion in Drosophila testes." Nat Cell Biol **12**(8): 806-811.

Li, L. H. and T. Xie (2005). "Stem cell niche: Structure and function." Annual Review of Cell and Developmental Biology **21**: 605-631.

Lifton, R. P., M. L. Goldberg, R. W. Karp and D. S. Hogness (1978). "The organization of the histone genes in Drosophila melanogaster: functional and evolutionary implications." Cold Spring Harb Symp Quant Biol **42 Pt 2**: 1047-1051.

Luger, K., T. J. Rechsteiner, A. J. Flaus, M. M. Waye and T. J. Richmond (1997). "Characterization of nucleosome core particles containing histone proteins made in bacteria." J Mol Biol **272**(3): 301-311.

Marshall, O. J. and A. H. Brand (2015). "damidseq_pipeline: an automated pipeline for processing DamID sequencing datasets." Bioinformatics **31**(20): 3371-3373.

Martin, C. and Y. Zhang (2007). "Mechanisms of epigenetic inheritance." Curr Opin Cell Biol **19**(3): 266-272.

Marzluff, W. F. and R. J. Duronio (2002). "Histone mRNA expression: multiple levels of cell cycle regulation and important developmental consequences." Curr Opin Cell Biol **14**(6): 692-699.

Miller, M. R., K. J. Robinson, M. D. Cleary and C. Q. Doe (2009). "TU-tagging: cell type-specific RNA isolation from intact complex tissues." Nat Methods **6**(6): 439-441.

Miyazato, A., S. Ueno, K. Ohmine, M. Ueda, K. Yoshida, Y. Yamashita, T. Kaneko, M. Mori, K. Kirito, M. Toshima, Y. Nakamura, K. Saito, Y. Kano, S. Furusawa, K. Ozawa and H. Mano (2001). "Identification of myelodysplastic syndrome-specific genes by

DNA microarray analysis with purified hematopoietic stem cell fraction." Blood **98**(2): 422-427.

Morris, L. X. and A. C. Spradling (2011). "Long-term live imaging provides new insight into stem cell regulation and germline-soma coordination in the Drosophila ovary." Development **138**(11): 2207-2215.

Morris, L. X. and A. C. Spradling (2012). "Steroid signaling within Drosophila ovarian epithelial cells sex-specifically modulates early germ cell development and meiotic entry." PLoS One **7**(10): e46109.

Neira, M. and E. Azen (2002). "Gene discovery with laser capture microscopy." Methods Enzymol **356**: 282-289.

Parisi, M. J., V. Gupta, D. Sturgill, J. T. Warren, J. M. Jallon, J. H. Malone, Y. Zhang, L. I. Gilbert and B. Oliver (2010). "Germline-dependent gene expression in distant non-gonadal somatic tissues of Drosophila." Bmc Genomics **11**.

Perera, S. C., S. Zheng, Q. L. Feng, P. J. Krell, A. Retnakaran and S. R. Palli (2005). "Heterodimerization of ecdysone receptor and ultraspiracle on symmetric and asymmetric response elements." Arch Insect Biochem Physiol **60**(2): 55-70.

Roy, P. J., J. M. Stuart, J. Lund and S. K. Kim (2002). "Chromosomal clustering of muscle-expressed genes in Caenorhabditis elegans." Nature **418**(6901): 975-979.

Song, X., C. H. Zhu, C. Doan and T. Xie (2002). "Germline stem cells anchored by adherens junctions in the Drosophila ovary niches." Science **296**(5574): 1855-1857.

Southall, T. D., K. S. Gold, B. Egger, C. M. Davidson, E. E. Caygill, O. J. Marshall and A. H. Brand (2013). "Cell-type-specific profiling of gene expression and chromatin

binding without cell isolation: assaying RNA Pol II occupancy in neural stem cells." Dev Cell **26**(1): 101-112.

Tang, F., C. Barbacioru, S. Bao, C. Lee, E. Nordman, X. Wang, K. Lao and M. A. Surani (2010). "Tracing the derivation of embryonic stem cells from the inner cell mass by single-cell RNA-Seq analysis." Cell Stem Cell **6**(5): 468-478.

Thomas, A., P. J. Lee, J. E. Dalton, K. J. Nomie, L. Stoica, M. Costa-Mattioli, P. Chang, S. Nuzhdin, M. N. Arbeitman and H. A. Dierick (2012). "A versatile method for cell-specific profiling of translated mRNAs in Drosophila." PLoS One **7**(7): e40276.

Tran, V., L. Feng and X. Chen (2013). "Asymmetric distribution of histones during Drosophila male germline stem cell asymmetric divisions." Chromosome Res **21**(3): 255-269.

Tran, V., C. Lim, J. Xie and X. Chen (2012). "Asymmetric division of Drosophila male germline stem cell shows asymmetric histone distribution." Science **338**(6107): 679-682.

Tricoire, H., V. Battisti, S. Trannoy, C. Lasbleiz, A. M. Pret and V. Monnier (2009). "The steroid hormone receptor EcR finely modulates Drosophila lifespan during adulthood in a sex-specific manner." Mech Ageing Dev **130**(8): 547-552.

Tsai, C. C., H. Y. Kao, T. P. Yao, M. McKeown and R. M. Evans (1999). "SMRTER, a Drosophila nuclear receptor coregulator, reveals that EcR-mediated repression is critical for development." Molecular Cell **4**(2): 175-186.

Tulina, N. and E. Matunis (2001). "Control of stem cell self-renewal in Drosophila spermatogenesis by JAK-STAT signaling." Science **294**(5551): 2546-2549.

van Steensel, B., J. Delrow and S. Henikoff (2001). "Chromatin profiling using targeted DNA adenine methyltransferase." Nat Genet **27**(3): 304-308.

van Steensel, B. and S. Henikoff (2000). "Identification of in vivo DNA targets of chromatin proteins using tethered dam methyltransferase." Nat Biotechnol **18**(4): 424-428.

Xie, J., M. Wooten, V. Tran, B. C. Chen, C. Pozmanter, C. Simbolon, E. Betzig and X. Chen (2015). "Histone H3 Threonine Phosphorylation Regulates Asymmetric Histone Inheritance in the Drosophila Male Germline." Cell.

Yamanaka, N., K. F. Rewitz and M. B. O'Connor (2013). "Ecdysone control of developmental transitions: lessons from Drosophila research." Annu Rev Entomol **58**: 497-516.

Yu, J., M. A. Vodyanik, K. Smuga-Otto, J. Antosiewicz-Bourget, J. L. Frane, S. Tian, J. Nie, G. A. Jonsdottir, V. Ruotti, R. Stewart, Slukvin, II and J. A. Thomson (2007). "Induced pluripotent stem cell lines derived from human somatic cells." Science **318**(5858): 1917-1920.

Figure legends

Figure 1.1 Illustration of a wild-type *Drosophila* testis and ovary

(**A**) Illustration of a wild-type *Drosophila* testis. Non-dividing hub cells (yellow) are surrounded by germline stem cells (GSCs, dark red) and cyst stem cells (CySCs, dark green). GSCs with round fusomes (red) divide asymmetrically and produce differentiated spermatogonia (green) with branched fusomes. CySCs divide asymmetrically to form cyst cells and support normal development of surrounding germ cells. (**B**) Illustration of a wild-type *Drosophila* germarium and egg chambers. GSCs (dark red) are attached to the supporting cap cells (grey) and divide asymmetrically to form cystoblasts, which further divide to form 16-cell cysts that become surrounded by follicle cells (green). The cysts and their surrounding follicle cells then bud from the germarium as individual egg chambers. As the egg chambers continue to grow, they move to the posterior and form a chain of egg chambers connected by stalk cells (blue).

Figure 1.2 Diagram of the *Drosophila* ecdysone pathway.

The hormone twenty-hydroxyecdysone 20E (blue dots) activates this pathway by binding to a heterodimeric receptor composed of EcR and USP. EcR and USP each contain a ligand binding domain (LBD). EcR can bind 20E and a DNA binding domain (DBD) that can recognize the ecdysone response element (EcRE) and regulate downstream gene expression (pink dots).

Figure 1.3 Schematic representation of the histone gene cluster in *Drosophila* and experimental strategy for studying histone function in *Drosophila*

(**A**) *Drosophila* histone genes form a gene cluster (~100 copies) on the left arm of chromosome II, and each repeat contains five canonical histone genes, His1, His2A, His2B, His3, and His4. (**B**) The entire histone cluster was removed from *Drosophila* using CRISPR/Cas9 and replaced by different copy numbers of histone genes. (**C**) The replacement histone genes were constructed with mutations in histone H3 or H4.

Figure 1.4 Illustration of the Targeted DamID (TaDa) experimental design

Cell-type specific analysis of genes that are being transcribed by RNA polymerase II (Pol II) can be achieved through TaDa. DNA adenine methyltransferase is fused to Pol II and methylates the adenine in the sequence GATC close to where Pol II binds. The methylated sites will then be identified through digestion by methylation specific restriction enzyme, PCR amplification and high-throughput sequencing. The expression of Dam-Pol II fusion protein is mediated by the GAL4-UAS system, which allows spatial and temporal control of expression. Metagene profile for Dam-Pol II obtained from TaDa can be used to predict cell-type specific or sex-specific gene expression.

Figure 1.1

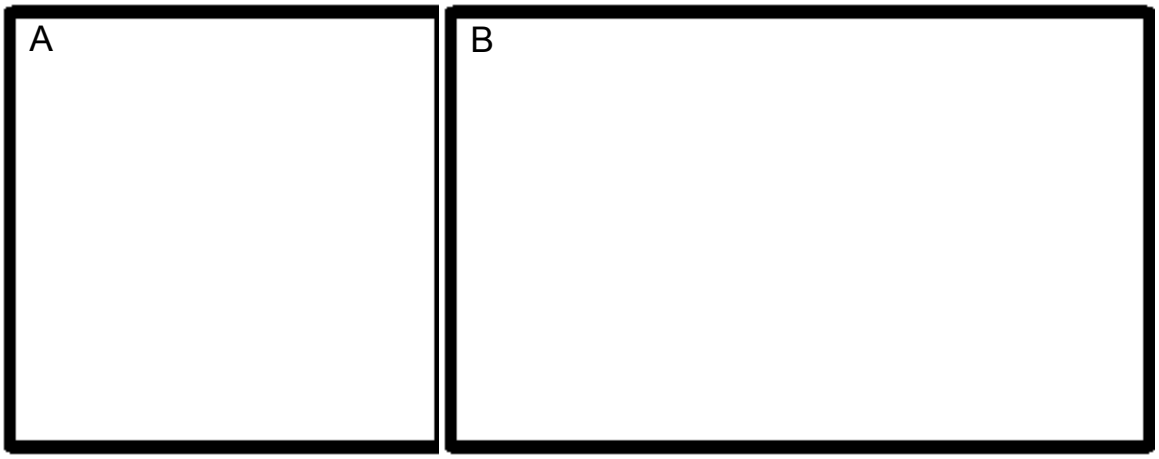

Figure 1.2

Figure 1.3

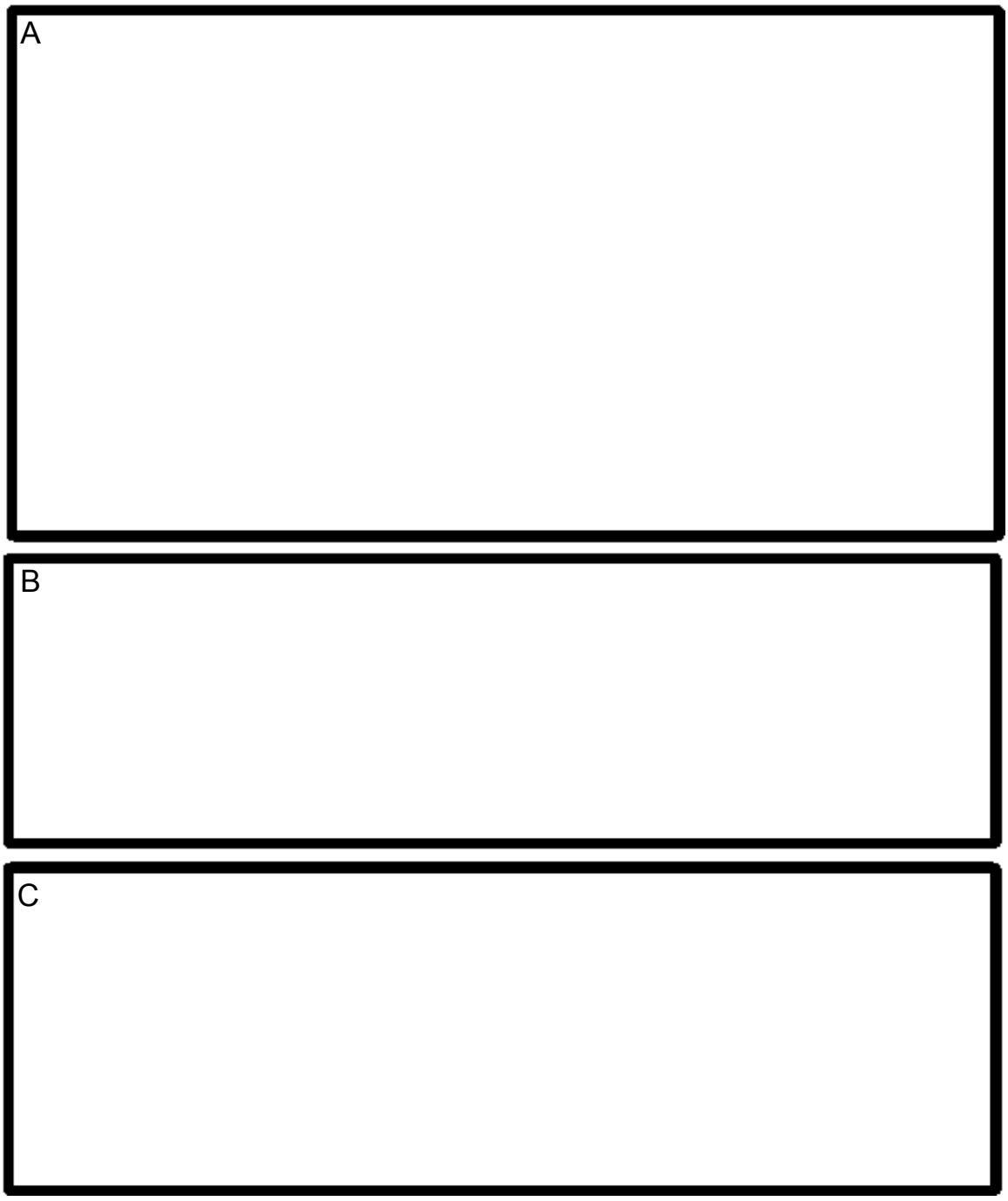

Figure 1.4

Cell type-specific profiling of transcription without cell isolation

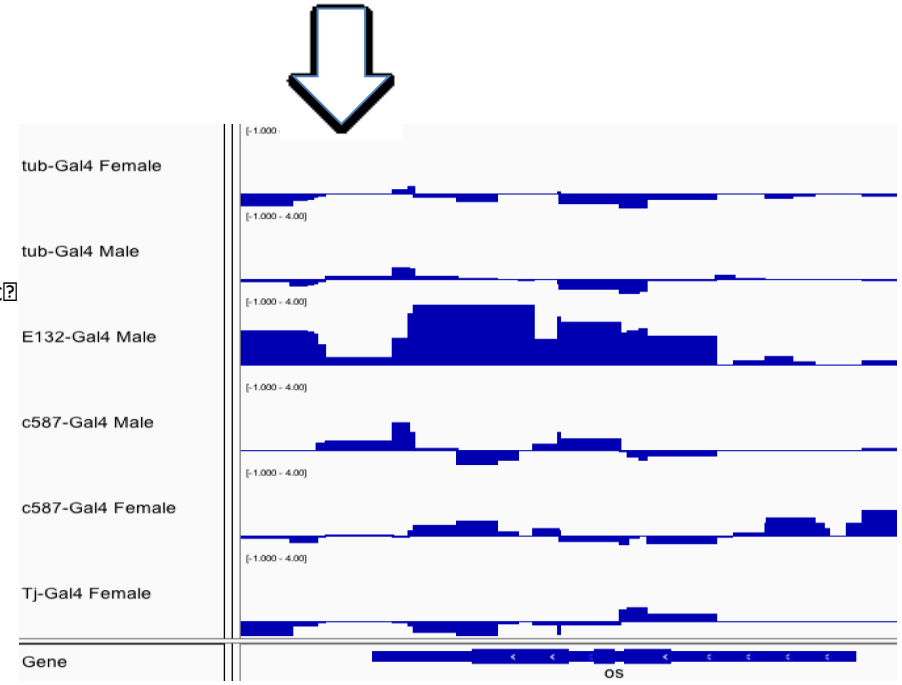

Chapter 2

Steroid Signaling Promotes Stem Cell Maintenance in the Drosophila Testis

This chapter is a modified version of the manuscript, "Li Y, Ma Q**,** Cherry CM, Matunis E. (2014) Steroid signaling promotes stem cell maintenance in the Drosophila testis. *Developmental Biology* 394: 129-141."

Summary

Stem cell regulation by local signals is intensely studied, but less is known about the effects of hormonal signals on stem cells. In *Drosophila,* the primary steroid twenty-hydroxyecdysone (20E) regulates ovarian germline stem cells (GSCs) but was considered dispensable for testis GSC maintenance. Male GSCs reside in a microenvironment (niche) generated by somatic hub cells and adjacent cyst stem cells (CySCs). Here, we show that depletion of free 20E from adult males by overexpressing a dominant negative form of the *Ecdysone receptor* (*EcR*) or its heterodimeric partner *ultraspiracle* (*usp*) causes GSC and CySC loss that is rescued by 20E feeding, uncovering a requirement for 20E in stem cell maintenance. EcR and USP are expressed, activated and autonomously required in the CySC lineage to promote CySC maintenance, as are downstream genes *ftz-f1* and *E75*. In contrast, GSCs non-autonomously require ecdysone signaling. Global inactivation of *EcR* increases cell death in the testis that is rescued by expression of *EcR-B2* in the CySC lineage, indicating that ecdysone signaling supports stem cell viability primarily through a specific receptor isoform. Finally, *EcR* genetically interacts with the NURF chromatin-remodeling complex, which we previously showed maintains CySCs. Thus, although 20E levels are lower in males than females, ecdysone signaling acts through distinct cell types and effectors to ensure both ovarian and testis stem cell maintenance.

Introduction

Adult stem cells, which are essential for the maintenance of many tissues, reside in niches, or local microenvironments, where distinct signals prevent their differentiation (or promote their maintenance) (Li and Xie 2005, de Cuevas and Matunis 2011). Stem cells can respond to both local and systemic signals including nutrition and hormones, which convey information about the organism's environment to the tissues and coordinate responses to physiological change (Drummond-Barbosa and Spradling 2001, Ito, Hirao et al. 2004, Li and Xie 2005, Drummond-Barbosa 2008, Hsu, LaFever et al. 2008, McLeod, Wang et al. 2010, Gancz and Gilboa 2013). Some of the best-characterized niches are found in the *Drosophila* gonads, where germline stem cells (GSCs) and supporting somatic stem cells remain active throughout adulthood, ensuring a lifetime supply of sperm or eggs (Spradling, Fuller et al. 2011). However, the role of hormonal signaling in stem cell maintenance is not fully understood, especially in the *Drosophila* testis (Gancz and Gilboa 2013).

In *Drosophila*, the steroid hormone twenty-hydroxyecdysone (20E), generated from the prohormone ecdysone, is essential for coordinating development at all stages, including embryogenesis, larval molting, puparium formation, and metamorphosis (Baehrecke 1996, Yamanaka, Rewitz et al. 2013). 20E acts by binding to a heterodimeric nuclear hormone receptor complex composed of *Ecdysone receptor* (*EcR*) and *ultraspiracle* (*usp*), which are mammalian orthologues of *farnesoid X receptor*/*liver X receptor* and *retinoid X receptor*, respectively (Hayward, Bastiani et al. 1999, King-Jones and Thummel 2005). This complex binds to specific promoter sequences, called Ecdysone Response Elements (EcREs), and can activate or repress the expression of

hundreds of target genes which vary in response depending on the presence or absence of cell-type-specific co-activators (Tsai, Kao et al. 1999, Perera, Zheng et al. 2005, Jang, Chang et al. 2009, Francis, Zorzano et al. 2010, Carbonell, Mazo et al. 2013) (Figure 2.1A). Additional temporal and spatial control of 20E signaling is generated through alternative splicing of transcripts encoded by the *EcR* gene to yield three isoforms, *EcR-A*, *EcR-B1*, and *EcR-B2*; these receptors share common ligand binding domains (LBDs) and DNA binding domains (DBDs) but vary at their amino-termini. Each *EcR* isoform has a distinct expression pattern and response to 20E throughout development (Talbot, Swyryd et al. 1993).

Although ecdysone signaling has been studied primarily during metamorphosis, 20E is also present, albeit at lower levels, in adult *Drosophila* (Hodgetts, Sage et al. 1977, Handler 1982, Bownes, Dubendorfer et al. 1984, Kozlova and Thummel 2000). Adult 20E titers respond to changes in diet and environment (Riehle and Brown 1999, Tu, Yin et al. 2002) and can also be modulated genetically. In this case, however, conditional manipulation of hormone levels is necessary due to the essential roles of 20E during development. 20E feeding can also serve as a tool to increase hormone titers (Garen, Kauvar et al. 1977).

Although 20E has been shown to regulate a few aspects of adult *Drosophila* behavior including sleep and longevity, the effects of this hormone are best understood during female reproduction, where ecdysone signaling regulates multiple stages of oogenesis (Carney and Bender 2000, Ishimoto, Sakai et al. 2009, Tricoire, Battisti et al. 2009, Ishimoto and Kitamoto 2010). Oogenesis is initiated through asymmetric GSC divisions, and *EcR*, *usp*, and the ecdysone target gene and ETS-domain DNA-binding

protein *Ecdysone-induced protein 74EF* (*E74)* are required directly in ovarian GSCs for their maintenance and proliferation. Both *EcR* and *E74* interact genetically with components of the Nucleosome remodeling factor (NURF) complex, suggesting that ecdysone signaling regulates GSCs by modulating their epigenetic state (Ables and Drummond-Barbosa 2010). Ovarian GSCs are also regulated indirectly by ecdysone signaling: *EcR*, *usp*, and the ecdysone target and nuclear hormone receptor *Ecdysone-induced protein 75B* (*E75)* are required in the somatic escort cells of the ovary for GSC maintenance (Morris and Spradling 2012). Ecdysone signaling is also required for many subsequent steps in oogenesis including germline differentiation, entry into meiosis, and formation and progression of egg chambers past mid-oogenesis (Buszczak, Freeman et al. 1999, Konig, Yatsenko et al. 2011, Morris and Spradling 2012).

In contrast to the wealth of information regarding the roles of ecdysone signaling in the ovary, little is known of its requirements in male reproduction. Adult *Drosophila* males contain lower titers of 20E than females, and although the hormone has been detected in the testis (Hodgetts, Sage et al. 1977, Handler 1982, Bownes, Dubendorfer et al. 1984, Parisi, Gupta et al. 2010), ecdysone signaling was recently described as being dispensable for GSC maintenance and early germ cell development in males (Morris and Spradling 2012). However, we previously found that the NURF complex is required for stem cell maintenance in the testis (Cherry and Matunis 2010). In light of the physical and genetic interactions between NURF and ecdysone pathway components during development and oogenesis (Badenhorst, Xiao et al. 2005, Ables and Drummond-Barbosa 2010), we were prompted to look more closely at the role of ecdysone signaling in the testis stem cell niche.

The *Drosophila* testis stem cell niche resides in the testis apex, where a cluster of non-mitotic somatic cells called the hub produces signals that maintain surrounding GSCs and cyst stem cells (CySCs) (Figure 2.1B). GSCs generate gonialblast daughters, which mitotically amplify and ultimately differentiate into sperm; CySCs produce non-mitotic daughters called cyst cells, two of which envelop each gonialblast and its descendants, supporting their differentiation into sperm. Here, we report that ecdysone signaling pathway components are expressed and activated in CySC lineage cells and are required directly in these cells to maintain both GSCs and CySCs, which do not survive in the absence of ecdysone signaling. Moreover, we show that *EcR* interacts genetically with *Enhancer of bithorax* (*Nurf301*), a component of the NURF complex, to maintain stem cells in the testis niche. Thus, steroid signaling is required for stem cell maintenance in both the ovary and testis of *Drosophila*, where it might act in part by regulating the epigenetic state of the stem cells.

Results

Ecdysone signaling components are expressed and activated in the *Drosophila* testis

To determine whether ecdysone signaling plays a role in the adult *Drosophila* testis, we began by asking whether ecdysone receptors and downstream targets of the pathway are expressed in this tissue. We used immunostaining to determine the expression patterns of *EcR*, *usp*, and the downstream targets *broad* (*br), E75* and *ftz transcription factor 1* (*ftz-f1*) in the testis apex. We found that USP is expressed in the hub and CySC lineage cells (Figure 2.1C), while EcR and Br are enriched in the CySC lineage (Figure 2.1D and E). Although transcripts encoding E75 and Ftz-f1 were detected in the testis by RNA-seq (Gan, Chepelev et al. 2010), these proteins are below the level of detection via immunostaining in adult testes (although they were detected in other tissues; data not shown). Thus, several key ecdysone pathway components are present within the testis apex, and their expression is largely confined to somatic cells.

Since ecdysone pathway members are expressed in the testis apex, we next asked which cells in this tissue actively transduce ecdysone signaling. Transgenic flies containing chimeric receptors are well-established tools for detecting ecdysone receptor complex (EcR and USP) activation within tissues. These receptors contain the ligand-binding domain from either EcR or USP fused to the yeast GAL4 DNA-binding domain (*GAL4-EcR* or *GAL4-usp*) under control of a heat-inducible promoter, which allows for precise temporal control of their expression (Kozlova and Thummel 2002). Binding of GAL4-EcR or GAL4-USP to a second transgene encoding a reporter (lacZ or GFP) under control of an upstream activating sequence (UAS), which is recognized by the Gal4 DNA-binding domain, reveals cells with active ecdysone signaling. When flies carrying

both transgenes are exposed to high temperature, chimeric receptors are expressed throughout the fly; however, UAS-reporter genes are expressed only in cells containing 20E and the cognate receptor (USP or other binding partners for *GAL4-EcR*; EcR or other binding partners for *GAL4-usp*) (Figure 2.1F) (Kozlova and Thummel 2002, Palanker, Necakov et al. 2006). We first examined testes from late 3rd instar larvae expressing GAL4-EcR, because at this stage, the stem cell niche is fully functional but the endogenous 20E levels are higher than in adults (Hardy, Tokuyasu et al. 1979, Kozlova and Thummel 2000). We observed weak GFP expression in a few hub cells and stronger expression in late cyst cells (Figure 2.1G). However, when flies develop to adulthood and 20E titers have diminished (Schwedes and Carney 2012), GFP expression is no longer detectable within the testis (Figure 2.1H). Therefore, we hypothesized that in larval testes, endogenous 20E levels are sufficient to induce *GAL4-EcR* activation in the somatic lineage, but in adult testes, 20E availability might be a limiting factor. To test this hypothesis, we fed exogenous 20E to adult flies containing *GAL4-EcR* and *UAS-lacZ* and then examined the reporter gene expression within the testis. We found that 20E feeding caused *GAL4-EcR* activation in the hub and CySC lineage in a pattern similar to that seen in 3rd instar larval testes in response to endogenous hormone (Figure 2.1I). We conclude that adult hub and CySC lineage cells are competent to respond to 20E via EcR, but that the levels of 20E needed to produce a detectable signal using this reporter are insufficient when flies are fed standard food. When we repeated the 20E feeding with flies expressing *GAL4-usp*, we again saw GFP expression in the hub and late cyst cells (Figure 2.1J). We expected to see activation of these reporters in the CySC lineage, but were surprised to find GFP expression in the hub; *GAL4-usp* requires a binding partner to function, and we

did not detect endogenous EcR expression in the hub (Figure 2.1D). Perhaps low levels of EcR are present in the hub (but undetectable by immunostaining) and are sufficient to activate reporter gene expression. However, *usp*, unlike *EcR*, can signal through additional binding partners such as *Hormone receptor-like in 38* (*DHR38*) (Jones, Wozniak et al. 2001, Baker, Shewchuk et al. 2003); these partners, which have not been characterized in the testis, may permit activation of *GAL4-usp*. We observed that the activation of both ecdysone activity reporters was limited to only a few cells, and we suspect that this is due to a limited supply of binding partners. In support of this idea, *GAL4-usp* activation becomes detectable in almost all hub and CySC lineage cells upon co-expression of EcR (data not shown). This finding suggests that the low levels of endogenous EcR detected by immunostaining in the CySC lineage are insufficient to activate *GAL4-usp* in all cells. Similarly, expression of a constitutively active form of the EcR co-activator *taiman* (*tai*) yielded *GAL4-EcR* reporter activation in almost all hub and CySC lineage cells in the testis apex (data not shown). Taken together, our results indicate that EcR and USP can be activated specifically within hub cells and CySC lineage cells in the presence of their binding partners in both larval and adult testes, and that receptor complex activation in the adult testis is ligand-dependent.

20E is required for male germline and somatic stem cell maintenance

Since ecdysone signaling components are expressed and can be activated in the testis, we hypothesized that 20E plays a role in this tissue even though its endogenous titer is very low. To test this hypothesis, we asked whether 20E is required to maintain

adult male GSCs or CySCs. To reduce the effective concentration of 20E, we used the *GAL4-EcR* and *GAL4-usp* constructs described above, which have been widely used as dominant negative (DN) receptors when overexpressed for an extended period of time (Kozlova and Thummel 2002, Kozlova and Thummel 2003, Hackney, Pucci et al. 2007, Konig, Yatsenko et al. 2011). For example, both heat-shocked *Gal4-EcR* flies and flies expressing *UAS-EcR.B1-ΔC655.F645A*, a DN form of *EcR*, in border cells develop a similar thin eggshell phenotype (Hackney, Pucci et al. 2007). Testes from control flies, which carry the *GAL4-EcR* or *GAL4-usp* construct but are un-induced, appear normal (Figure 2.2B and S2.1A). After extended overexpression of either construct, however, testes lose most of their GSCs, early germline cells, and CySCs (Figure 2.2C, E and S2.1B), suggesting that signaling via 20E contributes to the maintenance of both stem cell populations in the testis. Because the endogenous titer of 20E in the adult testis is very low, we speculated that these constructs could act as DN receptors by binding with endogenous receptors and then competing with endogenous heterodimers for the limited amount of 20E, similar to a 20E "sponge" (Fig. 2.2A). To ask whether the loss of stem cells is due to reduced titers of 20E by *GAL4-EcR* or *GAL4-usp*, we repeated the above experiment but added 20E to the fly food to increase hormone levels. We expected that if 20E is no longer the limiting factor, endogenous *EcR* and *usp* should function normally; therefore, feeding 20E should rescue the phenotype caused by overexpression of *GAL4-EcR* or *GAL4-usp*. Consistent with our hypothesis, 20E feeding significantly rescued the GSC and CySC loss caused by extended overexpression of *GAL4-EcR* or *GAL4-usp* (Figure 2D ,E and S2.1C). We conclude that although 20E is present only at very low levels in the testis, it is required to maintain GSCs and CySCs.

ecd plays an ecdysone-independent role in GSC and CySC maintenance

As an alternate approach to reducing ecdysteroid levels in the testis, we used a temperature-sensitive allele of *ecdysoneless* (ecd^1). This steroid-deficient fly strain has long been used to study the effects of ecdysone signaling in *Drosophila*, but it has both ecdysone-dependent and independent functions (Garen, Kauvar et al. 1977, Gaziova, Bonnette et al. 2004, Ables and Drummond-Barbosa 2010, Claudius, Romani et al. 2014). Therefore, rescue of *ecd* phenotypes by 20E feeding is important to distinguish between these possibilities. After shifting adult ecd^1 flies to the non-permissive temperature for 7 days, we found that their testes contained significantly fewer GSCs than un-shifted control testes. We expected that we could rescue this GSC loss phenotype by feeding 20E to the flies. However, we found that the phenotype was not rescued by 20E feeding (Figure S2.2A-D), although the same feeding paradigm was sufficient to activate *GAL4-EcR* (Figure 2.1I and J). We conclude that *ecd*-dependent GSC loss is caused by an ecdysone-independent role of *ecd*. Moreover, mosaic analysis revealed that *ecd* is required cell-autonomously in the GSCs and CySCs for their maintenance (Figure S2.2E, Table S2.1). The inability of adjacent wild-type cells to compensate for loss of *ecd* function further indicates that ecdysteroid production is not the main role for *ecd* in the testis niche. We conclude that *ecd* is required to maintain GSCs and CySCs in the testis niche; however, since its requirement is independent of 20E, *ecd* is not a useful tool for studying the role of ecdysone signaling in this tissue.

EcR and *usp* are required in the CySC lineage to maintain GSCs and CySCs

Knowing that 20E is required to maintain stem cells in the testis, we next asked whether the ecdysone receptors *EcR* and *usp* are also required. Flies carrying a temperature sensitive allele of *EcR*, EcR^{A483T}, in trans with a null allele, EcR^{M554fs}, have normal numbers of GSCs and CySCs when raised at permissive temperature (Figure 2.3B). However, after 7 days at restrictive temperature, $EcR^{A483T/M554fs}$ (EcR^{ts}) flies have significantly fewer GSCs and CySCs than heterozygous control flies under the same conditions (Figure 2.3A-D). In addition, we found differentiating spermatogonial cells next to the hub in 23% of mutant testes at restrictive temperature (n = 31); this phenotype, which does not occur in wild-type testes (Figure 2.3C), is indicative of GSC depletion. The stem cell loss phenotype of EcR^{ts} testes shows that *EcR* promotes stem cell maintenance in the testis, but does not reveal which cells autonomously require *EcR,* since this mutant combination yields a global reduction in receptor activity. Since EcR and USP are undetectable in germ cells but are present in the CySC lineage, we hypothesized that these receptors are required autonomously within somatic stem cells for their maintenance. The genomic location of *usp* (on the X chromosome) and *EcR* (very close to the centromere) precludes mosaic analysis of these genes in the testis. However, RNAi-mediated knockdown is a feasible alternative. We used the CySC and early cyst-cell driver *c587-Gal4* in combination with a temperature-sensitive allele of the *Gal4* repressor *Gal80* to conditionally express transgenic RNAi or DN constructs of *EcR* or *usp* specifically in the adult testis. After 14 days of transgene induction at 29˚C, we observed a significant decrease in the number of CySCs in all four experimental genotypes (Figure 2.4A-E, S2.3 and S2.4). Although we could not detect EcR in the hub, we did detect USP there, so we also asked whether there is a requirement for each

receptor in hub cells. However, hub cells in testes containing RNAi-mediated knock down of *EcR* or *usp* in the hub were indistinguishable from those in control testes; in addition there was no significant effect on CySC numbers (Figure S2.4). These results indicate that *EcR* and *usp* are cell-autonomously required in the CySC lineage, but not in hub cells, for CySC maintenance. After *EcR* or *usp* knockdown in the CySC lineage, we also found that the number of GSCs decreased significantly (Figure 2.4E), which suggests that *EcR* and *usp* are required indirectly in the CySC lineage for GSC maintenance. GSCs could be lost simply as a consequence of CySC loss, but it is also possible that they rely on ecdysone-dependent maintenance signals from CySCs. We have never observed expression or activation of ecdysone signaling pathway components in GSCs, or significant GSC loss, when *EcR* or *usp* are knocked down by RNAi in the germline (data not shown). We conclude that *EcR* and *usp* are required autonomously in the CySC lineage, and non-autonomously for GSC maintenance.

We next asked whether expression of EcR only in the CySC lineage is sufficient to rescue the stem cell loss phenotype of EcR^{ts} testes and whether the requirement of *EcR* is isoform-specific. To answer this question, we expressed each isoform (*EcR-A*, *EcR-B1*, or *EcR-B2*) independently in the CySC lineage in the EcR^{ts} mutant background. Interestingly, we found that expression of *EcR-B2*, but not *EcR-A* or *EcR-B1*, in the CySC lineage is able to fully rescue the EcR^{ts} stem cell loss phenotype (Figure 2.4F-J). In contrast, expression of *EcR-A*, *EcR-B1*, or *EcR-B2* in hub cells did not rescue the EcR^{ts} phenotype (Figure S2.5). These results indicate that within the CySC lineage, *EcR* is necessary for stem cell maintenance in the testis, and its requirement is specific to the

EcR-B2 isoform, which can act as a strong ligand-dependent transcriptional activator (King-Jones and Thummel, 2005).

EcR is required for cell survival in the testis

Ecdysone signaling is known to regulate apoptosis during development, and in the ovary, developing germline cysts lacking ecdysone signaling die more often than control cysts (Ables and Drummond-Barbosa 2010, Zirin, Cheng et al. 2013). Therefore, we asked whether stem cell loss in EcR^{ts} testes at restrictive temperature could be caused by increased cell death. We used terminal deoxynucleotidyl transferase dUTP nick end labeling (TUNEL) to detect fragmented DNA in dying cells, and we counted the number of dying cells in testes from EcR^{ts} flies that remained at permissive temperature (control testes) or were shifted to restrictive temperature for 2 days. As expected, dying cells were rarely found within the stem cell zone (within 2 cell diameters of the hub) in control testes, but in testes at restrictive temperature we observed significantly more of them (Figure 2.5 A, B and D). These testes also had significantly more germ cell death in the differentiating cell zone than did control testes (Figure 2.5E). To confirm that the increase in cell death is due to dysfunction of *EcR*, we expressed the *EcR-B2* isoform in the CySC lineage in EcR^{ts} testes at restrictive temperature and found that it rescues the increased cell death phenotype (Figure 2.5C-E). Taken together, these results suggest that *EcR-B2* in the CySC lineage is necessary for promoting cell survival in the testis stem cell niche. However, it is possible that GSCs and CySCs are also lost due to early differentiation of stem cells.

The 20E targets *E75* and *ftz-f1*, but not *br,* promote stem cell maintenance in the testis

Ecdysone signaling is mediated by multiple target genes which vary by tissue type and developmental stage (Andres and Thummel 1992). To identify potential 20E target genes in the adult testis niche, we surveyed testis RNA-seq data for the expression of known ecdysone-responsive genes (RPKM>1 in wild type testes) (Gan, Chepelev et al. 2010), espeically those with known requirements in other adult stem cell-based tissues, including the ovary and intestine (Ables and Drummond-Barbosa 2010, Gan, Chepelev et al. 2010, Morris and Spradling 2012, Zeng and Hou 2012). Using these criteria, we found three candidate ecdysone targets, *E75*, *ftz-f1* and *br*, and tested the requirement for each gene in CySC maintenance using RNAi-mediated knockdown in the CySC lineage. We found that *E75* or *ftz-f1* knockdown causes a loss of GSCs and CySCs that is similar to the phenotype resulting from knockdown of *EcR* or *usp* (Figure 2.6C-E). In contrast, knockdown of *br* in the CySC lineage shows no effect on stem cell maintenance even though we observed significant reduction of Br protein level in the cyst stem cell lineage, confirming the efficacy of *br* knockdown (Figure 2.6A, B and E). Mosaic analysis of *E75* and *ftz-f1* confirmed that these two factors are cell autonomously required for CySC maintenance (Figure 2.6F-J, Table 2.1 and 2.2). We conclude that the 20E target genes *E75* and *ftz-f1,* but not *br,* are required for CySC maintenance.

***EcR* genetically interacts with *Nurf301* to maintain stem cells in the testis**

In the *Drosophila* ovary, *EcR* interacts genetically with *Nurf301*, which encodes a component of the NURF chromatin remodeling complex, to promote GSC maintenance (Ables and Drummond-Barbosa, 2010). Since we had previously found that NURF is also autonomously required to promote the maintenance of male GSCs and CySCs (Cherry and Matunis 2010), we wondered if *EcR* and *Nurf301* function together in the testis. To test this hypothesis, we asked whether reduced *Nurf301* expression levels could enhance the stem cell loss phenotype of EcR knockdown. We accomplished this by knocking down *EcR* expression specifically in the CySC lineage in a *Nurf301* heterozygous background. *Nurf301* heterozygous mutant testes are indistinguishable from wild-type testes and have normal numbers of GSCs and CySCs (Cherry and Matunis 2010). In contrast, reducing *EcR* expression in *Nurf301* heterozygous CySCs causes a significant reduction in the number of GSCs and CySCs (Figure 2.7). This result suggests that the ecdysone signaling pathway functions together with the NURF chromatin-remodeling complex to promote stem cell maintenance in both the ovary and the testis.

Discussion

Our work shows that the steroid hormone 20E plays an important role in maintaining stem cells in the *Drosophila* testis: 20E, receptors of ecdysone signaling, and downstream targets are required directly in CySCs for their maintenance. When ecdysone signaling is lost in CySCs, GSCs are also lost, but it is unclear if their maintenance requires an ecdysone-dependent or independent signal from the CySCs. We also show that the requirement for EcR in the testis is isoform-specific: expression of *EcR-B2* in the CySC lineage is sufficient to rescue loss of GSCs and CySCs and increased cell death in *EcR* mutant testes, suggesting that there might be a temporal and spatial control of ecdysone signaling in the adult testis. In addition, we provide evidence that ecdysone signaling, as in the ovary, is able to interact with an intrinsic chromatin-remodeling factor, *Nurf301*, to promote stem cell maintenance. Therefore, our studies have revealed a novel role for ecdysone signaling in *Drosophila* male reproduction.

Hormone signaling in the ovary and testis

Although ecdysone signaling is required in both ovaries and testes for stem cell maintenance, the responses in each tissue are likely to be sex-specific. In the ovary, 20E controls GSCs directly, by modulating their proliferation and self-renewal, and it acts predominantly through the downstream target gene *E74* (Ables and Drummond-Barbosa 2010). In contrast, male GSCs require ecdysone signaling only indirectly: we found that ecdysone signaling is required in the CySC lineage to maintain both CySCs and GSCs. In a previous study, RNAi-mediated knockdown of *EcR*, *usp* or *E75* in the CySC lineage did not result in a significant loss of GSCs (Morris and Spradling, 2012); however, the

number of CySCs was not determined, and the phenotype was examined after 4 or 8 days, not 14 days as in our study. We suspect that the earlier time points used in that study may not have allowed enough time for a significant number of GSCs to be lost.

Spatial and temporal regulation of ecdysone signaling

During development, 20E is produced in the prothoracic gland (PG) and further metabolized to 20E in target tissues, but the PG does not persist into adulthood (Gilbert, Rybczynski et al. 2002, Huang, Warren et al. 2008). In adult female *Drosophila*, the ovary is a source of 20E (Schwartz, Kelly et al. 1985). In contrast, the identification of steroidogenic tissues in adult male *Drosophila* remains the subject of active investigation. The level of 20E in adult males is significantly lower than in adult females, but it can be detected in the testis (Hodgetts, Sage et al. 1977, Handler 1982, Bownes, Dubendorfer et al. 1984, Schwedes and Carney 2012). Furthermore, RNA-seq data show that *shade*, which encodes the enzyme that metabolizes the prohomone ecdysone to 20E, is expressed in the adult testis, suggesting that the adult testis may produce 20E (Petryk, Warren et al. 2003, Gan, Chepelev et al. 2010). However, the sources of 20E production in adult *Drosophila* males remain to be determined experimentally.

20E, like other systemic hormones, can have tissue-specific effects or differential effects on the same cell type as development proceeds. These differences are mediated at least in part by the particular downstream target genes that are activated in each case. For example, in female 3rd instar larval ovaries, ecdysone signaling upregulates *br* expression to induce niche formation and PGC differentiation(Gancz, Lengil et al. 2011), but *br* is not required for GSC maintenance in the adult ovary; instead, *E74* plays this role (Ables

and Drummond-Barbosa 2010). Similarly, *br* is required for the establishment of intestinal stem cells (ISCs) in the larval and pupal stages but not for ISC function in adults (Zeng and Hou 2012). Here, we show that ecdysone signaling in the adult testis is mediated by different target genes than in the ovary: *E74*, but not *E75* or *br*, regulate stem cell function in the ovary, whereas *E75* and *ftz-f1* are important for stem cell maintenance in the testis. Since E75 is itself a nuclear hormone receptor that responds to the second messenger nitric oxide (Reinking, Lam et al. 2005, Caceres, Necakov et al. 2011), it will be interesting to know whether E75's partner DHR3 also plays a role in CySCs. An intriguing question for future studies will be how different ecdysone target genes interact with the various signaling pathways that maintain stem cells in the ovary or testis.

Environmental changes, stem cells and hormonal signals

Since 20E levels can actively respond to physiological changes induced by environmental cues, it is possible that the effect of 20E on testis stem cell maintenance might reflect changes in diet, stress, or other environmental cues. For example, in *Aedes aegypti*, ecdysteroid production in the ovary is stimulated by blood feeding and this is an insulin-dependent process (Riehle and Brown 1999). In *Drosophila*, ecdysone signaling is known to interact with the insulin pathway in a complex way. Ovaries from females with hypomorphic mutations in the insulin-like receptor have reduced levels of 20E (Tu, Yin et al. 2002). Furthermore, ecdysone signaling can directly inhibit insulin signaling and control larval growth in the fat body (Colombani, Bianchini et al. 2005). Thus, ecdysone signaling may interact with insulin signaling during testis stem cell

maintenance. Previously, it was shown that GSCs in the ovary and testis can respond to diet through insulin signaling, which is required to promote stem cell maintenance in both sexes (Drummond-Barbosa and Spradling 2001, Flatt, Min et al. 2008, Hsu and Drummond-Barbosa 2009, Ueishi, Shimizu et al. 2009, McLeod, Wang et al. 2010, Wang, McLeod et al. 2011, Roth, Chiang et al. 2012). It is possible that diet can affect 20E levels and thus regulate stem cell maintenance. In addition to diet, stress can also affect 20E levels, as is the case in *Drosophila virilis*, where 20E levels increase significantly under high temperature stress (Rauschenbach, Sukhanova et al. 2000). A similar effect has been found in mammals, where the steroid hormone cortisol is released in response to psychological stressors (McGaugh 2004, Burke, Davis et al. 2005). Finally, 20E levels are also influenced by mating. In *Anopheles gambiae*, males transfer 20E to blood-fed females during copulation, which is important for egg production (Baldini, Gabrieli et al. 2013). In female *Drosophila*, whole body ecdysteroid levels also increase after mating (Harshman, Loeb et al. 1999). Studying the roles of hormonal signaling in mediating stem cell responses to stress and other environmental cues will be an exciting topic for future studies. From our work it is now clear that, as in mammals, steroid signaling plays critical roles in adult stem cell function during both male and female gametogenesis.

Experimental Procedures

Fly stocks and cultures

Fly stocks were raised at 25˚C on standard molasses/yeast medium unless otherwise indicated. The following fly stocks were used: *c587-Gal4* (Kai and Spradling 2003), *E132-Gal4* (from H. Sun), *w;; Nurf301*^{2}*/TM6B, Tb* and *w;; Nurf301*^{3}*/TM3, Ser* (from P. Badenhorst), *ftz-f1*^{ex7} *FRT2A* (from C. Dauphin-Villemant), *E75*$^{\Delta 51}$ *FRT80B* and *EcR*^{A483T}*/SM6b (*from D. Drummond-Barbosa*), and ecd*^{2} *FRT2A* (from M. Jindra). Other fly stocks came from the Bloomington Drosophila Stock Center (BDSC) or Vienna Drosophila RNAi Center (VDRC).

Immunofluorescence microscopy

Testes were dissected, fixed, and stained as described previously (Matunis 1997). The following antibodies were used: rabbit anti-Vasa (d-260) and goat anti-Vasa (dN-13) (Santa Cruz Biotechnology, 1:400); chicken anti-Vasa (from K. Howard, 1:5000); rabbit anti-GFP (Torrey Pines Biolabs, 1:10,000); chicken anti-GFP (Abcam, 1:10,000); mouse anti-β-Galactosidase (Promega, 1:1000); mouse 1B1 (1:25), mouse anti-Armadillo (N2 7A1; 1:50), mouse anti-EcR (DDA2.7; 1:50), mouse anti-EcR (Ag10.2; 1:50), and mouse anti-Broad-core (25E9.D7; 1:50) (Developmental Studies Hybridoma Bank at the University of Iowa); rabbit anti-ZFH1 (from R. Lehmann, 1:5000); guinea pig anti-ZFH1 (from J. Skeath; 1:1000); guinea pig anti-Tj (from D. Godt, 1:4000); and mouse anti-USP (from D. Montell, 1:20)(Christianson, King et al. 1992). Alexa fluor-conjugated secondary IgG (H+L) antibodies were diluted at 1:200 for 568 and 633 conjugates and 1:400 for 488 conjugates. Secondary antisera were: goat anti-rat 488, goat anti-rabbit 488 and 568, goat anti-mouse 488, 568 and 633, goat anti-chicken 488 and 568, and goat anti

guinea-pig 568 and 633 (Molecular Probes/Invitrogen). DNA was stained with 4,6-diamidino-2-phenylindole (DAPI; Sigma) at 1 ug/ml. Fixed testes were mounted in Vectashield (Vector Labs) for imaging.

Analysis of confocal images

Confocal images were obtained with a Zeiss LSM 5 Pascal or a Zeiss LSM 510 Meta microscope and were collected as serial confocal sections at similar detection settings unless otherwise noted. Images were analyzed using the Zeiss LSM Image Browser software or Zen 2009 Light edition software. GSCs were scored as Vasa-positive cells (with a spherical fusome) making contact with the hub. CySCs were scored as Zfh1-positive cells (Leatherman and Dinardo 2008), with medium to strong staining according to the rainbow indicator in the Zeiss Pascal software. All graphs were created using Prism 5 (GraphPad Software, Inc.). Statistical analysis of stem cell number was performed using Prism 5. Student's T-test was used to compare two populations, and unpaired ANOVA analysis was used to compare three or more populations.

20E feeding experiment

20E (Sigma-Aldrich) was dissolved in 10% ethanol to prepare a 25 mM stock solution. To visualize reporter activity: Adult males with the genotype *hs-EcR-LBD-GAL4; UAS-stinger* (or *UAS-lacZ*) or *hs-usp-LBD-GAL4; UAS-stinger* (or *UAS-lacZ*) were heat shocked 3 x 30 minutes at 37˚C and then placed in vials containing normal food covered with a piece of filter paper soaked with 100-150 ul of 1mM 20E (diluted in apple juice) plus green food coloring (McCormick, 1:50). A small hole was cut out of the filter paper

to give the flies access to the normal food below. After 1 day, flies with green guts (indicating that they had ingested the 20E) were dissected and stained with GFP or lacZ antibody.

To use reporters as dominant negative constructs: Adult males with the genotype *hs-EcR-LBD-GAL4; UAS-stinger*, or *hs-usp-LBD-GAL4; UAS-stinger,* or *hs-ECR-LBD-Gal4,* or *hs-usp-LBD-Gal4* were heat shocked twice every day for 30 minutes each time (once in the early morning and once at night) for 4-5 days. For 20E rescue experiments, flies were placed in vials containing 20E (as described above) after each heat shock and dissected one day after the last heat shock. Flies were fed an equivalent concentration of ethanol dissolved in apple juice as a control.

Loss-of-function experiments

To assay the effect of loss of *ecd* on stem cell maintenance, 0-5 day old ecd^{1} males raised at 18˚C were shifted to the non-permissive temperature (29˚C) for 7 days, and then testes were dissected and analyzed. *y w* males were processed in parallel as controls. To assay whether 20E feeding can rescue the ecd^{1} testis phenotype, we fed flies with 0.1 mM or 1 mM 20E using the method described for the 20E feeding experiment. Flies were fed an equivalent concentration of ethanol dissolved in apple juice as a control.

To assay the effect of loss of *EcR* on stem cell maintenance in adult testes, EcR^{M554fs}*/SM6b* (null allele) and EcR^{A483T}*/SM6b* (temperature sensitive allele) flies were crossed at the permissive temperature (18˚C) and shifted to the non-permissive temperature (31˚C) for 7 days, and testes were then dissected and analyzed. Heterozygous sibling males were processed in parallel as controls.

Temperature sensitive EcR rescue experiment

UAS-EcR.A, UAS-EcR.B1, and *UAS-EcR.B2* constructs were driven by *c587-Gal4* (cyst lineage) or *hh-Gal4* (BDSC 45546; hub cells) in the temperature-sensitive *EcR* mutant background *(EcR^{M554fs}/ EcR^{A483T})*. *UAS-GFP-nls* was used as a control. Flies were grown at 18˚C and transferred to 31˚C as adults to induce expression of the UAS constructs.

RNAi and dominant negative (DN) knockdown experiments

The following RNAi or DN constructs were used for cell type-specific knockdown of ecdysone pathway components:

Gene	Genotype	Stock number
EcR	*UAS-EcR-RNAi*	VDRC 37058
	UAS-EcR-RNAi	BDSC 9726
	UAS-EcR.B1-ΔC655.F645A	BDSC 6869
	UAS-EcR.B1-ΔC655.W650A	BDSC 6872
	UAS-EcR.A.F645A	BDSC 9450
	UAS-EcR.A.W650A	BDSC 9451
	UAS-EcR.B2.F645A	BDSC 9450
USP	*UAS-USP-RNAi*	VDRC 16893
	UAS-USP-RNAi	BDSC 27258
E75	*UAS-E75-RNAi*	VDRC *44851*
ftz-f1	*UAS-ftz-f1-RNAi*	VDRC *108995*
	UAS-ftz-f1-RNAi	BDSC *27659*
br	*UAS-br-RNAi*	BDSC *27272*

Male flies carrying these constructs were crossed to females with the genotype *c587-Gal4; tubGAL80^{ts}* (cyst lineage) *or E132-Gal; tubGAL80^{ts}* (hub cells) *at* 18˚C. Males were shifted to 29˚C upon eclosion and dissected after 1-5 days. *UAS-GFP RNAi* (BDSC 9330) was used as a control for RNAi experiments and *UAS-GFP* (BDSC 4776) as a control for DN experiments. Flies carrying UAS constructs alone, without a driver, were processed in parallel to check for leakiness of each UAS construct. To look for genetic interaction between ecdysone signaling and NURF, we expressed *UAS-EcR-RNAi* (BDSC 37058) in the CySC lineage in a *Nurf301^{3}* or *Nurf301^{2}* heterozygous background. *UAS-GFP-RNAi* was used as a control for this experiment.

Mosaic analysis

Negatively marked clones were induced using the FLP, FRT-mediated mitotic recombination technique (Xu and Rubin 1993) in flies of the genotype: *y w, P[hs-FLP]/Y; P[Ubi-GFP.nls] P[w^{+} FRT]2A /ftz-f1^{ex7} P[w^{+} FRT]2A* or *y w, P[hs-FLP]/Y; P[Ubi-GFP.nls] P[w^{+} FRT]2A /ecd^{2} P[w^{+} FRT]2A* or *y w, P[hs-FLP]/Y; P[Ubi-GFP] P[neoFRT]80B/E75$^{\Delta 51}$ P[neoFRT]80B ry^{506}*. Control clones were induced in *y w, P[hs-FLP]/Y; P[Ubi-GFP.nls] P[w^{+} FRT]2A/P[w^{+} FRT]2A* or *P[hs-FLP]/Y; P[Ubi-GFP] P[neoFRT]80B/P[neoFRT]80B ry^{506}*. GSC clones were identified as cells that were Zfh1-negative, GFP-negative, and making broad contact with the hub. CySC clones were identified as cells that were Zfh1-positive, GFP-negative, and within 2 cell diameters of the hub.

Positively marked clones were induced using the mosaic analysis with a repressible cell

marker (MARCM) technique (Lee and Luo 1999) in flies of the genotype *y w, P[hs-FLP], P[tub-Gal4] P[UAS-CD8-GFP]; P[tub-Gal80] P[w+ FRT]2A/ftz-f1^{ex7} P[w+ FRT]2A*. Control clones were induced in *y w, P[hs-FLP], P[tub-Gal4] P[UAS-CD8-GFP]; P[tub-Gal80] P[w$^+$ FRT]2A/P[w$^+$ FRT]2A* (Wang and Struhl 2004) (a gift from G. Struhl). CySC clones were identified as cells that were Zfh-1 positive, GFP-positive, and within 2 cell diameters of the hub.

To induce clones, 0-5 day old males were heat shocked for 3 x 30 minutes at 37˚C separated by 30-minute intervals at 25˚C. Flies were kept at 25˚C for 2, 4, 8, or 10 days after clone induction before dissection.

Apoptosis detection

Cells undergoing apoptosis were detected by terminal deoxynucleotidyl transferase dUTP nick end labeling (TUNEL; Chemicon International) as described (Sheng, Brawley et al. 2009). TUNEL-positive stem cells and early daughters were identified by the position of their nuclei (within two cell diameters of the hub). TUNEL-positive spermatogonia were identified as spots with a diameter greater than 5 μm and located more than two cell diameters from the hub.

Author Contributions

Y.L., Q.M., C.C. and E.M. designed the experiments; Y.L., Q.M., and C.C. performed the experiments; Y.L. and Q.M. analyzed the data; Y.L. and E.M wrote the manuscript.

References

Ables, E. T. and D. Drummond-Barbosa (2010). "The steroid hormone ecdysone functions with intrinsic chromatin remodeling factors to control female germline stem cells in Drosophila." Cell Stem Cell **7**(5): 581-592.

Andres, A. J. and C. S. Thummel (1992). "Hormones, puffs and flies: the molecular control of metamorphosis by ecdysone." Trends Genet **8**(4): 132-138.

Badenhorst, P., H. Xiao, L. Cherbas, S. Y. Kwon, M. Voas, I. Rebay, P. Cherbas and C. Wu (2005). "The Drosophila nucleosome remodeling factor NURF is required for Ecdysteroid signaling and metamorphosis." Genes Dev **19**(21): 2540-2545.

Baehrecke, E. H. (1996). "Ecdysone signaling cascade and regulation of Drosophila metamorphosis." Arch Insect Biochem Physiol **33**(3-4): 231-244.

Baker, K. D., L. M. Shewchuk, T. Kozlova, M. Makishima, A. Hassell, B. Wisely, J. A. Caravella, M. H. Lambert, J. L. Reinking, H. Krause, C. S. Thummel, T. M. Willson and D. J. Mangelsdorf (2003). "The Drosophila orphan nuclear receptor DHR38 mediates an atypical ecdysteroid signaling pathway." Cell **113**(6): 731-742.

Baldini, F., P. Gabrieli, A. South, C. Valim, F. Mancini and F. Catteruccia (2013). "The Interaction between a Sexually Transferred Steroid Hormone and a Female Protein Regulates Oogenesis in the Malaria Mosquito Anopheles gambiae." Plos Biology **11**(10).

Bownes, M., A. Dubendorfer and T. Smith (1984). "Ecdysteroids in Adult Males and Females of Drosophila-Melanogaster." Journal of Insect Physiology **30**(10): 823-830.

Bryant, Z., L. Subrahmanyan, M. Tworoger, L. LaTray, C. R. Liu, M. J. Li, G. van den Engh and H. Ruohola-Baker (1999). "Characterization of differentially expressed genes

in purified Drosophila follicle cells: toward a general strategy for cell type-specific developmental analysis." Proc Natl Acad Sci U S A **96**(10): 5559-5564.

Burke, H. M., M. C. Davis, C. Otte and D. C. Mohr (2005). "Depression and cortisol responses to psychological stress: A meta-analysis." Psychoneuroendocrinology **30**(9): 846-856.

Buszczak, M., M. R. Freeman, J. R. Carlson, M. Bender, L. Cooley and W. A. Segraves (1999). "Ecdysone response genes govern egg chamber development during mid-oogenesis in Drosophila." Development **126**(20): 4581-4589.

Caceres, L., A. S. Necakov, C. Schwartz, S. Kimber, I. J. Roberts and H. M. Krause (2011). "Nitric oxide coordinates metabolism, growth, and development via the nuclear receptor E75." Genes Dev **25**(14): 1476-1485.

Carbonell, A., A. Mazo, F. Serras and M. Corominas (2013). "Ash2 acts as an ecdysone receptor coactivator by stabilizing the histone methyltransferase Trr." Molecular Biology of the Cell **24**(3): 361-372.

Carney, G. E. and M. Bender (2000). "The Drosophila ecdysone receptor (EcR) gene is required maternally for normal oogenesis." Genetics **154**(3): 1203-1211.

Cherry, C. M. and E. L. Matunis (2010). "Epigenetic regulation of stem cell maintenance in the Drosophila testis via the nucleosome-remodeling factor NURF." Cell Stem Cell **6**(6): 557-567.

Christianson, A. M., D. L. King, E. Hatzivassiliou, J. E. Casas, P. L. Hallenbeck, V. M. Nikodem, S. A. Mitsialis and F. C. Kafatos (1992). "DNA binding and heteromerization of the Drosophila transcription factor chorion factor 1/ultraspiracle." Proc Natl Acad Sci U S A **89**(23): 11503-11507.

Claudius, A. K., P. Romani, T. Lamkemeyer, M. Jindra and M. Uhlirova (2014). "Unexpected role of the steroid-deficiency protein ecdysoneless in pre-mRNA splicing." PLoS Genet **10**(4): e1004287.

Colombani, J., L. Bianchini, S. Layalle, E. Pondeville, C. Dauphin-Villemant, C. Antoniewski, C. Carre, S. Noselli and P. Leopold (2005). "Antagonistic actions of ecdysone and insulins determine final size in Drosophila." Science **310**(5748): 667-670.

de Cuevas, M. and E. L. Matunis (2011). "The stem cell niche: lessons from the Drosophila testis." Development **138**(14): 2861-2869.

Drummond-Barbosa, D. (2008). "Stem cells, their niches and the systemic environment: an aging network." Genetics **180**(4): 1787-1797.

Drummond-Barbosa, D. and A. C. Spradling (2001). "Stem cells and their progeny respond to nutritional changes during Drosophila oogenesis." Dev Biol **231**(1): 265-278.

Flatt, T., K. J. Min, C. D'Alterio, E. Villa-Cuesta, J. Cumbers, R. Lehmann, D. L. Jones and M. Tatar (2008). "Drosophila, germ-line modulation of insulin signaling and lifespan." Proceedings of the National Academy of Sciences of the United States of America **105**(17): 6368-6373.

Francis, V. A., A. Zorzano and A. A. Teleman (2010). "dDOR Is an EcR Coactivator that Forms a Feed-Forward Loop Connecting Insulin and Ecdysone Signaling." Current Biology **20**(20): 1799-1808.

Gan, Q., I. Chepelev, G. Wei, L. Tarayrah, K. Cui, K. Zhao and X. Chen (2010). "Dynamic regulation of alternative splicing and chromatin structure in Drosophila gonads revealed by RNA-seq." Cell Res **20**(7): 763-783.

Gancz, D. and L. Gilboa (2013). "Hormonal control of stem cell systems." Annu Rev Cell Dev Biol **29**: 137-162.

Gancz, D., T. Lengil and L. Gilboa (2011). "Coordinated Regulation of Niche and Stem Cell Precursors by Hormonal Signaling." Plos Biology **9**(11).

Garen, A., L. Kauvar and J. A. Lepesant (1977). "Roles of ecdysone in Drosophila development." Proc Natl Acad Sci U S A **74**(11): 5099-5103.

Gaziova, I., P. C. Bonnette, V. C. Henrich and M. Jindra (2004). "Cell-autonomous roles of the ecdysoneless gene in Drosophila development and oogenesis." Development **131**(11): 2715-2725.

Gilbert, L. I., R. Rybczynski and J. T. Warren (2002). "Control and biochemical nature of the ecdysteroidogenic pathway." Annual Review of Entomology **47**: 883-916.

Hackney, J. F., C. Pucci, E. Naes and L. Dobens (2007). "Ras signaling modulates activity of the ecdysone receptor EcR during cell migration in the Drosophila ovary." Dev Dyn **236**(5): 1213-1226.

Handler, A. M. (1982). "Ecdysteroid titers during pupal and adult development in Drosophila melanogaster." Dev Biol **93**(1): 73-82.

Hardy, R. W., K. T. Tokuyasu, D. L. Lindsley and M. Garavito (1979). "The germinal proliferation center in the testis of Drosophila melanogaster." J Ultrastruct Res **69**(2): 180-190.

Harshman, L. G., A. M. Loeb and B. A. Johnson (1999). "Ecdysteroid titers in mated and unmated Drosophila melanogaster females." J Insect Physiol **45**(6): 571-577.

Hayward, D. C., M. J. Bastiani, J. W. Trueman, J. W. Truman, L. M. Riddiford and E. E. Ball (1999). "The sequence of Locusta RXR, homologous to Drosophila Ultraspiracle, and its evolutionary implications." Dev Genes Evol **209**(9): 564-571.

Hodgetts, R. B., B. Sage and J. D. O'Connor (1977). "Ecdysone titers during postembryonic development of Drosophila melanogaster." Dev Biol **60**(1): 310-317.

Hsu, H. J. and D. Drummond-Barbosa (2009). "Insulin levels control female germline stem cell maintenance via the niche in Drosophila." Proc Natl Acad Sci U S A **106**(4): 1117-1121.

Hsu, H. J., L. LaFever and D. Drummond-Barbosa (2008). "Diet controls normal and tumorous germline stem cells via insulin-dependent and -independent mechanisms in Drosophila." Dev Biol **313**(2): 700-712.

Huang, X., J. T. Warren and L. I. Gilbert (2008). "New players in the regulation of ecdysone biosynthesis." Journal of Genetics and Genomics **35**(1): 1-10.

Ishimoto, H. and T. Kitamoto (2010). "The steroid molting hormone Ecdysone regulates sleep in adult Drosophila melanogaster." Genetics **185**(1): 269-281.

Ishimoto, H., T. Sakai and T. Kitamoto (2009). "Ecdysone signaling regulates the formation of long-term courtship memory in adult Drosophila melanogaster." Proc Natl Acad Sci U S A **106**(15): 6381-6386.

Ito, K., A. Hirao, F. Arai, S. Matsuoka, K. Takubo, I. Hamaguchi, K. Nomiyama, K. Hosokawa, K. Sakurada, N. Nakagata, Y. Ikeda, T. W. Mak and T. Suda (2004). "Regulation of oxidative stress by ATM is required for self-renewal of haematopoietic stem cells." Nature **431**(7011): 997-1002.

Jang, A. C., Y. C. Chang, J. Bai and D. Montell (2009). "Border-cell migration requires integration of spatial and temporal signals by the BTB protein Abrupt." Nat Cell Biol **11**(5): 569-579.

Jones, G., M. Wozniak, Y. Chu, S. Dhar and D. Jones (2001). "Juvenile hormone III-dependent conformational changes of the nuclear receptor ultraspiracle." Insect Biochem Mol Biol **32**(1): 33-49.

Kai, T. and A. Spradling (2003). "An empty Drosophila stem cell niche reactivates the proliferation of ectopic cells." Proc Natl Acad Sci U S A **100**(8): 4633-4638.

King-Jones, K. and C. S. Thummel (2005). "Nuclear receptors--a perspective from Drosophila." Nat Rev Genet **6**(4): 311-323.

Konig, A., A. S. Yatsenko, M. Weiss and H. R. Shcherbata (2011). "Ecdysteroids affect Drosophila ovarian stem cell niche formation and early germline differentiation." EMBO J **30**(8): 1549-1562.

Kozlova, T. and C. S. Thummel (2000). "Steroid regulation of postembryonic development and reproduction in Drosophila." Trends Endocrinol Metab **11**(7): 276-280.

Kozlova, T. and C. S. Thummel (2002). "Spatial patterns of ecdysteroid receptor activation during the onset of Drosophila metamorphosis." Development **129**(7): 1739-1750.

Kozlova, T. and C. S. Thummel (2003). "Essential roles for ecdysone signaling during Drosophila mid-embryonic development." Science **301**(5641): 1911-1914.

Leatherman, J. L. and S. Dinardo (2008). "Zfh-1 controls somatic stem cell self-renewal in the Drosophila testis and nonautonomously influences germline stem cell self-renewal." Cell Stem Cell **3**(1): 44-54.

Lee, T. and L. Luo (1999). "Mosaic analysis with a repressible cell marker for studies of gene function in neuronal morphogenesis." Neuron **22**(3): 451-461.

Li, L. H. and T. Xie (2005). "Stem cell niche: Structure and function." Annual Review of Cell and Developmental Biology **21**: 605-631.

Matunis, E. (1997). "punt and schnurri regulate a somatically derived signal that restricts proliferation of committed progenitors in the germline." Development **124**: 4383-4391.

McGaugh, J. L. (2004). "The amygdala modulates the consolidation of memories of emotionally arousing experiences." Annu Rev Neurosci **27**: 1-28.

McLeod, C. J., L. Wang, C. Wong and D. L. Jones (2010). "Stem cell dynamics in response to nutrient availability." Curr Biol **20**(23): 2100-2105.

Morris, L. X. and A. C. Spradling (2012). "Steroid signaling within Drosophila ovarian epithelial cells sex-specifically modulates early germ cell development and meiotic entry." PLoS One **7**(10): e46109.

Palanker, L., A. S. Necakov, H. M. Sampson, R. Ni, C. Hu, C. S. Thummel and H. M. Krause (2006). "Dynamic regulation of Drosophila nuclear receptor activity in vivo." Development **133**(18): 3549-3562.

Parisi, M. J., V. Gupta, D. Sturgill, J. T. Warren, J. M. Jallon, J. H. Malone, Y. Zhang, L. I. Gilbert and B. Oliver (2010). "Germline-dependent gene expression in distant non-gonadal somatic tissues of Drosophila." Bmc Genomics **11**.

Perera, S. C., S. Zheng, Q. L. Feng, P. J. Krell, A. Retnakaran and S. R. Palli (2005). "Heterodimerization of ecdysone receptor and ultraspiracle on symmetric and asymmetric response elements." Arch Insect Biochem Physiol **60**(2): 55-70.

Petryk, A., J. T. Warren, G. Marques, M. P. Jarcho, L. I. Gilbert, J. Kahler, J. P. Parvy, Y. T. Li, C. Dauphin-Villemant and M. B. O'Connor (2003). "Shade is the Drosophila P450 enzyme that mediates the hydroxylation of ecdysone to the steroid insect molting hormone 20-hydroxyecdysone." Proceedings of the National Academy of Sciences of the United States of America **100**(24): 13773-13778.

Rauschenbach, I. Y., M. Z. Sukhanova, A. Hirashima, E. Sutsugu and E. Kuano (2000). "Role of the ecdysteroid system in the regulation of Drosophila reproduction under environmental stress." Dokl Biol Sci **375**: 641-643.

Reinking, J., M. M. Lam, K. Pardee, H. M. Sampson, S. Liu, P. Yang, S. Williams, W. White, G. Lajoie, A. Edwards and H. M. Krause (2005). "The Drosophila nuclear receptor e75 contains heme and is gas responsive." Cell **122**(2): 195-207.

Riehle, M. A. and M. R. Brown (1999). "Insulin stimulates ecdysteroid production through a conserved signaling cascade in the mosquito Aedes aegypti." Insect Biochem Mol Biol **29**(10): 855-860.

Roth, T. M., C. Y. A. Chiang, M. Inaba, H. B. Yuan, V. Salzmann, C. E. Roth and Y. M. Yamashita (2012). "Centrosome misorientation mediates slowing of the cell cycle under limited nutrient conditions in Drosophila male germline stem cells." Molecular Biology of the Cell **23**(8): 1524-1532.

Schwartz, M. B., T. J. Kelly, R. B. Imberski and E. C. Rubenstein (1985). "The Effects of Nutrition and Methoprene Treatment on Ovarian Ecdysteroid Synthesis in Drosophila-Melanogaster." Journal of Insect Physiology **31**(12): 947-&.

Schwedes, C. C. and G. E. Carney (2012). "Ecdysone signaling in adult Drosophila melanogaster." J Insect Physiol **58**(3): 293-302.

Sheng, X. R., C. M. Brawley and E. L. Matunis (2009). "Dedifferentiating spermatogonia outcompete somatic stem cells for niche occupancy in the Drosophila testis." Cell Stem Cell **5**(2): 191-203.

Spradling, A., M. T. Fuller, R. E. Braun and S. Yoshida (2011). "Germline stem cells." Cold Spring Harb Perspect Biol **3**(11): a002642.

Talbot, W. S., E. A. Swyryd and D. S. Hogness (1993). "Drosophila tissues with different metamorphic responses to ecdysone express different ecdysone receptor isoforms." Cell **73**(7): 1323-1337.

Tang, F., C. Barbacioru, S. Bao, C. Lee, E. Nordman, X. Wang, K. Lao and M. A. Surani (2010). "Tracing the derivation of embryonic stem cells from the inner cell mass by single-cell RNA-Seq analysis." Cell Stem Cell **6**(5): 468-478.

Tricoire, H., V. Battisti, S. Trannoy, C. Lasbleiz, A. M. Pret and V. Monnier (2009). "The steroid hormone receptor EcR finely modulates Drosophila lifespan during adulthood in a sex-specific manner." Mech Ageing Dev **130**(8): 547-552.

Tsai, C. C., H. Y. Kao, T. P. Yao, M. McKeown and R. M. Evans (1999). "SMRTER, a Drosophila nuclear receptor coregulator, reveals that EcR-mediated repression is critical for development." Molecular Cell **4**(2): 175-186.

Tu, M. P., C. M. Yin and M. Tatar (2002). "Impaired ovarian ecdysone synthesis of Drosophila melanogaster insulin receptor mutants." Aging Cell **1**(2): 158-160.

Ueishi, S., H. Shimizu and H. I. Y (2009). "Male germline stem cell division and spermatocyte growth require insulin signaling in Drosophila." Cell Struct Funct **34**(1): 61-69.

Wang, L., C. J. McLeod and D. L. Jones (2011). "Regulation of adult stem cell behavior by nutrient signaling." Cell Cycle **10**(16): 2628-2634.

Wang, W. and G. Struhl (2004). "Drosophila Epsin mediates a select endocytic pathway that DSL ligands must enter to activate Notch." Development **131**(21): 5367-5380.

Xu, T. and G. M. Rubin (1993). "Analysis of genetic mosaics in developing and adult Drosophila tissues." Development **117**(4): 1223-1237.

Yamanaka, N., K. F. Rewitz and M. B. O'Connor (2013). "Ecdysone control of developmental transitions: lessons from Drosophila research." Annu Rev Entomol **58**: 497-516.

Zeng, X. K. and S. X. Hou (2012). "Broad relays hormone signals to regulate stem cell differentiation in Drosophila midgut during metamorphosis." Development **139**(21): 3917-3925.

Zirin, J., D. J. Cheng, N. Dhanyasi, J. Cho, J. M. Dura, K. VijayRaghavan and N. Perrimon (2013). "Ecdysone signaling at metamorphosis triggers apoptosis of Drosophila abdominal muscles." Developmental Biology **383**(2): 275-284.

Figure Legends

Figure 2.1: Ecdysone signaling components are expressed and activated in the *Drosophila* testis niche.

(A) Diagram of the *Drosophila* testis. Around 10 GSCs (3 shown, pink) are attached to the hub. GSCs divide asymmetrically to produce daughter gonialblasts (GB) that are displaced from the hub. GBs go on to form spermatogonial cysts. Fusomes (red) are spherical in GSCs and branched in spermatogonia. Approximately 2 CySCs (blue) flank each GSC and contact the hub with cytoplasmic extensions. CySCs divide to produce cyst cell daughters; two envelop each GB and its descendants. **(B)** Diagram of the *Drosophila* ecdysone pathway. 20E (blue dots) activates this pathway by binding to a heterodimer composed of EcR and USP. Both EcR and USP contain a LBD that can bind 20E and a DBD that can recognize the EcRE and regulate downstream gene expression (pink dots). **(C-E)** Testes from adult *y w* flies stained with germline marker anti-Vasa (red), DNA stain DAPI (blue), and antibodies (green) against: **(C)** USP (hub and CySC lineage); **(D)** EcR (CySC lineage); or **(E)** ecdysone signaling target Br (CySC lineage). Insets show green channel alone. **(F)** Diagram of the *GAL4-EcR* reporter construct, which is composed of the LBD from EcR fused to the DBD from Gal4 and is under control of the hsp-70 promoter. When expressed at low levels, this reporter shows where the pathway can be activated: in the presence of 20E and EcR's binding partners, Gal4 is activated and induces expression of *UAS-lacZ* or *UAS-GFP* (green dots). A similar *GAL4-usp* construct (not shown) is activated by ecdysone and USP's binding partners. **(G)** Late 3rd instar larval testis carrying the *GAL4-EcR* reporter and stained with DAPI (blue), anti-Vasa (red), and anti-GFP (green). Without 20E feeding, endogenous 20E

drives GFP expression in the larval hub and CySC lineage. Inset shows green channel alone. **(H-J)** Adult testes stained with DAPI (blue), somatic cell marker anti-Tj (red), and anti-lacZ (green). Without 20E feeding **(H)**, adult testes carrying the *Gal4-EcR* reporter (or *Gal4-usp* reporter, not shown) do not express lacZ. After adult flies carrying the *Gal4-EcR* reporter **(I)** or *Gal4-usp* reporter **(J)** are fed 1 mM 20E overnight, testes express lacZ in the hub and CySC lineage. Hub, asterisk or arrow; CySC lineage cells, arrowhead. Scale bar in J, for all panels, = 20 μm.

Figure 2.2: 20E hormone is required for stem cell maintenance

(A) Diagram showing how *Gal4-EcR* or *Gal4-usp* can act as dominant negative constructs (20E "sponges"): when expressed at high levels, they bind with endogenous receptors, compete for endogenous 20E and reduce its effective concentration, thus preventing endogenous EcR or USP from functioning normally (Hackney et al. 2007). (B-D) Testes from adult flies carrying *Gal4-EcR* stained with anti-Vasa (red), DAPI (blue), anti-Zfh1 (green; CySCs and their immediate daughters), anti-Hts/1B1 (white; fusomes), and anti-Arm (white; hub cells). Before overexpression (B), testes look normal; after heat-shock induced overexpression of *Gal4-EcR* (C), GSCs and CySCs are lost; feeding 20E to adult flies rescues the loss (D). Scale bar in D, for B-D, = 20 μm. (E) Bar graphs showing number of GSCs or Zfh1-positive cells per testis for this experiment. Data are represented as mean ± standard error of the mean (SEM). ** P-value < 0.005; *** P-value < 0.0005.

Figure 2.3: *EcR* is required in the testis to maintain GSCs and CySCs.

Testes from adult flies stained with anti-Vasa (red), DAPI (blue), anti-Zfh1 (green), anti-Hts/1B1, and anti-Arm. **(A)** *EcR* heterozygous mutant testes look wild-type after 7 days at 31˚C. $EcR^{A483T/M554fs}$ mutant testes look normal at permissive temperature **(B)** but lose GSCs and CySCs after 7 days at restrictive temperature **(C)**. At restrictive temperature, spermatogonial cysts are sometimes found touching the hub; a 8-cell cyst (identified by elongated fusome) is outlined. Hub, asterisk. Scale bar in C, for A-C, = 20 μm. **(D)** Bar graphs showing number of GSCs or Zfh1-positive cells per testis for this experiment. Data are represented as mean ± SEM. *** P-value < 0.0005.

Figure 2.4: *EcR* and *usp* are required in the CySC lineage to maintain CySCs and GSCs.

(A-D, F-I) Testes from adult flies stained with anti-Vasa (red), DAPI (blue), anti-Zfh1 (green), anti-Hts/1B1, and anti-Arm. **(A)** Mock disruption of GFP by RNAi in the CySC lineage does not affect GSC or CySC maintenance. **(B-D)** Disruption of EcR by RNAi **(B)** or DN **(C)** or disruption of USP by RNAi **(D)** in the CySC lineage causes loss of GSCs, early germline cells, and CySCs. **(E)** Bar graphs showing the number of Zfh1-positive cells or GSCs per testis for the experiments depicted in panels A-D. **(F)** Testes from *c587-Gal4;* $EcR^{A483T/M554fs}$*; TM6B/+* flies lose GSCs and CySCs at restrictive temperature (similar to Figure 2.3C). Expression of *UAS-EcR-B2* **(I)** but not *UAS-GFP* **(G)** or *UAS-EcR-A* **(H)** in the CySC lineage is able to rescue the stem cell loss phenotype in EcR^{ts} testes. Outlined cells are differentiated spermatogonia near the hub. Hub, asterisk. Scale bars in D, for A-D; in I, for F-I = 20 μm. **(J)** Bar graphs showing the number of Zfh1-positive cells or GSCs per testis for the experiments depicted in panels

F-I. In (E) and (J), data are represented as mean ± SEM. ** P-value < 0.005; *** P-value < 0.0005.

Figure 2.5: *EcR* is required for cell survival in the testis.

Testes from adult flies stained with anti-Vasa (red), DAPI (blue), anti-Zfh1, and TUNEL (green) to visualize apoptotic cells. *c587-Gal4; $EcR^{A483T/M554fs}$; TM6B/+* testes contain more TUNEL-positive cells at restrictive temperature **(B)** than at permissive temperature **(A)**. TUNEL-positive cells are rarely found within 2 cell diameters of the hub under normal conditions, but their number increases at restrictive temperature (arrowhead) suggesting that *EcR* is required for early cell survival in the testis. **(C)** Expression of *UAS-EcR.B2* in the CySC lineage is able to rescue the increased cell death phenotype in the EcR^{ts} testes. Hub, asterisk. Scale bar in C, for A-C, = 20 μm. **(D, E)** Column scatter graphs showing the number of TUNEL-positive cells within 2 cell diameters of the hub (D) and the number of TUNEL-positive germ cells (diameter > 5 μm) (E) per testis for these experiments. Bars indicate mean ± SEM. * P-value < 0.05; ** P-value < 0.005.

Figure 2.6: *E75* and *ftz-f1*, but not *br*, are potential ecdysone targets that regulate stem cell maintenance in the testis.

(A, B) Testes from adult flies stained anti-Vasa (red), DAPI (blue), anti-Br (green). Disruption of Br by RNAi in the CySC lineage can effectively reduce Br level by immunostaining, but it does not cause GSC or CySC loss. **(C, D)** Testes from adult flies stained with anti-Vasa (red), DAPI (blue), anti-Zfh1 (green), anti-Hts/1B1, and anti-Arm. Disruption of *E75* **(C)** or *ftz-f1* **(D)** by RNAi in the CySC lineage causes CySC and GSC loss. **(E)** Bar graphs showing the number of Zfh1-positive cells or GSCs per testis for

these experiments. Data are represented as mean ± SEM. *** P-value < 0.0005. **(F-I)** Testes from adult flies stained with anti-GFP (green), DAPI (blue), anti-Zfh1 (red). *ftz-f1*^{ex7} CySC (GFP positive, Zfh1 positive) and cyst clones (GFP positive, Zfh1 negative) are induced at a similar rate but lost faster than wild type clones. ACI, after clone induction.

Figure 2.7: *EcR* genetically interacts with *Nurf301* to maintain stem cells in the testis.

Induction of *EcR RNAi* (7 days at 29˚C) in the CySC lineage using *c587-Gal4* driver causes GSC and CySC loss; in a *Nurf301*^{3}/+ heterozygous background, the loss is enhanced. Data are represented as mean ± SEM. * P-value < 0.05; *** P-value < 0.0005.

Figure S2.1: Ecdysone hormone is required for stem cell maintenance.

Testes from adult flies *Gal4-usp* stained with anti-Vasa (red), DAPI (blue), anti-Zfh1 (green), anti-Hts/1B1, and anti-Arm. Before overexpression **(A)**, testes look normal; after heat-shock induced overexpression of *Gal4-usp* **(B)**, GSCs and CySCs are lost; feeding 20E to adult flies rescues the loss **(C)**. Scale bar in C, for A-C, = 20 μm.

Figure. S2.2 : *Ecdysoneless* (*ecd*) has ecdysone-independent functions in the testis.

Testes from adult temperature sensitive *ecd*^{1} flies stained with anti-Vasa (red), DAPI (blue), anti-Zfh1 (green), anti-Hts/1B1, and anti-Arm. **(A)** At permissive temperature (18˚C), testes appear normal. At restrictive temperature (29˚C), testes show GSC loss **(B)** and cannot be rescued by 20E feeding **(C)**. Scale bar in C for A-C = 20 μm. **(D)** Bar

graph showing number of GSCs per testis for this experiment. Data are represented as mean ± SEM. **(E)** Negatively marked clonal analysis shows that *ecd*^{2} (null allele) stem cell clones are lost faster than control clones, which indicates that *ecd* is required cell autonomously in the GSCs and CySCs for their maintenance.

Figure S2.3: Different alleles of *EcR RNAi*, *EcR DN* or *usp RNAi* lines causes stem cell loss.

(A) Bar graphs showing the number of Zfh1-positive cells or GSCs per testis for *EcR* knockdown experiment using different alleles of *EcR RNAi* or *DN*. **(B)** Bar graphs showing the number of Zfh1-positive cells or GSCs per testis for *usp* knockdown experiment using different transgenes for *usp RNAi*. Data are represented as mean ± SEM. *** P-value < 0.0005.

Figure S2.4: *EcR* and *usp RNAi* constructs have leaky expression.

(A) Bar graphs showing the number of Zfh1-positive cells or GSCs per testis for *EcR RNAi* with or without driver. *EcR RNAi* without driver causes similar stem cell loss as RNAi driven by *E132-Gal4* driver, but is less severe than RNAi driven by *c587-Gal4* driver. **(B)** Bar graphs showing the number of Zfh1-positive cells or GSCs per testis for *usp RNAi* with or without driver. *usp RNAi* without driver causes stem cell loss but is less severe than RNAi driven by *c587-Gal4* driver, but not RNAi driven by *E132-Gal4* driver. Data are represented as mean ± SEM. * P-value < 0.05, ** P-value < 0.005, *** P-value < 0.0005.

Figure S2.5: *EcR* is not required in the hub cells to maintain CySCs and GSCs. Testes from adult flies stained with anti-Vasa (red), DAPI (blue), anti-GFP (green). **(A)** *c587-Gal4* driver drives the expression of GFP in the CySC lineage. **(B)** *hh-Gal4* driver drives the expression of GFP in the hub cells. **(C)** Testes from adult flies stained with anti-Vasa (red), DAPI (blue), anti-Zfh1 (green), anti-Hts/1B1. Expression of *UAS-EcR.B2* in the hub cells cannot rescue the stem cell loss phenotype in EcR^{ts} testes. Hub, asterisk. Scale bar in C, for A-C, = 20 μm. **(D)** Bar graphs showing the number of Zfh1-positive cells or GSCs per testis for EcR hub rescue experiment. Data are represented as mean ± SEM. *** P-value < 0.0005 .

Table 2.1. *ftz-f1* is required cell autonomously for GSC and CySC maintenance

Part A *ftz-f1* negative clonal analysis

Genotype	0d ACI	2dACI	6dACI	8dACI
Percentage of testis with CySC clones				
ftz-f1^{ex7} FRT2A	17% (3/18)	17% (7/30)	7% (2/30)	5% (1/20)
Ctrl *FRT2A*	0% (0/17)	77% (26/34)	40%(6/15)	35% (10/29)

Part B *ftz-f1* MARCM

Genotype	0d ACI	2d ACI	4d ACI	6d ACI	8d ACI
Percentage of testes with CySC clones					
ftz-f1^{ex7} FRT2A	5% (1/21)	72% (13/18)	5% (1/22)	0% (0/24)	5% (1/23)
Ctrl *FRT2A*	0% (0/25)	83% (15/18)	63% (14/22)	55% (12/22)	50% (10/22)
Percentage of testis with cyst cell clones					
ftz-f1^{ex7} FRT2A	5% (1/21)	83% (15/18)	32% (7/22)	5% (1/24)	0% (0/23)
Ctrl *FRT2A*	12% (3/25)	94% (17/18)	86% (19/22)	68% (15/22)	70% (14/20)

Table 2.2 *E75* clonal analysis indicates that *E75* is cell autonomously required for GSC and CySC maintenance

Genotype	0d ACI	2d ACI	8d ACI
Percentage of testis with CySC clones			
$E75^{\Delta 51}$ *FRT80B*	10% (2/20)	30% (7/23)	11% (4/35)
Ctrl *FRT80B*	9% (2/22)	36% (9/25)	25% (7/29)

Table S2.1. *ecd* is required cell autonomously in the GSCs and CySCs for their maintenance. (These data are presented graphically in Figure S4.3D.)

Genotype	0d ACI	2d ACI	4d ACI	6d ACI	8d ACI	10d ACI
Percentage of testes with GSC clones						
ecd^{2} FRT2A	12% (3/25)	64% (16/25)	31% (9/29)	0% (0/23)	2.4% (1/42)	0% (0/6)
Ctrl FRT2A	12% (2/17)	82% (28/34)	56% (19/34)	47% (7/15)	70% (20/29)	59% (14/24)
Percentage of testes with CySC clones						
ecd^{2} FRT2A	12% (3/25)	72% (18/25)	17% (5/29)	8.7% (2/23)	12% (5/42)	17% (1/6)
Ctrl FRT2A	0% (0/17)	77% (26/34)	47% (16/34)	40% (6/15)	35% (10/29)	42% (10/24)

Figure 2.1

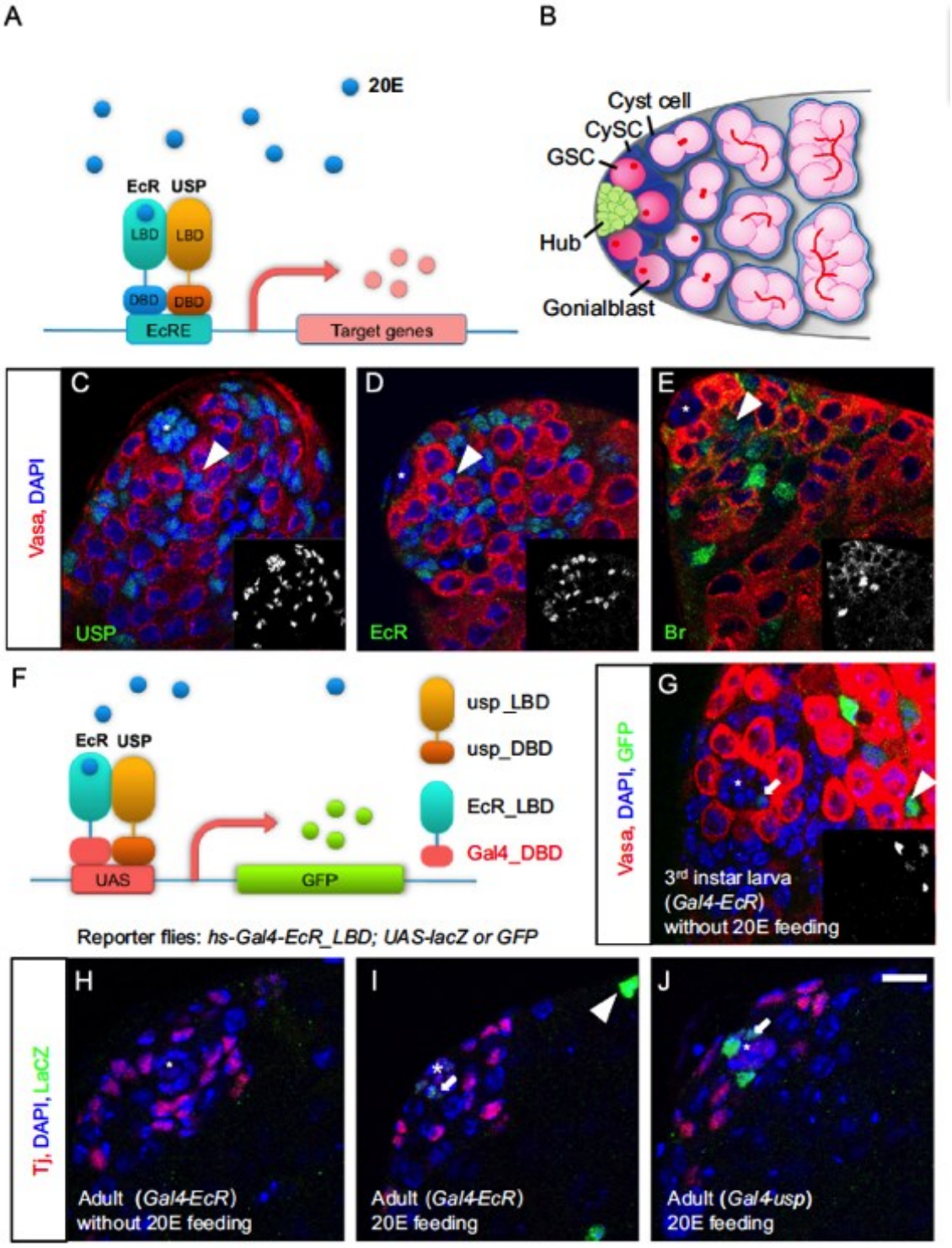
A
20E
EcR USP
LBD LBD
DBD DBD
EcRE
Target genes
B
Cyst cell
CySC
GSC
Hub
Gonialblast
C
Vasa, DAPI
USP
D
EcR
E
Br
F
EcR USP
UAS
GFP
usp_LBD
usp_DBD
EcR_LBD
Gal4_DBD
Reporter flies: hs-Gal4-EcR_LBD; UAS-lacZ or GFP
G
Vasa, DAPI, GFP
3rd instar larva
(Gal4-EcR)
without 20E feeding
H
Tj, DAPI, LacZ
Adult (Gal4-EcR)
without 20E feeding
I
Adult (Gal4-EcR)
20E feeding
J
Adult (Gal4-usp)
20E feeding

Figure 2.2

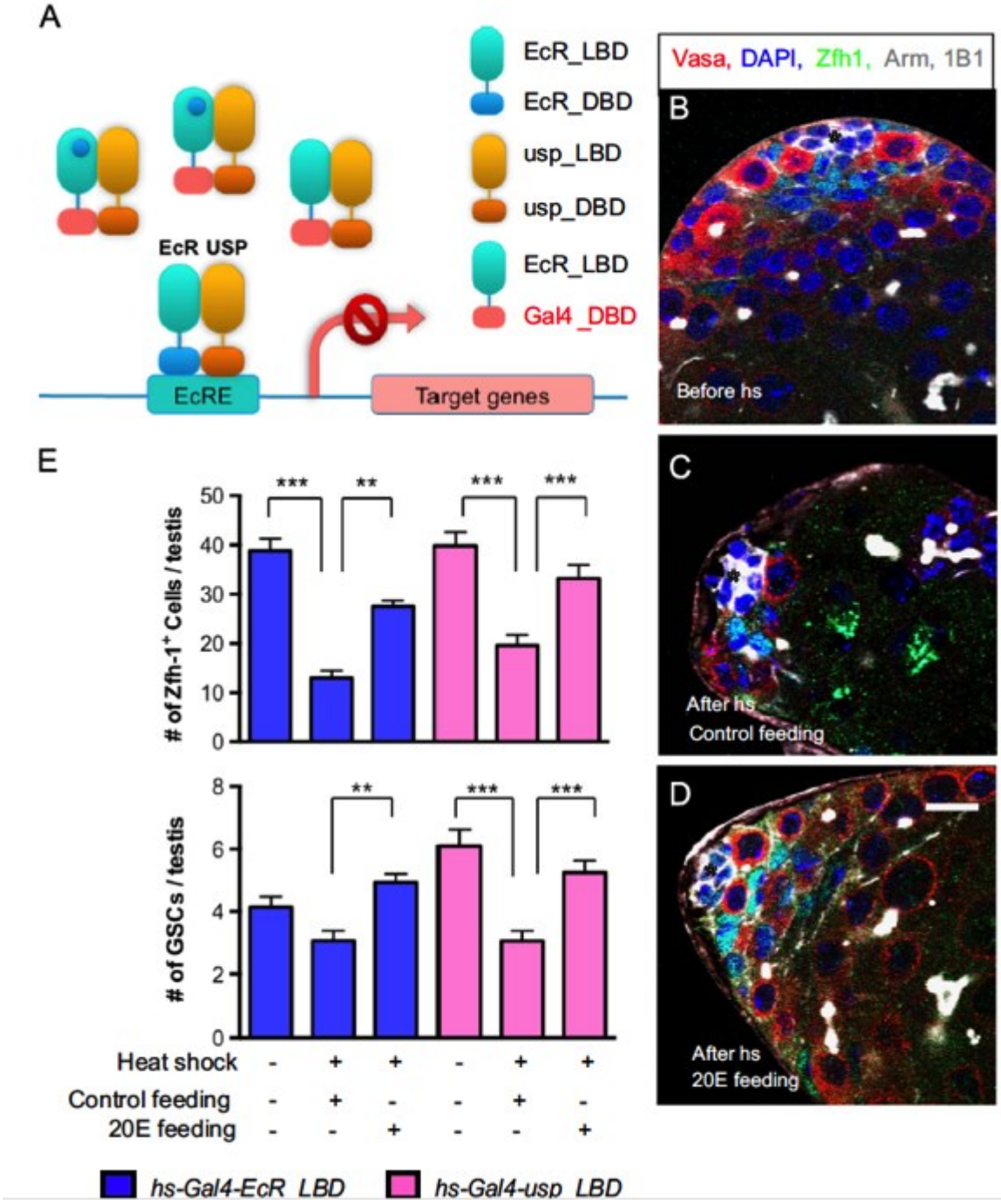
A
EcR_LBD
EcR_DBD
usp_LBD
usp_DBD
EcR_LBD
Gal4 _DBD
EcR USP
EcRE
Target genes
Vasa, DAPI, Zfh1, Arm, 1B1
B
Before hs
C
After hs
Control feeding
D
After hs
20E feeding
E
# of Zfh-1+ Cells / testis
# of GSCs / testis
Heat shock
Control feeding
20E feeding
hs-Gal4-EcR LBD
hs-Gal4-usp LBD

Figure 2.3

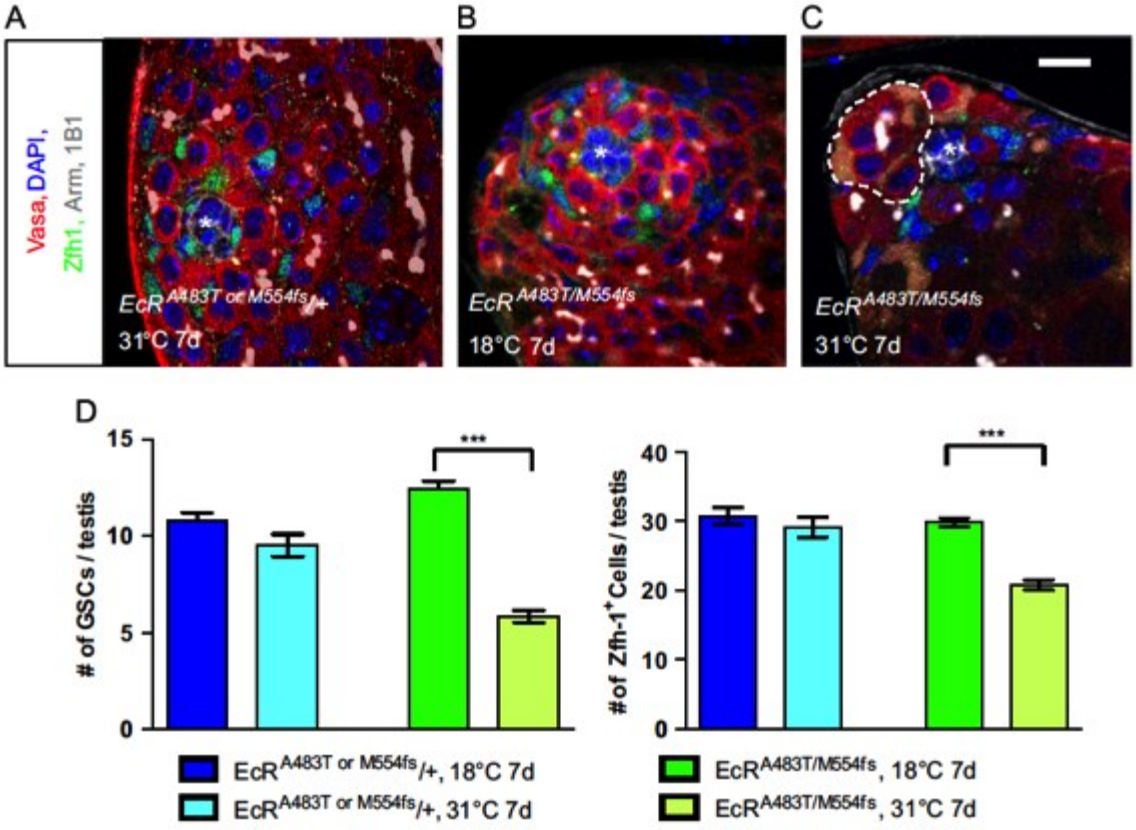
A
B
C
Vasa, DAPI,
Zfh1, Arm, 1B1
EcR A483T or M554fs /+
31°C 7d
EcR A483T/M554fs
18°C 7d
EcR A483T/M554fs
31°C 7d
D
# of GSCs / testis
15
10
5
0
***
#of Zfh-1+ Cells / testis
40
30
20
10
0
***
EcR A483T or M554fs /+, 18°C 7d
EcR A483T or M554fs /+, 31°C 7d
EcR A483T/M554fs, 18°C 7d
EcR A483T/M554fs, 31°C 7d

Figure 2.4

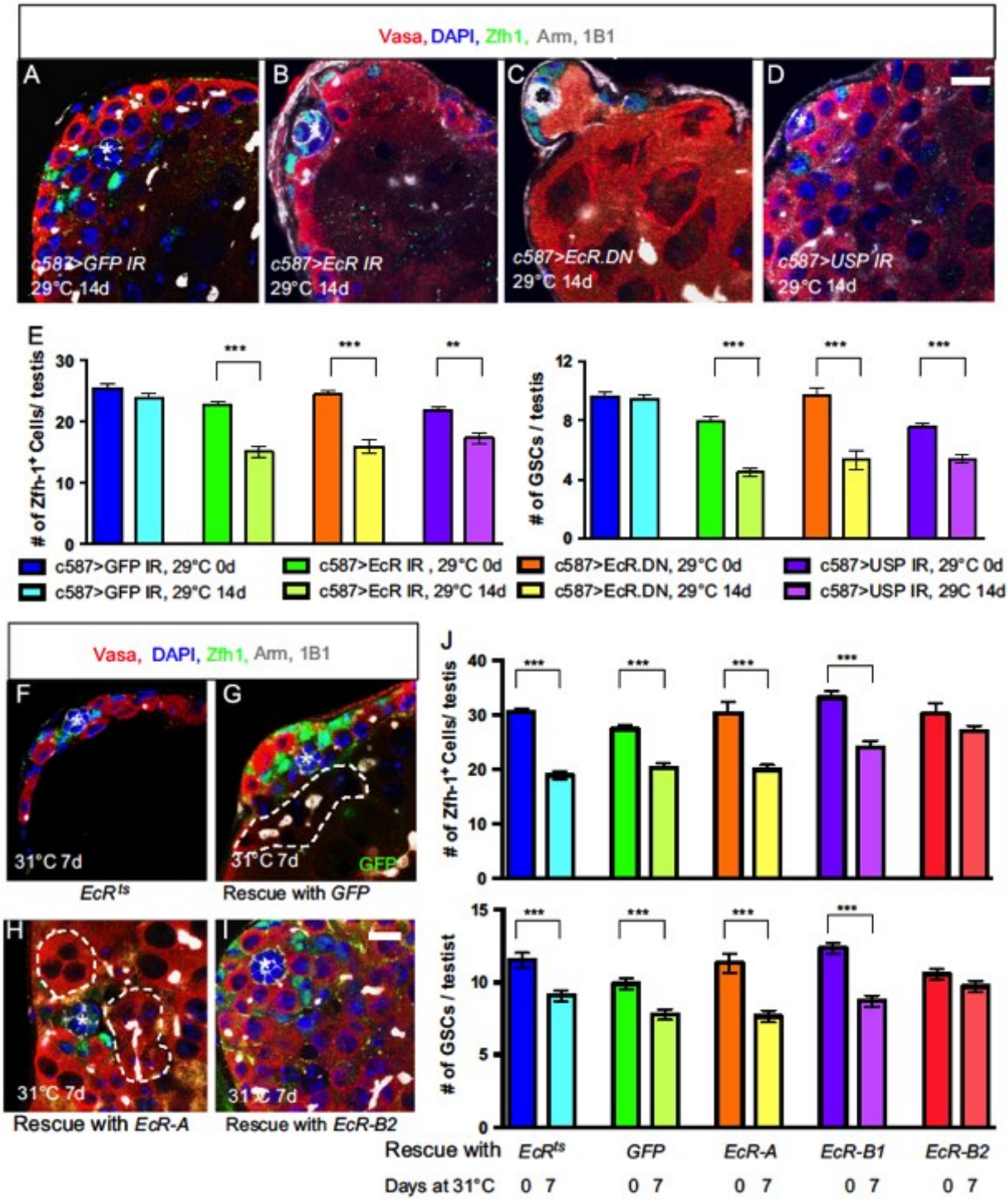
Vasa, DAPI, Zfh1, Arm, 1B1
A
B
C
D
c587>GFP IR
29°C 14d
c587>EcR IR
29°C 14d
c587>EcR.DN
29°C 14d
c587>USP IR
29°C 14d
E
# of Zfh-1+ Cells/ testis
# of GSCs / testis
c587>GFP IR, 29°C 0d
c587>GFP IR, 29°C 14d
c587>EcR IR , 29°C 0d
c587>EcR IR, 29°C 14d
c587>EcR.DN, 29°C 0d
c587>EcR.DN, 29°C 14d
c587>USP IR, 29°C 0d
c587>USP IR, 29C 14d
Vasa, DAPI, Zfh1, Arm, 1B1
F
G
31°C 7d
EcRts
Rescue with GFP
H
I
Rescue with EcR-A
Rescue with EcR-B2
J
# of Zfh-1+ Cells/ testis
# of GSCs / testist
Rescue with EcRts GFP EcR-A EcR-B1 EcR-B2
Days at 31°C 0 7 0 7 0 7 0 7 0 7

Figure 2.5

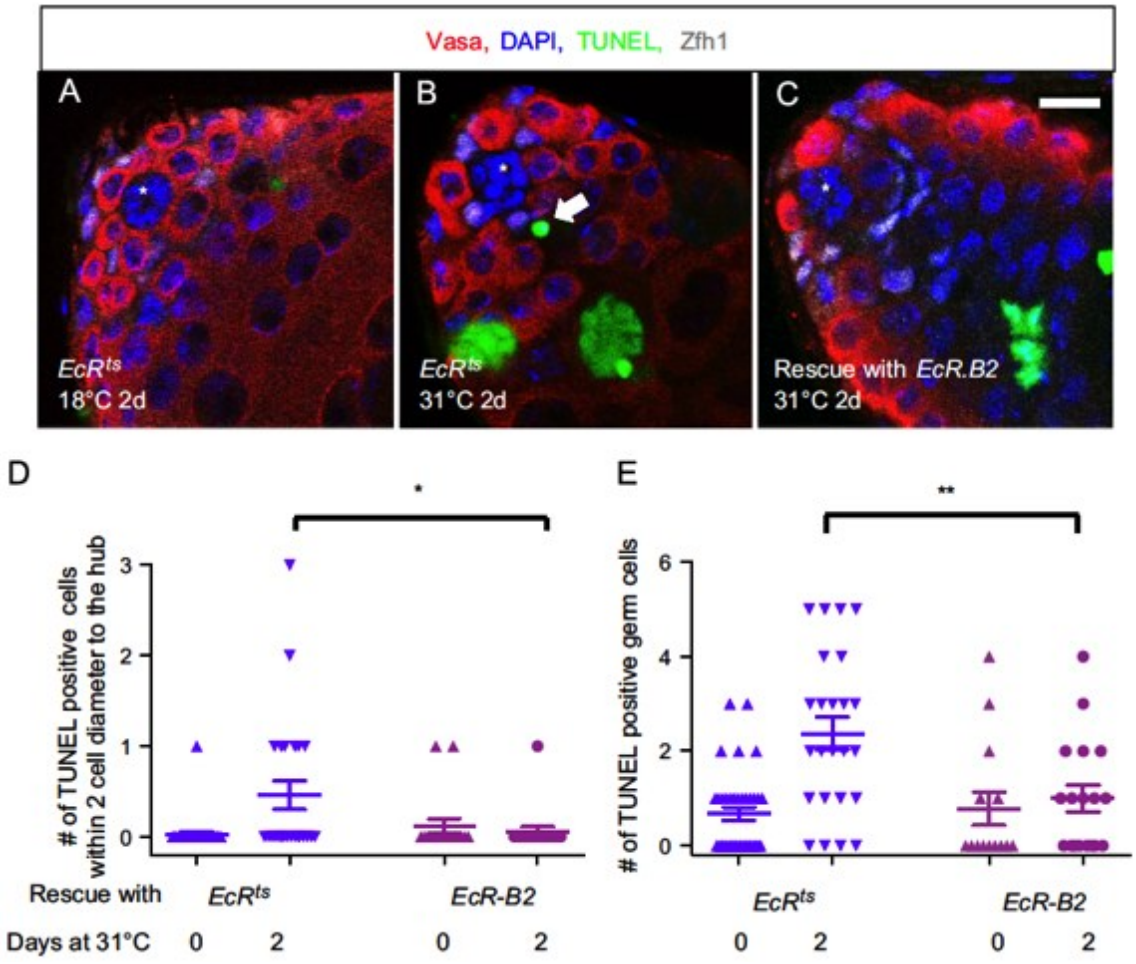
Vasa, DAPI, TUNEL, Zfh1
A
EcR^ts
18°C 2d
B
EcR^ts
31°C 2d
C
Rescue with EcR.B2
31°C 2d
D
*
# of TUNEL positive cells within 2 cell diameter to the hub
3
2
1
0
Rescue with
EcR^ts
EcR-B2
Days at 31°C
0
2
0
2
E
**
# of TUNEL positive germ cells
6
4
2
0
EcR^ts
EcR-B2
0
2
0
2

Figure 2.6

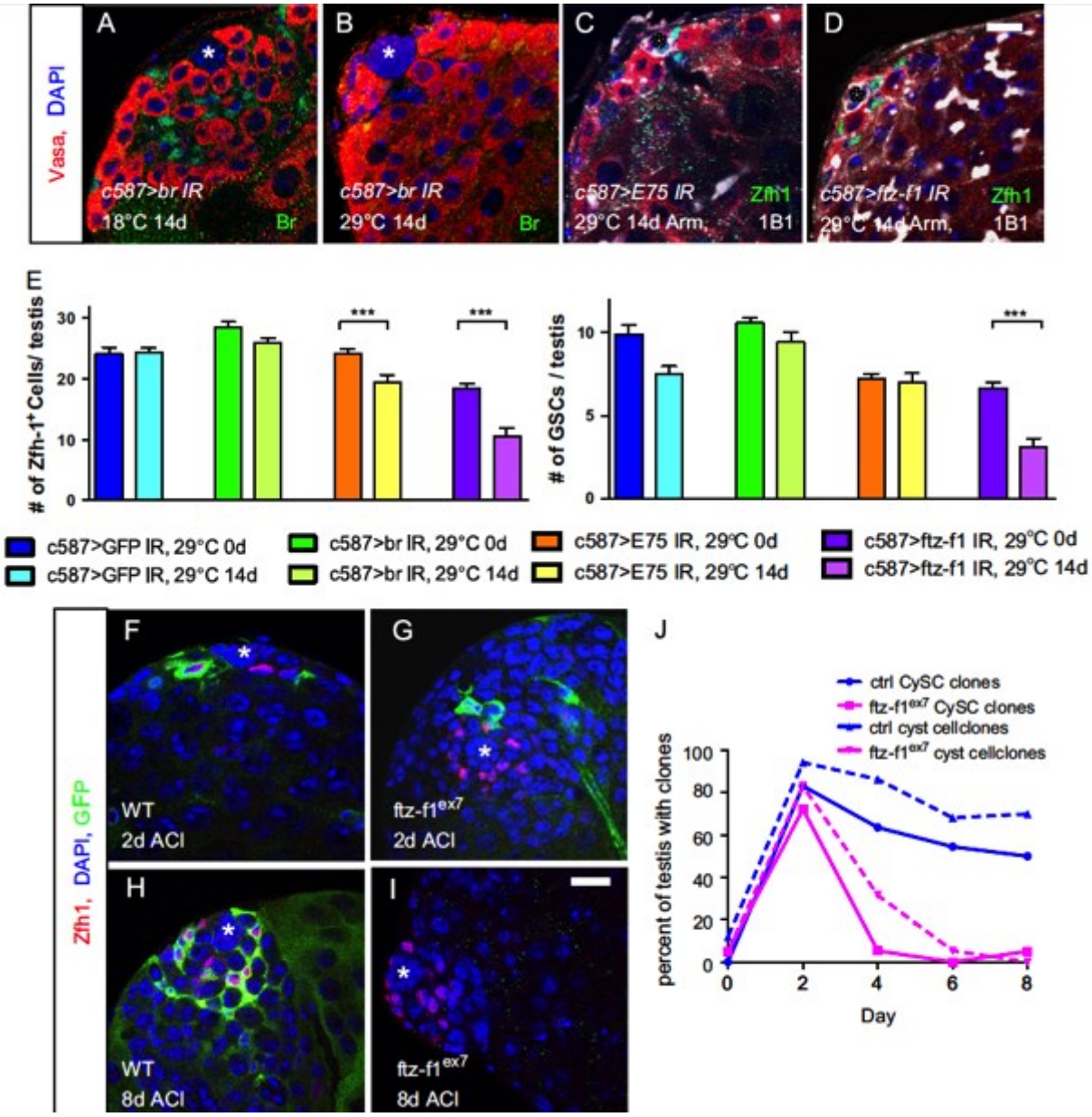
A
B
C
D
Vasa, DAPI
c587>br IR
18°C 14d
Br
c587>br IR
29°C 14d
Br
c587>E75 IR
29°C 14d Arm,
Zfh1
1B1
c587>ftz-f1 IR
29°C 14d Arm,
Zfh1
1B1
# of Zfh-1+ Cells/ testis
# of GSCs / testis
***
c587>GFP IR, 29°C 0d
c587>GFP IR, 29°C 14d
c587>br IR, 29°C 0d
c587>br IR, 29°C 14d
c587>E75 IR, 29°C 0d
c587>E75 IR, 29°C 14d
c587>ftz-f1 IR, 29°C 0d
c587>ftz-f1 IR, 29°C 14d
Zfh1, DAPI, GFP
F
G
H
I
WT
2d ACI
ftz-f1ex7
2d ACI
WT
8d ACI
ftz-f1ex7
8d ACI
J
ctrl CySC clones
ftz-f1ex7 CySC clones
ctrl cyst cellclones
ftz-f1ex7 cyst cellclones
percent of testis with clones
Day

Figure 2.7

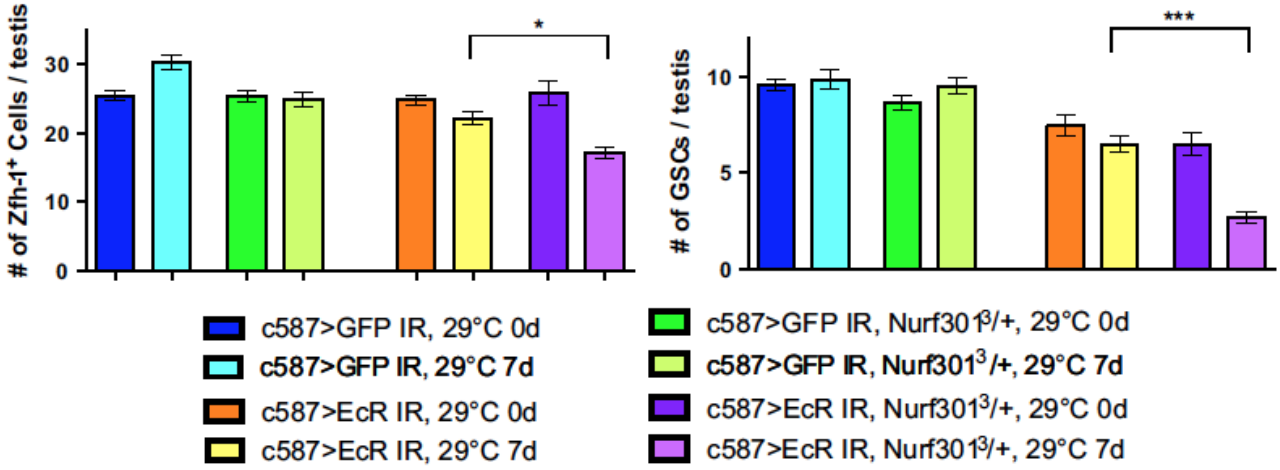
# of Zfh-1+ Cells / testis
30
20
10
0
*
# of GSCs / testis
10
5
0
***
c587>GFP IR, 29°C 0d
c587>GFP IR, 29°C 7d
c587>EcR IR, 29°C 0d
c587>EcR IR, 29°C 7d
c587>GFP IR, Nurf301^3/+, 29°C 0d
c587>GFP IR, Nurf301^3/+, 29°C 7d
c587>EcR IR, Nurf301^3/+, 29°C 0d
c587>EcR IR, Nurf301^3/+, 29°C 7d

Figure S2.1

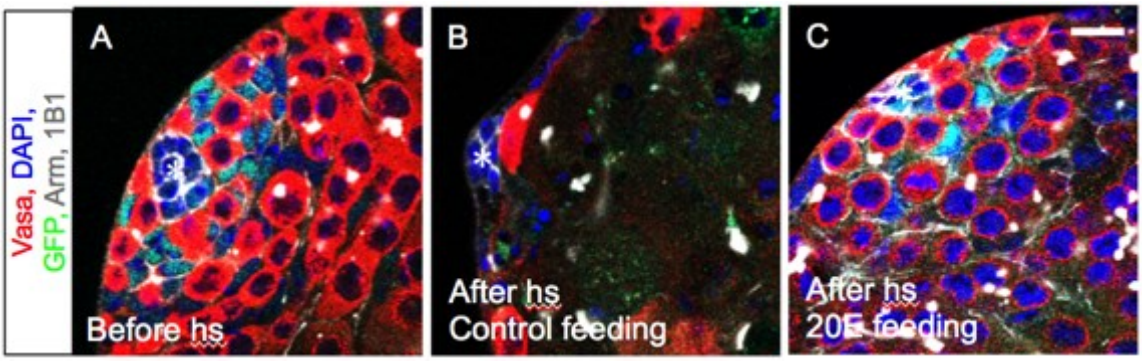
Vasa, DAPI,
GFP, Arm, 1B1
A
Before hs
B
After hs
Control feeding
C
After hs
20E feeding

Figure S2.2

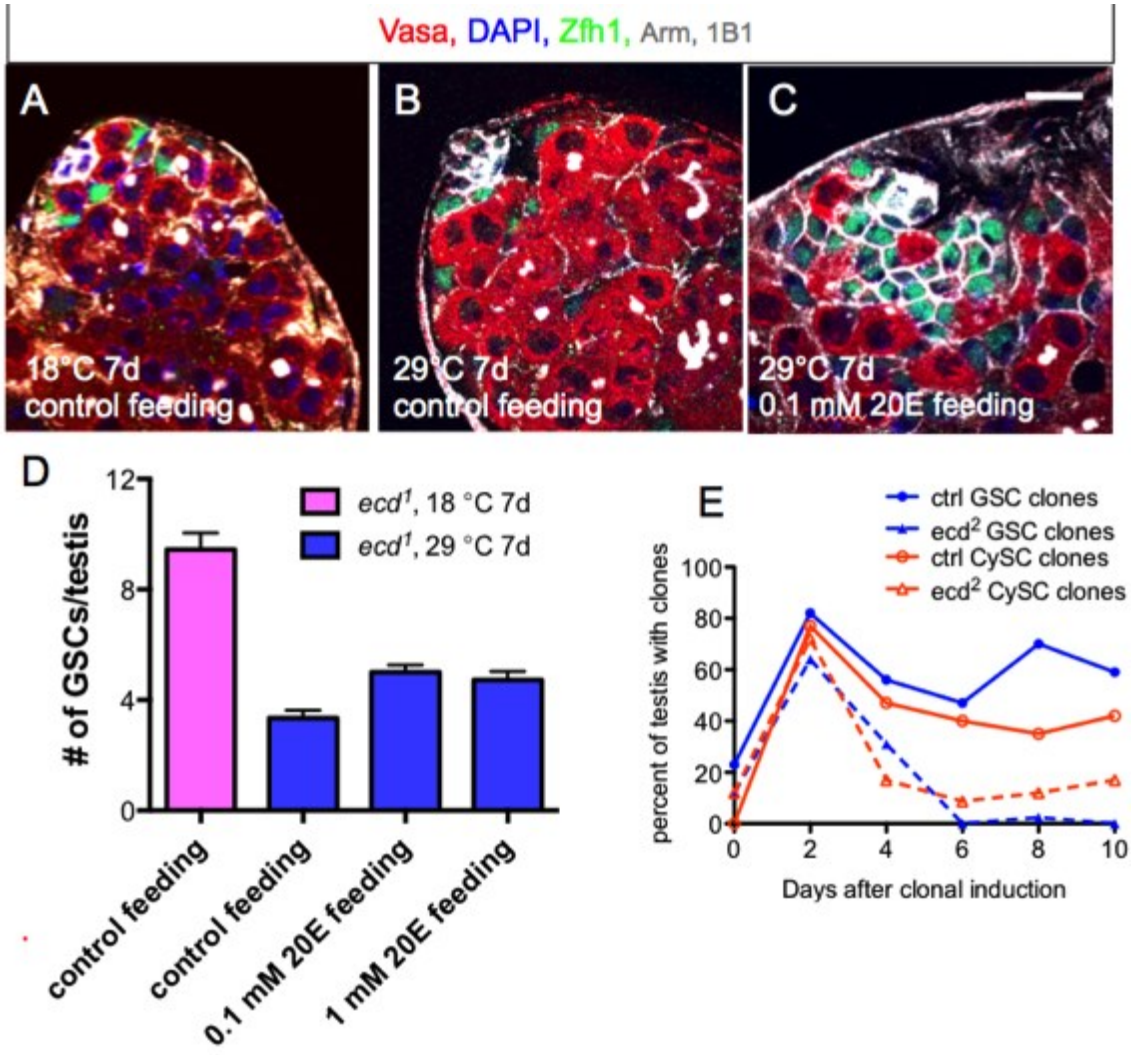
Vasa, DAPI, Zfh1, Arm, 1B1
A
18°C 7d
control feeding
B
29°C 7d
control feeding
C
29°C 7d
0.1 mM 20E feeding
D
# of GSCs/testis
ecd1, 18 °C 7d
ecd1, 29 °C 7d
control feeding
control feeding
0.1 mM 20E feeding
1 mM 20E feeding
E
ctrl GSC clones
ecd2 GSC clones
ctrl CySC clones
ecd2 CySC clones
percent of testis with clones
Days after clonal induction

Figure S2.3

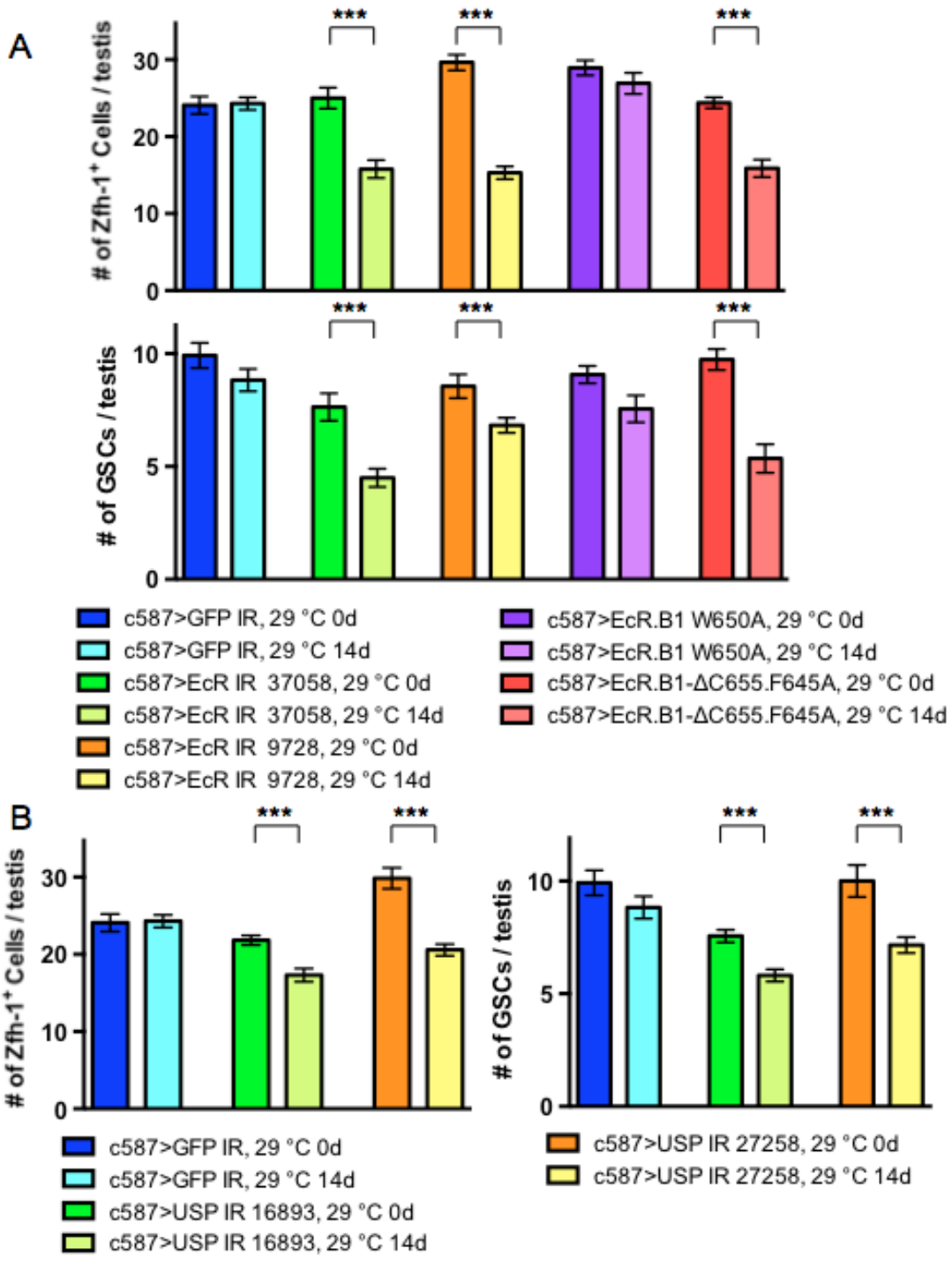
A
# of Zfh-1+ Cells / testis
# of GSCs / testis
***
c587>GFP IR, 29 °C 0d
c587>GFP IR, 29 °C 14d
c587>EcR IR 37058, 29 °C 0d
c587>EcR IR 37058, 29 °C 14d
c587>EcR IR 9728, 29 °C 0d
c587>EcR IR 9728, 29 °C 14d
c587>EcR.B1 W650A, 29 °C 0d
c587>EcR.B1 W650A, 29 °C 14d
c587>EcR.B1-ΔC655.F645A, 29 °C 0d
c587>EcR.B1-ΔC655.F645A, 29 °C 14d
B
# of Zfh-1+ Cells / testis
# of GSCs / testis
c587>GFP IR, 29 °C 0d
c587>GFP IR, 29 °C 14d
c587>USP IR 16893, 29 °C 0d
c587>USP IR 16893, 29 °C 14d
c587>USP IR 27258, 29 °C 0d
c587>USP IR 27258, 29 °C 14d

Figure S2.4

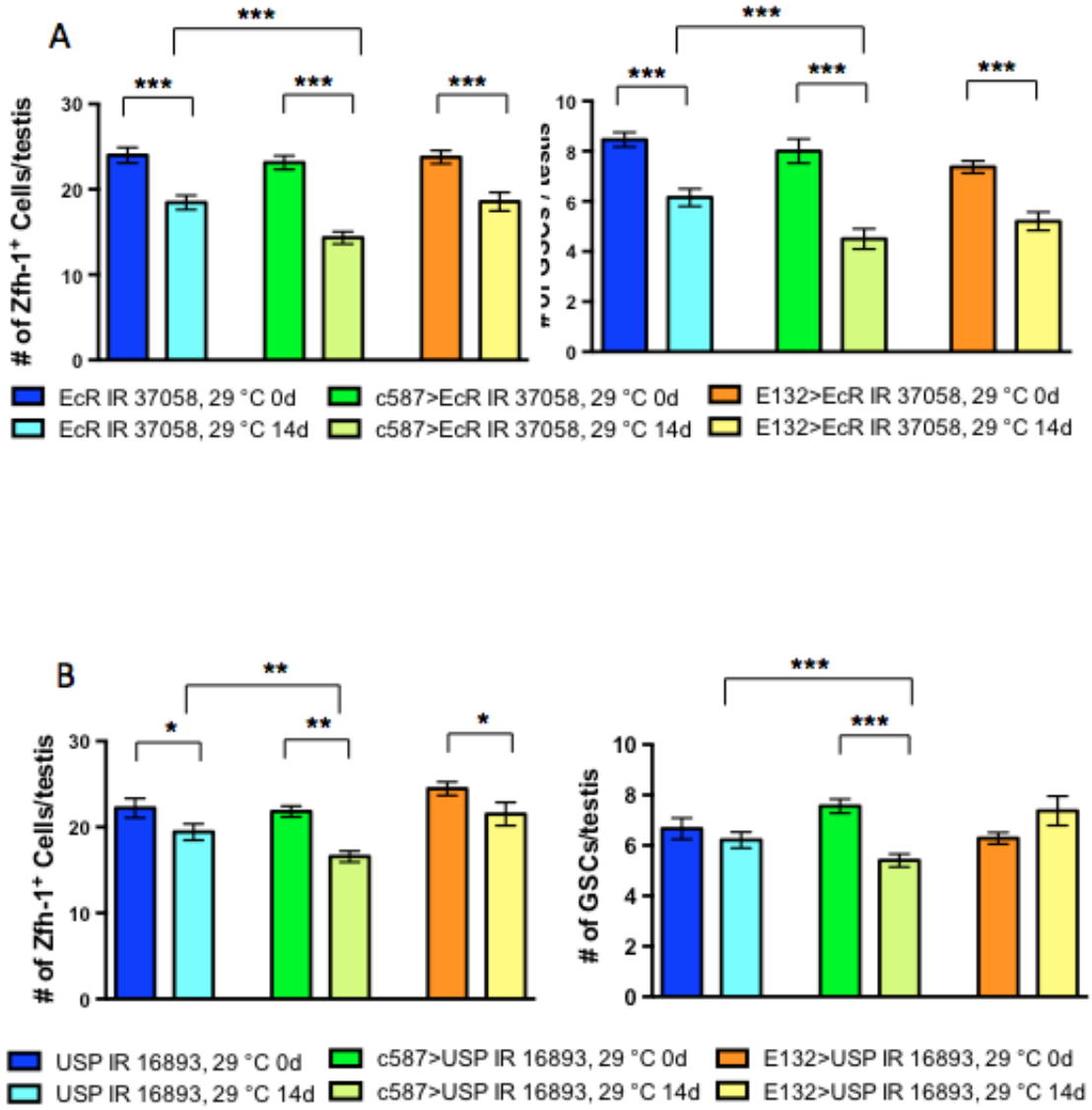
A
# of Zfh-1+ Cells/testis
EcR IR 37058, 29 °C 0d
EcR IR 37058, 29 °C 14d
c587>EcR IR 37058, 29 °C 0d
c587>EcR IR 37058, 29 °C 14d
E132>EcR IR 37058, 29 °C 0d
E132>EcR IR 37058, 29 °C 14d
B
# of Zfh-1+ Cells/testis
# of GSCs/testis
USP IR 16893, 29 °C 0d
USP IR 16893, 29 °C 14d
c587>USP IR 16893, 29 °C 0d
c587>USP IR 16893, 29 °C 14d
E132>USP IR 16893, 29 °C 0d
E132>USP IR 16893, 29 °C 14d

Figure S2.5

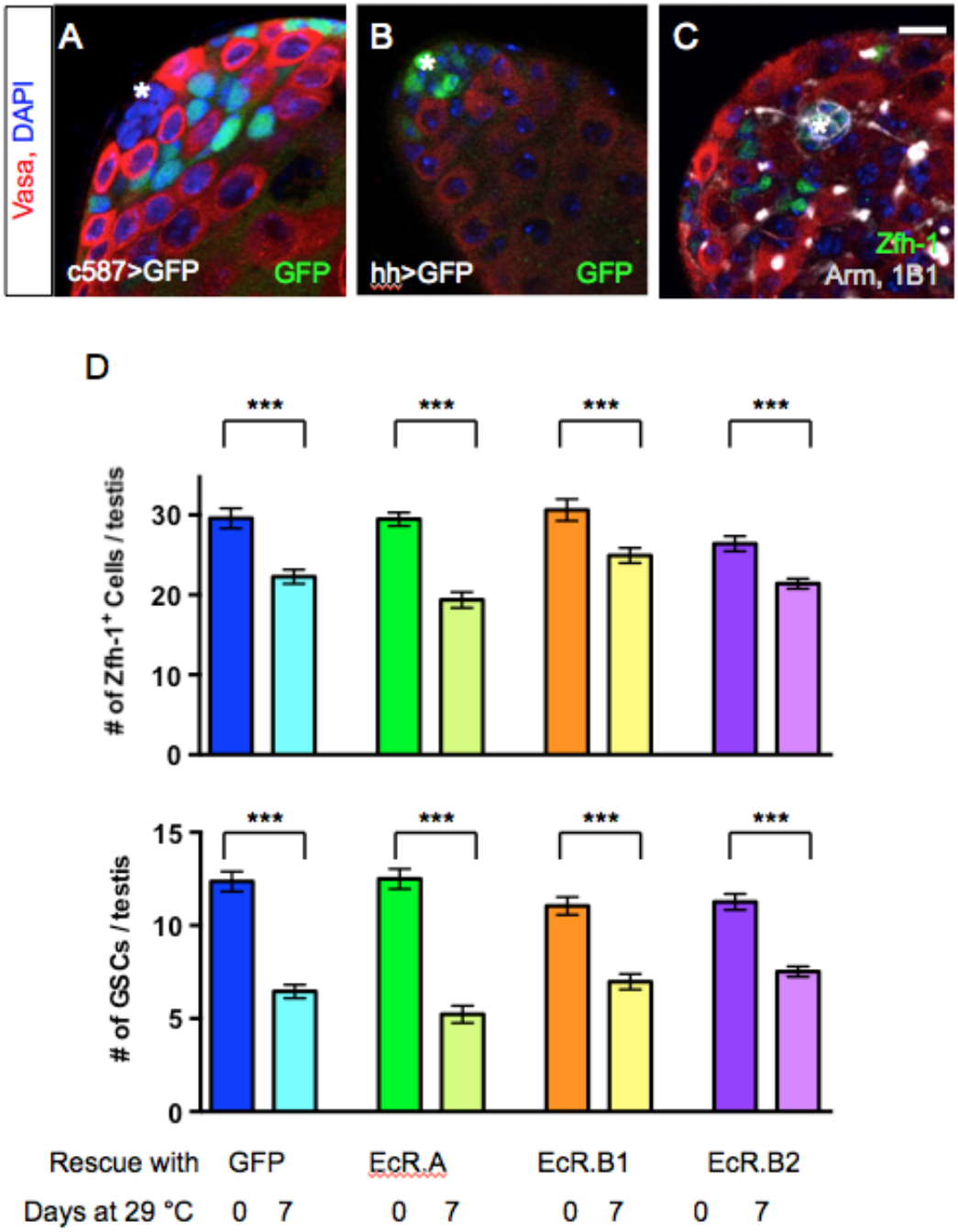
Vasa, DAPI
A
c587>GFP
GFP
B
hh>GFP
GFP
C
Zfh-1
Arm, 1B1
D
# of Zfh-1+ Cells / testis
30
20
10
0
***
# of GSCs / testis
15
10
5
0
Rescue with GFP EcR.A EcR.B1 EcR.B2
Days at 29 °C 0 7 0 7 0 7 0 7

Chapter 3

Probing the function of metazoan histones with a systematic library of histone H3 and H4 mutants

This chapter is a modified version of the manuscript, "Zhang W[#], Xue Z[#], Li Y[#], Zhang X, Long L, Ren X, Zhang J, Ma Q, Matunis, E, Dai J, Gao G, in preparation, Probing the function of the metazoan histones with a systematic library of histone H3 and H4 mutants."

My contribution focused on the effect of that varying histone copy number had on testis and ovary development, and stem cell maintenance in their niches.

Summary

In addition to their roles as structural components of chromatin, histones are intimately involved in the regulation of DNA metabolism and transcription through their post-translational modifications. Using the CRISPR/Cas9 system, a histone deficiency line of *Drosophila melanogaster* was generated, enabling us to systematically probe the functions of each amino acid residue in core histone proteins in their original genomic context. We demonstrate that reducing histone copy number to as few as 8 can support development and adult viability, but results in deficiencies in both testis and ovary development, and a concomitant reduction in fertility. At least 20 copies of histone genes are required to generate a phenotypically wild-type fly. Moreover, using a hierarchical method, we systematically mutagenized all modifiable residues on histone H3 and H4, and probed the consequences of 38 mutations on viability, development, DNA-damage sensitivity and heterochromatin gene silencing. Through the study, we found mutations at several residues impair viability and fertility. Together, the new histone mutagenesis platform allows us to perform high-throughput studies on the function of each key residue in all five histones in *Drosophila melanogaster*.

Introduction

Eukaryotic genomes exist in the form of chromatin formed through DNA association with histones and accessory proteins, allowing them to be packaged into the nucleus. The fundamental building block of chromatin is the nucleosome, which consists of 147 base pairs of DNA wrapped around a histone octamer comprised of two copies each of histone proteins H3, H4, H2A and H2B (Luger et al., 1997; Van Holde, 1989; Wolffe, 2001). Histones do not merely provide a binding platform for DNA; they also actively participate in DNA related processes, such as transcription (Kouzarides, 2007). One mechanism for histones to carry out these functions is through their post-translational modifications (PTMs) (Rothbart and Strahl, 2014), which is a critical step in epigenetic regulation of gene expression.

In the past two decades, over 20 types of PTMs have been identified on histones including acetylation, methylation and phosphorylation (Bannister and Kouzarides, 2011; Kouzarides, 2007; Tessarz and Kouzarides, 2014). Among them, 12 PTMs are added to lysine residues (Huang et al., 2015; Huang et al., 2014). The N-terminal flexible "tail" domains of histones are the most heavily modified portions, presumably because they are more easily accessible to histone modifying enzymes. However, PTMs have also been detected within the globular core domain of histones (Masumoto et al., 2005; Ng et al., 2002; van Leeuwen et al., 2002; Xu et al., 2005; Ye et al., 2005). Histone PTMs are thought to function through two major mechanisms: they directly modulate the packaging conformation of chromatin to modulate gene expression, and they indirectly do so by regulating the assembly of specific chromatin-associated protein factors at particular sites within the genome (Strahl and Allis 2000).

To understand the function of a given histone modification, one can study its modifying enzymes by modulating their activity. However, modifying enzymes may have non-histone substrates or several other histone substrates, which will interfere with site-specific interpretations using this approach. Alternatively, one can mutate specific amino acid residues within the histone to mimic either a modified or an unmodified status, which can often indicate the function of that modification.

Mutagenesis studies on histones have been carried out extensively in the unicellular organism *Saccharomyces cerevisiae* (Dai et al., 2008; Nakanishi et al., 2008). However, similar studies remain very limited in other model systems. The major constraint comes from the copy number and distribution of histone-encoding genes in the genome. For example, there are 64 histone genes within the human genome, which are distributed at three major loci on different chromosomes (Marzluff et al., 2002). Supplying cells with histones derived solely from a mutated version of a histone gene requires inactivating all 64 copies of histone loci across three genomic sites which, if not impossible, is laborious and time-consuming with current gene knockout technologies. Furthermore, due to the critical role of histones in chromatin formation, multiple copies of each histone gene have to be maintained to keep the cells functional. It is not an easy task to construct an array of histone genes each harboring a specific mutation. Currently, the only multicellular organism in which histone mutagenesis has been performed is *Drosophila melanogaster*. This is possible because all the canonical histone genes in *D. melanogaster* reside at a single locus on the left arm of chromosome 2, including approximately 100 copies of the histone gene repeat units (His-GUs) (Lifton et al., 1978; McKay et al., 2015). Each His-GU (~5kb in length) contains the four core histone genes

presented as *His2A-His2B* and *His3-His4* pairs under the control of a divergent promoter, respectively, plus the linker histone, *His1*, which is regulated independently from the core histone genes (Figure S3.1) (Guglielmi et al., 2013; Isogai et al., 2007; Matsuo and Yamazaki, 1989).

In this study, we generated a new transgenic *Drosophila* strain in which the entire histone cluster was removed using the CRISPR/Cas9 system. In addition, two targeted recombination sites were introduced (Bischof et al., 2007), allowing us to integrate multiple histone genes back into the original histone gene locus on chromosome 2. This also circumvents any potential position effects that are often introduced when transgenic constructs are inserted at new sites in the genome. In addition, the presence of two recombination sites greatly reduces the difficulty to generate the histone arrays. For example, to generate a histone array with 12 copies of His-GUs (including core histones and histone H1), a single plasmid with six copies of the His-GUs is sufficient. Here, we demonstrate that as few as 8 copies of His-GUs can rescue lethality caused by complete histone deletion, and that at least 20 His-GUs are required to generate a phenotypically wild-type fly. We found that reduced histone copy number (< 20 His-GUs) is compatible with development and adult viability in *Drosophila*, but results in defects in both testis and ovary development, and a concomitant reduction in fertility, suggesting that sufficient histone expression is critical for development process in fly.

In addition, our new transgenic fly strains allowed a systematic mutagenesis study of histones. We developed a hierarchical method to construct histone mutants in any of the five-histone genes, systematically mutagenizing all modifiable residues on histone H3 and H4, and testing the consequences of these mutations (38 total) on viability,

development, DNA-damage sensitivity and heterochromatin gene silencing. We found that mutations at multiple residues impair viability. We also identified many histone residues, which, when mutated, greatly reduce fertility. Together, we have generated an optimized histone mutagenesis platform, which allows us to study the function of each residue in all five histones with much higher throughput.

Results

The construction of transgenic fly lines heterozygous for a deletion of the entire endogenous genomic histone locus

Previously, Herzig and colleagues constructed a histone deficient line termed *Df(2L)His*^{C} (*His*^{C}) by removing the entire histone cluster with the DrosDel system (Ryder et al., 2004), providing the only metazoan system for histone mutagenesis studies so far (Gunesdogan et al., 2010, 2014; McKay et al., 2015; Pengelly et al., 2013). This fly line, however, can only be rescued using transgenes targeted to either multiple ectopic loci or by a single locus using BAC-based, transgenic arrays, which avoids the potential position effect of the native histone genes.

In order to generate a heterozygous fly line with deletion of the entire histone cluster on one chromosome and to introduce a targeted integration site to facilitate *in situ* complementation, we initially designed a strategy to knock in two *loxP* donor sequences flanking the histone locus using homolog recombination (HR) mediated by traditional ends-out targeting method (Xie and Golic, 2004). However, we failed to obtain any desirable flies for unknown reasons. We speculated that the numerous repetitive sequences near the histone cluster might somehow interfere with the HR process. Therefore, we carried out the same deletion using our recently developed CRISPR/Cas9-mediated gene knock-in technology to generate two mutant fly lines simultaneously (Figure 3.1A) (Xue et al., 2014; Yu et al., 2013). In the first line, a donor plasmid containing an *FRT* (flipase recognition target) site and a phage attachment site (*attP*) was inserted, targeting the left side of the histone locus. To avoid disrupting flanking genes

and using repetitive sequences, we chose a target site adjacent to *CG8663* (2L: 21,394,202) (Figure S3.1). In the second line, a donor plasmid containing the *FRT* site, *attP* site and a *3×P3RFP* gene, was designed to integrate near CG3305 (2L: 21,559,013) at the right of the histone locus (Xue et al., 2014). Unexpectedly, in this experiment, we identified one founder line that contained not only the insertion of the desired sequences but also another copy of the entire donor plasmid. This resulted in a fly with a duplicated *FRT-attP-3×P3RFP* cassette (Figure 3.1A). After the two above-mentioned founder lines were crossed and flipase-mediated recombination was induced, we obtained flies with the entire histone locus deleted and replaced with duplicated *attP-FRT-3×P3RFP* sequences at its original locus, allowing *in situ* integration of modified histone arrays (Figure 3.1A). We designated this fly line as His^{D}. The presence of two *attP* sites and the entire donor plasmid was confirmed by PCR (Figure 3.1B), and the entire region was subsequently sequenced to verify the complete removal of all canonical histone genes. In summary, we have successfully constructed a heterozygous transgenic fly line in which all canonical histone genes were removed from one chromosome. In addition, this fly line enabled us to integrate two copies of a histone donor simultaneously at the endogenous histone locus in one injection experiment, avoiding the construction of a twelve-copy BAC clone or multiple rounds of transgene integration. This greatly enhanced our ability to systematically generate a fly library containing hundreds of histone mutants (see Figure S3.2A and below).

Since the histone mRNAs are maternally deposited into the developing embryo at high levels, there are enough histone proteins present to support the development of homozygous mutant His^{D} embryos through the first 14 cell cycles of embryogenesis

(Smith et al. 1993, Gunesdogan et al. 2014). Therefore, we were able to monitor the expression of zygotic histone genes at cycle 15. As depicted in Figure 3.1C, both His^{D} and $Df(2L)His^{C}$ lost signals by phospho-histone H3 staining (p-H3S28) (Yung et al., 2015) compared to the wild type (w^{1118}), indicating that in His^{D} mutant the cell cycle was completely arrested and H3 genes have been removed. In addition, resupplying the His^{D} mutant with 20 copies of His-GUs could fully rescue the cell-cycle arrest (Figure 3.1C, compare w^{1118} with 20 His-GUs allowing the embryos to develop into adulthood).

At least twenty copies of the histone genes are required to generate flies with wild-type morphology

Previously, it was reported that 2 copies and 6 copies of the His-GUs result in developmental defects and lethality, respectively, during larval development, and that 12 or more copies of His-GUs fully rescues this lethality (Gunesdogan et al., 2010; McKay et al., 2015). In order to evaluate the phenotypes of His^{D} transgenic flies, containing varying numbers of reintroduced His-GUs, transgenes containing His-GUs were introduced into the His^{D} background and the resulting flies and embryos were analyzed. Consistent with previous reports, we found that resupplying at least 8 His-GUs was necessary to produce viable flies, although the rescue ratio was quite low (less than 10%) (Figure 3.2A). The ratio improves with an increasing number of His-GUs. With 12 copies, the rescue ratio was about 75%. Near 100% efficiency of rescue is achieved in flies with 20 or more His-GUs (Figure 3.2A).

It has been reported that previously generated “24× His-GUs” transgenic flies showed no significant differences of histone expression at the protein or mRNA levels

compared to wild-type flies because of the histone gene dosage compensation mechanism (McKay et al., 2015). We tested if the dosage compensation could also help to keep a steady level of histone proteins when they were integrated at their original locus by monitoring the amount of histone H3, H4 and H2B in our flies complemented with different number of His-GUs. Consistently, we also found that histone proteins were expressed similarly in adult flies different numbers of His-GUs (Figure 3.2C and Figure S3.2A). Next, to test whether chromatin structure is affected by the number of His-GUs, we dissected the salivary glands from third instar larvae and analyzed the polytene chromosomes from both wild type and flies with 12, 16 or 20 copies of reintroduced His-GUs. However, we failed to observe any detectable abnormalities (Figure S3.2B). We conclude that 12 or more copies of histone genes leads to similar levels of histone expression in adult flies, agreeing with previous findings (McKay et al., 2015).

A recent study mentioned a defect in fertility with 12 copies of the histone gene (McKay et al., 2015), but without any further analyses. To test if different numbers of histone genes affect fertility in our system, we measured how many adults could be produced from either His^{D} mutant males crossed to wild-type females, or His^{D} mutant females crossed to wild-type males. As shown in Figure 3.2C, we found there is no obvious decrease in the number of adult progeny from males containing 12 to 24 His-GUs. However, a significant decrease in fertility was observed from female flies containing 16 or less His-GUs. Very few adult flies could be obtained when there are only 12 His-GUs. Increasing the number to 16 could produce more progeny compared to 12 His-GUs but still yielded significantly fewer flies compared to wild type. Only when the number of His-GUs increased to 20 or more, similar number of adults compared to wild

type could be obtained (Figure 3.2D). Therefore, the number of His-GUs affects fertility in female flies but not male flies, consistent with previous findings (McKay et al., 2015).

To find reasons for the fertility defects, we monitored the integrity of testes or ovaries in flies containing different numbers of histone genes. We classified the testis or ovary into three different categories based on their morphology defects (Figure 3.2E and 3.2F). We found that in male flies, around 80% or more testes appeared normal when males had at least 12 His-GUs (Figure 3.2E). A small portion (< 5%) of flies with mild phenotypes (shorter and thinner) could be observed even in His^{D} flies rescued with 24 or lower copy number of His-GUs. In female flies ovary development is severely disrupted in flies with 16 or less copies of histone genes (Figure 3.2F). Around 90% of ovaries in flies with 12 copies of His-GUs and 65% of ovaries in flies with 16 copies of His-GUs do not produce mature eggs. This is consistent with our female fertility results (Figure 3.2D). We conclude that a reduced number of histone genes leads to developmental defects of both the testis and the ovary, with more severe effects on ovary development.

Histone dosage affects fertility by interfering with oocyte development and spermatogenesis

In order to have a deeper understanding of how oogenesis and spermatogenesis are affected by reduced histone gene dosage, we immunostained ovaries and testes from flies carrying different copy numbers of histones and analyzed their morphology using serial confocal microscopy. The *Drosophila* ovary is composed of interconnected chains of egg chambers (ovarioles) and its germline stem cell niches are located at the tip of each ovariole within a structure called the germarium. At the anteriormost portion of the

germarium a group of non-dividing somatic cap cells is surrounded by 2-3 germline stem cells (GSCs) which continuously self-renew and produce differentiating germ cells. Follicle stem cells (FSCs) produce follicle cells and form a columnar epithelium to envelop the germline cyst as it moves through the germarium. After an egg chamber buds off the germarium, it grows in size. Five to eight follicle cells become stalk cells and separate adjacent egg chambers (Dobens and Raftery, 2000). Defects in budding processes cause egg chambers with excessive germline cysts, which leads to reduced fecundity or sterility (Edwards and Kiehart, 1996; Ruohola et al., 1991). Here we found that ovaries from female flies carrying 24 copies of histones appear phenotypically indistinguishable from wild-type ovaries. In female flies with 20 His-GUs, 56% of the ovaries look normal, while 44% of the ovaries have mild budding defects, whereas early stages of egg chamber fail to separate from the germarium. This might explain why more than 90% of females with 20 His-GUs produce mature eggs (Figure 3.2D). Ovaries from females with 16 or fewer copies of His-GUs show very strong defects in oogenesis. Mid-stage egg chambers are undetectable in ovaries with 16 His-GUs. All early to mid stages of egg chambers are missing from most of the ovaries with 12 His-GUs or less. We thought perhaps the budding defects might arise from decreased division rate of follicle cells due to reduced histone levels in vivo. In other words, high histone levels ($\geq$ 20 copies) may be required to keep germ cells dividing normally in order to produce eggs. Interestingly, we found that the germline stem cell niche (open arrow head) in the defective ovarioles looks quite normal, containing both stem cells and their differentiating progeny (Figure 3.3A). This suggests that mid levels of histone dosage (12~16 copies) are sufficient to support the normal divisions of GSCs in the ovary.

As in the ovary, the *Drosophila* testis stem cell niche is located at the testis apex, where a group of ~10-15 non-dividing somatic cells called the hub send signals to the surrounding GSCs and cyst stem cells (CySCs, dark green cells) (Hardy et al., 1979; Leatherman and Dinardo, 2010; Tulina and Matunis, 2001) (Figure 3.3B). The differentiating daughter of the GSC division, called a gonialblast, undergoes 4 rounds of synchronous mitotic divisions while further differentiating into 2-, 4-, 8- and 16-cell spermatogonial cysts and finally undergoes meiosis and spermiogenesis to become sperm. With the decrease of histone copy numbers in male flies, the number of GSCs also decreases accordingly. Male flies carrying 20 or more His-GUs appear wild type, containing around 10.4 GSCs. Around 4-5 GSCs are found in males with 10 His-GUs compared to around 11 GSCs in heterozygous histone deficiency flies. This indicates that histone dosage might also affect GSC division in the testis. Hubs from testes containing low copy number (≤ 16 copies) of His-GUs also appear smaller and contain fewer cells than wild-type flies. Therefore, it is also possible that since the hub is smaller in testes containing low copy number of His-GUs (≤ 16 copies), GSCs and CySCs are depleted as a secondary consequence. However, even flies with 8 His-GUs still have more than 4 GSCs per testis niche and therefore might still be able to produce enough sperm to maintain fertility. Together, these results suggest that spermatogenesis and oogenesis are both affected by histone gene dosage.

A hierarchical assembly method for high-throughput and systematic construction of histone mutant arrays

One limiting factor in high-throughput histone mutagenesis using the previously developed system is the construction of the arrays containing multiple copies of each mutant, which is tedious and time-consuming. To solve this problem, two important issues need to be addressed. One is to introduce a single mutation at a single defined site while keeping all the other histone genes intact. The other is to generate the repetitive histone groups, which contain multiple copies of the same mutants. Here, we introduced a hierarchical strategy, which allows rapid construction of many histone mutants that can be assembled into five-copy arrays (Figure 3.4A).

To facilitate mutagenesis of histone genes within each His-GU, we divided the five-histone genes among three vectors, harboring histone H3 and histone H4, histone H2A and histone H2B, and histone H1, respectively. This allowed simultaneous mutagenesis of each individual histone gene. Using pre-designed restriction enzymes, each histone gene could be reassembled into the original vector to form a complete His-GU bearing the mutation. This strategy not only allowed us to generate a histone group containing one particular mutation, but also the option to generate double or triple mutants, if necessary. Once a histone group is ready for making the desired arrays, it can be released from the vector and cloned back into the same vector to generate a plasmid containing two copies of the same mutated histone group. This step can be repeated once to generate an entry plasmid with three copies of the histone group. At the same time, the two copies of histone groups could be released and cloned into *pUASTattB* (Bischof et al., 2007) to facilitate injection for transgenesis. In the last step, the entry vector was recombined into the other plasmid using the Gateway system to yield the final plasmid

containing five copies of the same mutated His-GUs, which was used to inject the embryos.

This approach allows one to construct many histone mutants and assemble them into five-copy arrays in as few as ten days (Figure 3.4A). Combining this approach with the design of two *attP* sites at the endogenous histone locus, a single injection would allow us to incorporate ten copies of the same histone mutants. Only a single round of crossing is required to generate homozygous flies containing twenty copies of the same histone mutant. Therefore, this system allowed us to test numerous histone mutations in a short period of time, greatly enhancing our ability to understand the function of histones and their modifications in metazoan.

Validation of transgenic flies containing arrays of mutated histones

After injection, we initially generated heterozygous lines containing the mutated His-GUs on one chromosome and wild-type histone genes on the other chromosome (His^D). Therefore we worried that recombination could potentially occur between the mutated histone locus and the adjacent endogenous histone locus. To rule out this possibility, we performed several assays to validate each mutant line. Since a *Sal*I recognition site was inserted between histone H3/H4 and histone H2A/H2B to facilitate cloning, a pair of primers was designed to amplify the DNA flanking the *Sal*I site. The amplified DNA was digested with *Sal*I and the size of the fragments was analyzed. As shown in Figure 3.4B, none of the DNA is cut in the wild type line. However, the amplified DNA is completely digested in the homozygous mutant line. In the heterozygous mutant line, only a very small portion of amplified DNA could be digested,

which indicates the presence of both wild type and mutated genes. In addition, this assay allows us to estimate the copy number of histone genes, similar to a previous assay (ref). By quantifying the amount of digested and undigested DNA, we estimated the copy number to be about 83 using histone H4K8A mutant and 103 with H4K16A mutant (Figure 3.4B and Figure S3.14). This is consistent with the estimate of about 100 copies obtained previously (McKay et al., 2015).

Next, we designed a strategy to quickly identify the presence of mutated histone genes in heterozygous flies by designing primers spanning the *Sal*I site, which allowed us to distinguish flies containing the mutated histone genes (Figure 3.4C). Flies containing histone mutants were amplified using this strategy and the corresponding DNA fragments were sequenced to verify the presence of specific mutations (Figure 3.4C and Figure S3.14). Finally, a modification-specific antibody, if available, was used to detect the presence of the modification in wild-type flies but absence in the mutant flies, as exemplified in Figure 3.4D with anti-H4K8Ac antibody. All of our histone mutants that could be assayed using commercially available antisera to histone modifications yielded the expected results.

Alanine substitution mutations in many histone residues impair fly viability

Using the above strategy, we targeted 44 different amino acid residues on histone H3 and H4 known to be posttranslationally modified, generating a library of alanine substitution mutations. Among the 44 mutants, we obtained 42 lines with the His-GUs integrated at the original locus, including four lines in which the 5× His-GUs was only integrated at one of the two *attP* sites (not further investigated in this paper). Therefore,

we successfully constructed 38 histone mutant fly lines, which could allow us to evaluate the function of these modifications directly *in vivo*.

Each mutant was homozygosed to generate flies containing 20 copies of the mutated *His-GUs*. To our surprise, among the 38 lines, we found 17 (44.7%) are essential as we failed to obtain the desired homozygous flies after screening hundreds of individuals (Table 1). This number is much higher than what is observed in yeast, where ~ 90% of the mutants are dispensable for cell survival (Dai et al., 2008; Nakanishi et al., 2008). This implies that there are very different requirements for histone modifications between the single cell yeast system and multicellular organisms. Furthermore, by keeping the histone mutant lines over a GFP-marked balancer chromosome, (containing GFP on Chr 2, genotype: *Cyo, P[ActGFP]MR1*,) we could perform survival tracing tests of homozygous mutant embryos and larvae, by monitoring loss of GFP. This analysis allowed us to identify the stages where the histone mutants failed to pass, and therefore, potentially instructs further experiments. In addition, it also provides us with a platform to study the function of certain histone amino acid residues before the stages where they are required for viability, such as H3K27A (see below). Among the 17 mutants, we found that five are embryonic lethal, three are larval lethal and nine are pupal lethal (Table 3.1 and Figure S3.11 A). Moreover, some of the mutants which are not fully lethal show an obvious reduction in viability, including H3T3A, H4K16A and H4K77A, which produce 31.9%, 40.3% and 28.6% of the expected number of progeny compared to that of wild type, respectively. Interestingly, we found H4K16A showed a striking sex-specific bias in viability. The viability rate of homozygous females was 40.3%, but the rate decreased to 2.2% in homozygous males for unknown reasons.

Histone mutants impact fertility more than adult morphology

For all viable mutants, we examined the visible morphologies of adult flies including the mouth parts, antennae, eyes, legs, sex combs and wings. Only minor defects on wings were observed in H3R17A (28.6%) and H4K16A (33.3%) (Table 1, Figure S3.8), suggesting the majority of these viable mutations cause only very minor defects during development. Second, we measured the fertility of the mutant flies as described above by calculating the ratio of adult progeny between the mutant and the wild type (20 His-GUs) when they are crossed to a wild-type fly. We found that the fertility of female flies was more sensitive to the histone mutations than males (Table 1). A fertility ratio, generated by dividing the number of mutant adult progeny by the number of wild-type progeny, was used to represent fertility. This ratio was above 50% for all of the remaining males carrying the histone mutations except for H3R17A mutant males, which had a fertility ratio of 31.62% (Figure S3.10A). On the other hand, female flies containing H3T3A, H3R17A, H3K56A and H4K16A mutations were completely sterile, and those with H3K23A, H4R23A and H4R92A mutants were nearly sterile, with an average of ratio below 10% (Figure S3.10 B).

Since histone gene dosage affects fertility by interfering with oogenesis and spermatogenesis, we examined the testes and ovaries of flies with reduced histone gene copy number at five days of age, classifying them into three categories as defined above (Figure 3.2E and 3.2F). Consistent with what we observed in fertility tests, we found that most male mutant flies have phenotypically wild-type testes (>90%, Figure S3.10B). Only two mutants, H3T3A and H4K31A, had notable defects in over 20% of their testes (Figure S3.10B). On the other hand, a large portion (9/15) of the histone mutants showed

defects during oogenesis. In some mutants, such as H3K56A and H4K16A, none of the ovaries examined showed wild-type morphology and the majority (~90%) was severely affected, consistent with the female sterile phenotype described above. Together, our data support the conclusion that histone mutations preventing many different PTMs have a profound impact on oogenesis, and a small subset can affect spermatogenesis, but most have no effect on the visible morphology of adulthood.

Histone mutants and DNA damage

Various types of histone modifications have been documented to be functionally involved in the process of DNA damage response (DDR) in different model systems. For example, in the yeast *Saccharomyces cerevisiae*, both acetylation and deacetylation of histones H3K56 promotes cell survival in response to genotoxic stress (Celic et al., 2006; Hyland et al., 2005; Reid et al., 2011; Simoneau et al., 2015; Wurtele et al., 2012; Wurtele and Verreault, 2006). However, the functions of histone mutations related to genotoxic agent–induced DNA lesions are poorly understood in multicellular organisms. Therefore, we carried out a damage sensitivity screen using both UV and X-ray irradiation.

In general, we found that the histone mutant larvae are more sensitive to X-ray irradiation than UV irradiation (Figure S3.12). Consistent with previous reports in flies lacking the histone modifying enzyme CBP/p300 (Das et al., 2009), our H3K56A mutant, which prevents any modifications at this site, also showed a dramatically increased sensitivity to both UV and X-rays, underscoring a critical role of K56ac in both pathways. In addition, the H4T1A mutant exhibited severe sensitivity to X-rays and

minor sensitivity to UV irradiation, which is in agreement with the report that phosphorylation of H4S1 is induced at DSBs in *S. cerevisiae* (Cheung et al., 2005). Notably, several mutants showed differential responses to UV and X-ray, including H3T3A, H4R23A and H4R92A. These mutants showed no significant difference compared to wild type upon UV exposure but were significantly more sensitive to X-rays, particularly H3T3A and H4R23A. This presumably indicates the specificity of their involvement in DSB repair. Taken together, these histone mutations enabled us to reproduce the DNA-damage phenotypes known to occur by mutating the corresponding histone modifying enzymes, and to also identify new histone residues that might be intimately involved in regulating DDR in *Drosophila*.

Selective activation of retrotransposons in specific histone mutants

The transposable elements that shape most of the eukaryotic genome are kept silenced to prevent harmful mutagenesis (Mugnier et al., 2008). However, the regulatory mechanisms of their silencing are poorly understood. To evaluate the impacts of epigenetic regulation during this process in *Drosophila*, we analyzed the expression of copia, a heterochromatic LTR retrotransposon, which is usually silenced (de Setta et al., 2011). As shown in Figure S3.13A and summarized in Table 1, several histone mutants (H3K9A, H3K23A, H3K56A and H4R23A) showed strongly increased expression of copia, indicating the de-repression of this retrotransposon in the mutants. In *S. pombe*, it has been shown that the localization of Swi6, a homologue of *Drosophila* Heterochromatin Protein 1 (HP1), to heterochromatic regions requires methylation on H3K9 (Nakayama et al., 2001). This finding is consistent with the loss of copia repression we identified in the H3K9A mutants. Our work also suggests that several

additional histone PTMs, (Figure S3.14), may be involved in the process of retrotransposon silencing.

We therefore chose two histone mutants, H3K9A and H3K56A to ask if the expression of additional transposable elements including Het-A, I-element, mdg, Mst40 and ZAM was also upregulated. To our surprise, we found only the expression of copia was increased in both mutants. Mst40 and mdg are specifically upregulated in H3K9A and H3K56A respectively (Figure S3.13B-C), inferring the presence of distinct regulatory mechanisms. Further studies are required to dissect the underling mechanisms.

Discussion

A "designer" system to study histone function *in situ*

Currently the only system permitting the analysis of histone residue function in animal development is that established by Herzig and colleagues, in which the endogenous histone gene cluster is removed and complemented with plasmid-based transgenes (Gunesdogan et al., 2010, 2014; Hodl and Basler, 2012; Pengelly et al., 2013). More recently, a BAC-based transgene was established, reducing the amount of transgenes from a minimum of four to just one, which greatly shortened the time to test a given mutant (McKay et al., 2015). However, it is still quite time and labor intensive to create a BAC vector containing 12 copies of the histone gene cluster. Therefore, prior to our work, only less than ten mutations were assayed. In addition, since complementation is achieved by transgenes, it was not possible to test if the same phenotype could be produced when the histone genes were integrated at their original locus. Therefore, we designed a new system in *Drosophila* which enables us to 1) delete the entire histone gene cluster from the genome; 2) integrate the mutated histone genes at the endogenous locus; 3) reduce the transgenes needed to rescue histone null flies to a single plasmid and 4) perform systematic histone mutagenesis in an animal model.

Deletion of the histone cluster was achieved by incorporation of two FRT sites flanking the cluster using the CRISPR/Cas9 method. To allow *in situ* integration of the histone genes, *attP* was introduced simultaneously during the insertion of FRT sites, in a way that when the histone cluster was removed by inducing Flp recombinase, it will be retained to accept donor plasmids at high efficiency.

During the process of integrating the FRT site, we accidentally introduced two *attP* sites, which turned out to be a great advantage of our system. The time and labor consumption for the cloning of multiple His-GUs was reduced significantly. Only a plasmid containing six copies of His-GUs is required to generate the "24x His-GUs", which otherwise requires the construction of a BAC vector with 12x His-GUs (McKay et al., 2015). In order to further increase the throughput to generate the histone mutations, we arbitrarily divided His-GU into three parts, allowing mutagenesis of all five histones simultaneously. The individually mutated histone genes could be assembled into one His-GU by a simple subcloning step and subjected to further assembly into multiple copies for injection. We roughly calculated the amount of time to generate a batch of histone mutations using this design and found that one person could potentially finish cloning tens of plasmids containing multicopy His-GUs within 10-days. Therefore, the new system could enable us to achieve our goal to perform systematic histone mutagenesis in the animal model.

The lethality profile of histone mutants differs between yeast and animal

In budding yeast, only 5-15% of the histone H3 and H4 point mutants are lethal and none of them reside within the N-terminal tail domains (Dai et al., 2008; Nakanishi et al., 2008). In fact, although most of the PTMs occur in the tails, the N-terminal tails on histone H3 and H4 are dispensable for growth (Kayne et al., 1988; Morgan et al., 1991). These findings are surprising, given the high conservation of histones and the critical function of each modification. One possible explanation is that some of the functions of these modified residues may not be essential in a single cell organism. However, they

might become crucial when the regulation of chromatin-associated activities relies more on PTM-related epigenetic modifications in multicellular organisms.

In this study, we investigated 38 mutants on the modifiable residues on histone H3 and H4 in *Drosophila* and identified 17 residues that are essential for viability (Table 3.1). Among the 17 mutants, two of them, H3Y41A and H3T45A are known to be lethal in budding yeast. Another mutant, H4Y88A is not required for survival but the glutamate substitution at this site completely abolishes viability (Dai et al., 2008). In addition, several well-studied and functionally important modification sites, such as H3K4, H3K9 and H3K36, which are dispensable in budding yeast, become essential in flies. Together, these data support the hypothesis that additional essential functions are carried out by these modified residues in multicellular organism, which are not required in the single cell budding yeast. Consistently, a recent study also showed that the H3K36R mutant, which is viable in yeast, could not complete development in *Drosophila* (McKay et al., 2015). Furthermore, the function of each essential residue is apparently not the same since mutations on these residues blocks development at different stages.

Histone dosage is critical for normal development of the testis and ovary

Currently, the genome annotations (FlyBase) list only 23 copies of His-GUs on chromosome 2L. In contrast, recent studies suggest there are over 100 copies of the repeats (Lifton et al., 1978; McKay et al., 2015) and we also estimated a similar number (Figure 3.4B and Figure S3.14). However, as few as 8 His-GUs are required to obtain a viable fly (Figure 3.2A and Figure S3.4), and 12 His-GUs seem to be enough to produce flies with no obvious phenotypes (Figure S3.4) (Gunesdogan et al., 2010; McKay et al.,

2015), providing a chance to study the function of histone mutations without reconstructing the entire histone gene array.

A recent report indicated that reducing the number of histone genes to 24 or 12 copies resulted in the reduction of fertility in female flies, although the reason is unknown (McKay et al., 2015). Our results suggest that reduced copy number of His-GUs causes developmental defects in both testis and ovary, with more severe defects during ovary development (Figure 3.2D and 3.2E), consistent with their report. Interestingly, we find that the ovarian defects are not due to the loss of GSCs in the ovary, and instead the process of egg chamber budding from the germarium is impaired (Figure 3.3A), which leads to reduced fecundity or sterility (Edwards and Kiehart, 1996; Ruohola et al., 1991) and explains the severe fertility defects in females. On the other hand, we find that the number of GSCs in the testis is reduced with decreased histone gene copy number. One possibility is that the GSC division in the testis is delayed because it is known that histone supply regulates the length of S phase during cell cycle (Gunesdogan et al., 2014).

Experimental Procedures

Fly strains

The following fly stocks were used in this study: w^{1118}, *yw hs-flp122; Ubi-GFP FRT* (a gift from Renjie Jiao), *φc31* (Bischof et al., 2007), and w^{1118}*; Df(2L)BSC104/CyO* (Günesdogan et al., 2010), His^{C} (Bloomington Stock Center, BSC 8670). CyO/sna^{Sco} (BSC 2555). Flies were cultured at 25°C on standard cornmeal/sugar/agar media.

CRISPR/Cas9 mediated HisD fly mutant construction

The CRISPR/Cas9 system was established and applied to gene targeting in *Drosophila* (Yu et al., 2013). Two guide RNAs (gRNAs), whose target sites flank the histone gene cluster in chromosome 2, were used to introduce DNA double-strand breaks at each side of the histone gene cluster into two *w1118 flies*. To take advantage of site-specific homologous recombination (HR) in *Drosophila*, two *FRT* sites were integrated into each side of the histone gene cluster. His^{D} was generated by crossing and inducing the rearrangement of two *FRT* sites which deleted the entire histone cluster out from one chromosome. The sequences of gRNAs are listed below. Underlined sequences indicate the target sites for guide RNAs:

His-T7gRNA-L1:

TAATACGACTCACTATAGGGCTCATCGAAGCAGTTGTGTTTTAGAGCTAGAAAT

AGC

His-T7gRNA-R1:

TAATACGACTCACTATAGGACTTACAGCTGTACGTTGGTTTTAGAGCTAGAAAT

AGC

Plasmid construction and synthesis

The Gateway cloning system was modified and used to assemble multi-copy histone units into a vector suitable for transgenesis. The attL1 and attL2 sequences were amplified from the *pCR8/GW* vector (Invitrogen, K2500-20) and assembled into a *pSMART* vector. The *pSMART* vector contains a kanamycin resistance marker, into which KpnI and NotI restriction sites were added between two attL sequences. The newly generated vector was named *pSMART-attL*. The attR1 and attR2 sequences, together with a ccdB gene and chloromycetin resistance gene, were amplified from the *pDEST22* vector (Invitrogen, Gateway destination vector) and assembled into a *pUAST-attB-*w^+ vector (Bischof et al., 2007) by SbfI and NotI restriction sites. The newly generated vector was named *pUAST-attB-*w^+*-attR*. A primer pair that specifically targeted both sides of one histone unit in the chromosome was used for wild-type histone unit assembly. The forward primer contained KpnI and AgeI restriction sites, and the reverse primer contained NotI and XmaI restriction sites. KpnI and NotI restriction sites were used for shuttling one histone unit assembly from the *Drosophila* genome to the *pSMART-attL* vector. A SalI restriction site was introduced between histone H4 and histone H2A to facilitate histone mutagenesis.

In order to introduce amino acid mutations into specific histone modification sites, the wild-type histone unit was divided into three parts: histone H1, histone H2A and H2B, and histone H3 and H4. Each part was cloned into a single pUC19 vector using the following restriction enzyme combinations, XmaI/BglII, BspHI/SalI and SalI/KpnI respectively, creating three plasmids called pUC19-H1, pUC19-H2A/B and pUC19-H3/4.

Mutations were introduced through site-directed mutagenesis using primers that changed the destination codon to GCC (encoding alanine).

To increase the histone copy number within the *pSMART-attL* vector, KpnI and XmaI were used to excise a single histone unit and insert it back into the same plasmid, which was then linearized by AgeI and KpnI. Because AgeI and XmaI are isocaudomers, the same strategy was used to increase the histone unit copy number to three in this vector. In the *pUAST-attB-w*$^{+}$*-attR* vector, KpnI and NotI restriction sites were introduced upstream of the attR1-ccdB-cmR-attR2 cassette. Two histone units were inserted into the *pUAST-attB-w*$^{+}$*-attR* vector using KpnI and NotI. The Gateway LR clonase kit (Invitrogen, 11791-020) was used to insert three histone units into the *pUAST-attB-w+* destination vector. The final construct contains a total of five histone units, three from the *pSMART-attL* vector and the two from the *pUAST-attB-w+-attR* vector (Figure 3.4A).
In order to insert an attP-*FRT* cassette downstream of the histone cluster in the genome, a synthetic plasmid donor named *pAV-R*, which contains homologous arms (ArmC, left; ArmD, right), an attP-*FRT* cassette and a RFP selection marker, was synthesized by Wuxi Qinglan Biotechnology Inc.

To construct the conditional histone deletion system, the *pAV-R* donor plasmid was modified to include an eGFP marker driven by an ubiquitin promoter that was inserted between the left homologous arm and attB sites via the Golden gate cloning method.

Plasmid midi-preparation

The constructs containing five copies of mutated or wild-type histone units were transformed into DH5α competent cells and cultured at 30°C for 24 hours. A single

colony was inoculated into a 1L flask containing 200 mL of LB medium, and cultured at 30°C, 220 rpm for 24 hours. Bacteria wet weight was normalized to 1g after harvest. The plasmid was extracted using a Plasmid Midi kit (QIAGEN, 12143) following the recommended protocol, and the plasmid concentration was quantified using a 2000c NanoDrop. The plasmid was further purified by phenol/chloroform/isoamyl alcohol (25:24:1) and normalized to 1.5 μg/μL. The normalized plasmid was centrifuged at 18000rpm for 1 hour at 4°C. The supernatant was then transferred carefully to a new tube and stored at -20°C.

Drosophila embryo microinjection

His^{D} male flies were mated with φC31 virgin flies. Three or four days later, 0-1h embryos were harvested for microinjection (Miller et al., 2002). For each histone mutant construct, about 1000 embryos were injected.

Genomic DNA preparation and histone construct double integration verification

3-5 *Drosophila* adults were homogenized in 100 μL Lysis buffer (10mM Tris-HCl PH8.0, 0.5 mM NaCl, 20 mM EDTA, 50 μg/Ml RNase A and 1%SDS) and incubated at 30°C for 1 hour. Samples were then transferred to a 65°C heating block for 30 min. Next, 100 μL of phenol/chloroform/isoamyl alcohol was added and the tube was gently vortexed. The tube was then centrifuged at 15000 rpm for 10 min and the supernatant was transferred into a new tube. The DNA was precipitated with an equal volume of isopropanol at -20°C for 30 min then centrifuged at 15000 rpm at 4°C for 10 min. The supernatant was discarded, and the pelleted DNA was washed with 500 μL of 70%

ethanol and dried using a vacuum pump at RT for 5 min. The genomic DNA was resuspended in 15μL of TE buffer and stored at -20°C.

2xTaq Master Mix was used for histone construct double integration verification. 100 ng genomic DNA was used for each 10 μL PCR reaction. Both forward and reverse primers were diluted to 1 μM in 10μL of the reaction volume. The PCR program was set to 1 cycle of 94°C for 5 min, 32 cycles of 94°C/30 s, 60°C/30 s, 72°C/80 s, 1 cycle of 72°C for 7 min and 12°C keep. The PCR products were mixed with loading buffer and loaded onto a 1.5% agarose gel with 0.5 μg/mL EtBr for electrophoresis. The verification pattern was shown and discussed in Figure S3.5B.

Histone mutant sequencing validation

Drosophila histone mutants were verified by histone-specific sequencing from genomic DNA. Two different primer pairs were used for mutant gene amplification from homozygous or heterozygous adult flies. For homozygous mutants, general histone primers (WZO172 5'-taaacgtttcaaaggctaagctaaaaacc-3' and WZO101 5'-ctcattgaatctggtttgtggtcctg-3') were used to amplify a 1584bp fragment for sequencing. For heterozygous mutants, transgene specific primers (WZO371 5'-ccatttgtacagtctgtagtcgac-3' and WZO101) were used to amplify a 1320bp fragment for sequencing.

Homozygous fly mutants verification assay

A SalI digestion assay was used to distinguish between the endogenous and transgenic histone loci. In the transgenic histone unit, a SalI restriction site was

introduced between histone H4 and histone H2A. A pair of primers (WZO167 5'-gcaaagtcccgctcaaaccg-3' and WZO337 5'-ggtttttgtcgttttacctataaataggggc-3') flanking the SalI site was used to amplify a 1232bp fragment, which can then be digested by the SalI restriction enzyme into two equal length fragments. DNA fragments were mixed with the appropriate 6xDNA loading buffer and loaded onto a 1.5% agarose gel with 0.5μg/ml EtBr for electrophoresis. Gel images were generated using a TANON 1600 instrument and the DNA signal intensity was quantified via ImageJ software.

Viability statistics

Heterozygous mutant flies balanced over CyO were self-crossed to create homozygous histone mutants that were identified through the absence of the CyO balancer. The viability ratio for each histone mutant was determined by calculating the number of homozygous mutants over the total number of progeny. Three biological replicates were performed for each histone mutant.

Fertility test

Either male or virgin female histone mutant adult flies were crossed with three w^{1118} virgins of the opposite sex. Parents were allowed to mate for seven days and then discarded. The amount of progeny in each vial was counted to assess the fertility of the various histone mutants.

Morphological observation

In order to screen for morphological defects in each of the viable histone mutants and different copy of His-GUs rescued adults, the mouthparts, antennae, eyes, legs, sex combs, and wings were observed using a stereomicroscope and compared to those of w^{1118} control flies. Adult flies of the 10 His-GUs, 12 His-GUs, 16 His-GUs, 20 His-GUs and 24 His-GUs genotypes were analyzed.

To determine the phenotypes within the ovary and testis, virgin males and females were aged for five days and then their testes or ovaries were dissected and observed under optical microscope. Wing, ovary, and testis phenotypes were photographed with a Leica Mz10f microscope.

Identification of the lethal phases of histone mutants

Lethal histone mutants were balanced over *CyO, P{ActGFP}MR1* to identify homozygous mutant embryos or larvae by the absence of green fluorescent protein (GFP) expression. 150 GFP-positive first instar larvae and 150 GFP-negative first instar larvae were collected on an apple juice plate, and tracked until adulthood. For each histone mutant, the number of progeny at 2nd instar larval, 3rd instar larval, pupal, and adult stages were counted. Embryonic lethal mutants were identified by the absence of GFP-negative first instar larvae.

DNA damage sensitivity screen

Viable homozygous histone mutants, and heterozygous histone mutants balanced over *Cyo, P{ActGFP}MR1*, were screened for their DNA damage responses. GFP-positive and GFP-negative wandering 3rd instar larvae were selected and randomly

divided into control and experimental groups. The experimental groups were exposed to either 10mJ/cm^2 of UV radiation using a stratalinker 2400 (Stratagene Ltd.) or 30Gy X-ray radiation using a RS 2000 (Rad Source Technologies, Inc). After irradiation, all larvae were maintained under standard conditions for 7 days until eclosion when adults were collected and counted. The eclosion rate was calculated as: the number of eclosed flies / the number of input larvae. The eclosion rate of the experimental groups was then normalized to its paired control as follows: Normalized eclosion ratio (%) = Ratio (experimental group) / Ratio (control group) x 100. A two tailed Student's t test was performed between each mutant and the control (20 His GUs), with * indicating $p<0.05$ and ** indicating $p<0.01$.

RNA extraction and RT-qPCR

Total RNA was extracted from *Drosophila* larvae, adults or salivary glands using an RNA extraction kit according to the manufacturer's instructions (TIANGEN, DP431). The total RNA concentration was measured using a Nanodrop (Thermo 2000c), and 1ug of total RNA was then used for cDNA synthesis (TIANGEN, KR106). 2x SYBR green master mix (ABI, 4367659) was added to the RNA extract for Quantitative real-time PCR analysis using a Roche480 instrument, and the data were analyzed via LightCycler 480 software.

RNA sequencing

w^{1118}, 20 His-GUs and 12 His-GUs virgin male and female flies were collected and kept in vials for four days. Ovaries and testes were dissected for RNA sequencing.

Nucleoprotein extraction and Western blot

Drosophila larvae or adults were homogenized in Buffer M (50 mM Tris-HCl pH 7.5, 50 mM KCl, 5% Glycerol, 1 mM DTT, 0.5 mM PMSF and 0.5 mM EDTA). Nuclei were purified with miraclothes, transferred into 1.5 mL tubes, and centrifuged for 15 min at 4 °C. The supernatant was discarded and nuclei were resuspended with 100 μL Buffer M. 10 μL 3 M KCl was added to increase the final KCl concentration to 100 mM. Following genomic DNA sonification, 30 μL of 4x protein loading buffer (Takara) was added and the mixture heated for 6 min at 95 °C. Protein samples were loaded onto a 15% SDS-PAGE gel for electrophoresis. After transfer to PVDF membrane and blocking in 5% TBST dissolved in milk, protein samples were incubated with primary antisera at 4 °C overnight. Western blot signals were detected by ImageQuant LAS 4000 instrument.

Immunostaining

Testes and ovaries were dissected from 0-5 day old adult flies, and were then fixed, and stained as described previously (Matunis, 1997). The following antibodies were used: rabbit anti-Vasa (d-260) (Santa Cruz Biotechnology, 1:400); mouse anti-1B1 (1:25), mouse anti-Armadillo (N2 7A1; 1:50); guinea pig anti-ZFH1 (from J. Skeath; 1:1000). Alexa fluor-conjugated secondary IgG (H+L) antibodies (Molecular Probes/Invitrogen) were diluted at 1:200 for 568 and 633 conjugates and 1:400 for 488 conjugates. DNA was stained with 4, 6-diamidino-2-phenylindole (DAPI; Sigma) at 1 ug/ml. Fixed testes and ovaries were mounted in Vectashield (Vector Labs) for imaging.

Analysis of confocal images

Confocal images were obtained with a Zeiss LSM 5 Pascal or a Zeiss LSM 510 Meta microscope. GSCs were scored as Vasa-positive cells making contact with the hub and containing spherical fusomes. Statistical analysis of stem cell number was performed using Prism 5. Unpaired ANOVA analysis was used to compare three or more populations.

Polytene immunostaining:

Salivary glands from wandering 3rd instar larvae were dissected in 0.7M NaCl. For anti-HP1 (DSHB), anti-MSL2 and anti-MOF immunostaining, salivary glands were fixed for 7 minutes in 1.85% formaldehyde and 55% glacial acetic acid diluted in double distilled water, affixed to slides using high pressure treatment, then frozen in liquid nitrogen. The slides were washed with cold and room temperature 1xPBS for 10 min then washed for 3x15min in 0.1% PBST (TritonX-100). The slides were blocked in normal goat serum (CWBIO) for 1-2h at room temperature. After blocking, the slides were incubated in 40ul of primary antibody at 4°C overnight. Slides were washed for 3x15 min in 0.1% PBST (TritonX-100) and goat anti-mouse or goat anti-rabbit secondary antibodies were added to the slides for 2 h at RT in the dark. Slides were then washed 3x5 min in PBS and mounted in Vectashield (H-1200) containing 4', 6-diamidino-2-phenylindole (DAPI).

Ovary immunostaining:

Female flies were kept for 3, 5, and 7 days with a few male flies and transferred to fresh vials of food every other day. Ovaries were dissected in 1x PBS and fixed in 4% paraformaldehyde in PBS, pH 6.9, at room temperature for 15-20 min. Ovaries were washed in 0.5% PBST (TritonX-100) for 30 min followed by 3 x 15 min washes in 0.1% PBST (TritonX-100) at room temperature. Ovaries were then blocked with goat serum (CWBIO) for 90 min at room temperature and incubated at 4°C overnight in mouse monoclonal anti-1B1 (DSHB) antisera and rat anti-vasa (DSHB) antisera diluted in 0.1% PBST (TritonX-100). Ovaries were washed 4 x 15min with 0.1% PBST (TritonX-100), then incubated in the dark with goat anti-Rat (Invitrogen A-11007) and goat anti-mouse secondary antibodies for 2 h at room temperature. Ovaries were washed 4 x 15 min with 0.1% PBST (TritonX-100) again, eggs were discarded, and the remaining ovaries mounted in Vectashield (H-1200) containing 4', 6-diamidino-2-phenylindole (DAPI).

Antisera, (source), working concentration：

mouse anti-MSL2, (a gift from Peter B. Becker), 1:200

mouse anti-MOF, (a gift from Peter B. Becker), 1:200

mouse-anti-HP1, (DSHB, C1A9), 1:50-1:100

mouse anti-1B1, (DSHB, 7H9 1B1), 1:200

rabbit anti-H4K16ac, (Santa Cruz, SC8662-R), 1:50

rat anti-vasa (DSHB, anti-vasa),1:200

goat anti-Rat (Invitrogen A-11007), 1:200

goat anti-mouse, 1:200

goat anti-rabbit, 1:200

Embryo immunostaining

Embryo collections were obtained by restricting egg deposition to 30 min with subsequent aging at 25°C for the appropriate length of time. Embryos were dechorionated with 50% bleach, fixed in 1:1 heptane (Sigma, 24,665-4): 3.7% formaldehyde (Calbiochem, 344198) mixture for 20 min and then devitellinized in a 1:1 heptane/methanol mixture followed by washes and storage in methanol as described in *Drosophila protocols*. Embryos were re-hydrated in PBTA solution（1x PBS, 1% BSA, 0.1% Triton X-100, blocked for 30min at room temperature and incubated with primary antibodies at 4°C overnight in PBTA following washes in PBTA for 20 min, three times. Secondary antibody incubation was in PBTA for 1 h at room temperature. After incubation, embryos were washed for 20 min in PBTA three times, then mounted in Vectashield. Micrographs were acquired on a Zeiss LSM 780 upright confocal microscope.

Clonal analysis and wing disc staining

Embryos were collected for 24 hours in vials, and aged 1 day at room temperature then heat-shocked at 38°C for 1h, then incubated at 28 degrees until the third larval instar (about 4 days after heat-shocking). 3rd instar larvae were dissected in 1x PBS and fixed for 20 minutes in 4% paraformaldehyde (Sigma, 158127) in 1xPBS. Samples were washed for 15 min, three times with 0.1% Triton X-100 in PBS, then incubated in block solution (1% BSA, 0.1% Triton X-100 in PBS) at room temperature for 1h, then with primary antibodies in 0.1% Triton X-100 in PBS overnight at 4°C. After being washed three times for 15 min with 0.1% Triton X-100 in PBS, samples were incubated with

secondary antibodies before DAPI (diluted 1:1000) staining. Samples were washed three times for 15 min with 0.1% Triton X-100 in PBS . Imaginal discs were carefully removed from the cuticle and mounted in Vectashield. Wing discs were imaged using a Zeiss LSM780 upright confocal microscope.

The following antibodies were used:

Rabbit anti-CyclinB, 1:100;

Mouse anti-H3K27me3, PTM-651, 1:200;

Ubx, DSHB FP3.38, 1:200;

Abd-B, DSHB 1A2E9, 1:200;

Rabbit anti-GFP, Abcam ab6556, 1:500;

Mouse anti-H3K9me3, active motif 39285,1:200;

Goat anti-mouse, 1:200;

Goat anti-rabbit, 1:200;

Histone mutagenesis primer list

Mutants	Forward	Reverse
H3T3A	acgagccatctccgatttggg	gccaagcaaactgctcgcaaatcgac
H3K4A	ggtacgagccatctccgatttgg	gcccaaactgctcgcaaatcgac
H3T6A	ttgcttggtacgagccatctcc	gccgctcgcaaatcgactggtgg
H3R8A	agcagtttgcttggtacgagc	gccaaatcgactggtggaaaggcg
H3K9A	gcgagcagtttgcttggtacgag	gcctcgactggtggaaaggcgc
H3S10A	tttgcgagcagtttgcttggtac	gccactggtggaaaggcgccac
H3R17A	tggcgcctttccaccagtc	gccaaacaactggctactaaggccgc
H3K18A	gcgtggcgcctttccac	gcccaactggctactaaggccgctc

H3K23A	agtagccagttgtttgcgtgg	gccgccgctcgcaagagtgc
H3R26A	agcggccttagtagccagttg	gccaagagtgctccagccaccg
H3K27A	gcgagcggccttagtagccag	gccagtgctccagccaccggag
H3S28A	cttgcgagcggccttagtag	gccgctccagccaccggagg
H3K36A	cacacctccggtggctggagc	gccaagccccaccgctatcgc
H3T45A	tccagggcgatagcggtg	gccgtggccttgcgtgaaattcgtc
H3K56A	ttggtagcgacgaatttcacgcaag	gccagcaccgagcttctaatccg
H3K64A	gcggattagaagctcggtgc	gccctgcctttccagcgtctgg
H3K79A	aaagtcctgagcgatttcacgc	gccacggacttgcgattccagag
H4T1A	cattttcactgttctatactattatacacgcacagc	gccggtcgtggtaaaggaggcaaag
H4R3A	accagtcatttttcactgttctatactattatacacg	gccggtaaaggaggcaaaggcttgg
H4K5A	accacgaccagtcatttttcactg	gccggaggcaaaggcttgggaaag
H4K8A	gcctcctttaccacgaccagtc	gccggcttgggaaagggtggcg
H4K12A	tcccaagcctttgcctcctttac	gccggtggcgccaagcgtc
H4K16A	ggcgccacccttttcccaagc	gcccgtcatcgcaaagtgctgc
H4R23A	cagcactttgcgatgacgcttg	gccgataacatccaaggtatcacgaagc
H4Y51A	tatgagtccagatatgcgcttcacacc	gccgaggaaacgcgtggcgttc
H4K77A	ggcgtgttccgtgtaggtc	gccaggaagacagttacagccatggatg
H4Y88A	cacaacatccatggctgtaactgtc	gccgctctgaagaggcaaggccg
H4K91A	cagagcgtacacaacatccatgg	gccaggcaaggccgcacc
H4R92A	cttcagagcgtacacaacatccatgg	gcccaaggccgcaccctctacgg

Acknowledgements

This work was supported in part by National Science Foundation of China 31471254, Research Fund for the Doctoral Program of Higher Education of China 20120002110022, Chinese Minister Of Science and Technology 2012CB725201 and Tsinghua University Initiative Scientific Research Program 2011Z02296 to J.D. and by R01HD040307 to E.M.

Reference

Bannister, A.J., and Kouzarides, T. (2011). Regulation of chromatin by histone modifications. Cell Res *21*, 381-395.

Bischof, J., Maeda, R.K., Hediger, M., Karch, F., and Basler, K. (2007). An optimized transgenesis system for Drosophila using germ-line-specific phiC31 integrases. Proc Natl Acad Sci U S A *104*, 3312-3317.

Celic, I., Masumoto, H., Griffith, W.P., Meluh, P., Cotter, R.J., Boeke, J.D., and Verreault, A. (2006). The sirtuins hst3 and Hst4p preserve genome integrity by controlling histone h3 lysine 56 deacetylation. Curr Biol *16*, 1280-1289.

Cheung, W.L., Turner, F.B., Krishnamoorthy, T., Wolner, B., Ahn, S.H., Foley, M., Dorsey, J.A., Peterson, C.L., Berger, S.L., and Allis, C.D. (2005). Phosphorylation of histone H4 serine 1 during DNA damage requires casein kinase II in S. cerevisiae. Curr Biol *15*, 656-660.

Conrad, T., Cavalli, F.M., Holz, H., Hallacli, E., Kind, J., Ilik, I., Vaquerizas, J.M., Luscombe, N.M., and Akhtar, A. (2012a). The MOF chromobarrel domain controls genome-wide H4K16 acetylation and spreading of the MSL complex. Dev Cell *22*, 610-624.

Conrad, T., Cavalli, F.M., Vaquerizas, J.M., Luscombe, N.M., and Akhtar, A. (2012b). Drosophila dosage compensation involves enhanced Pol II recruitment to male X-linked promoters. Science *337*, 742-746.

Corona, D.F., Clapier, C.R., Becker, P.B., and Tamkun, J.W. (2002). Modulation of ISWI function by site-specific histone acetylation. EMBO Rep *3*, 242-247.

Dai, J., Hyland, E.M., Yuan, D.S., Huang, H., Bader, J.S., and Boeke, J.D. (2008). Probing nucleosome function: a highly versatile library of synthetic histone H3 and H4 mutants. Cell *134*, 1066-1078.

Dang, W., Steffen, K.K., Perry, R., Dorsey, J.A., Johnson, F.B., Shilatifard, A., Kaeberlein, M., Kennedy, B.K., and Berger, S.L. (2009). Histone H4 lysine 16 acetylation regulates cellular lifespan. Nature *459*, 802-807.

Das, C., Lucia, M.S., Hansen, K.C., and Tyler, J.K. (2009). CBP/p300-mediated acetylation of histone H3 on lysine 56. Nature *459*, 113-117.

de Setta, N., Van Sluys, M.A., Capy, P., and Carareto, C.M. (2011). Copia retrotransposon in the Zaprionus genus: another case of transposable element sharing with the Drosophila melanogaster subgroup. J Mol Evol *72*, 326-338.

Dobens, L.L., and Raftery, L.A. (2000). Integration of epithelial patterning and morphogenesis in Drosophila ovarian follicle cells. Developmental dynamics : an official publication of the American Association of Anatomists *218*, 80-93.

Edwards, K.A., and Kiehart, D.P. (1996). Drosophila nonmuscle myosin II has multiple essential roles in imaginal disc and egg chamber morphogenesis. Development *122*, 1499-1511.

Gelbart, M.E., Larschan, E., Peng, S., Park, P.J., and Kuroda, M.I. (2009). Drosophila MSL complex globally acetylates H4K16 on the male X chromosome for dosage compensation. Nat Struct Mol Biol *16*, 825-832.

Guglielmi, B., La Rochelle, N., and Tjian, R. (2013). Gene-specific transcriptional mechanisms at the histone gene cluster revealed by single-cell imaging. Mol Cell *51*, 480-492.

Gunesdogan, U., Jackle, H., and Herzig, A. (2010). A genetic system to assess in vivo the functions of histones and histone modifications in higher eukaryotes. EMBO Rep *11*, 772-776.

Gunesdogan, U., Jackle, H., and Herzig, A. (2014). Histone supply regulates S phase timing and cell cycle progression. eLife *3*, e02443.

Hardy, R.W., Tokuyasu, K.T., Lindsley, D.L., and Garavito, M. (1979). The germinal proliferation center in the testis of Drosophila melanogaster. Journal of ultrastructure research *69*, 180-190.

Hodl, M., and Basler, K. (2012). Transcription in the absence of histone H3.2 and H3K4 methylation. Curr Biol *22*, 2253-2257.

Huang, H., Lin, S., Garcia, B.A., and Zhao, Y. (2015). Quantitative proteomic analysis of histone modifications. Chem Rev *115*, 2376-2418.

Huang, H., Sabari, B.R., Garcia, B.A., Allis, C.D., and Zhao, Y. (2014). SnapShot: histone modifications. Cell *159*, 458-458 e451.

Hyland, E.M., Cosgrove, M.S., Molina, H., Wang, D., Pandey, A., Cottee, R.J., and Boeke, J.D. (2005). Insights into the role of histone H3 and histone H4 core modifiable residues in Saccharomyces cerevisiae. Mol Cell Biol *25*, 10060-10070.

Isogai, Y., Keles, S., Prestel, M., Hochheimer, A., and Tjian, R. (2007). Transcription of histone gene cluster by differential core-promoter factors. Genes Dev *21*, 2936-2949.

Kayne, P.S., Kim, U.J., Han, M., Mullen, J.R., Yoshizaki, F., and Grunstein, M. (1988). Extremely conserved histone H4 N terminus is dispensable for growth but essential for repressing the silent mating loci in yeast. Cell *55*, 27-39.

Kimura, A., Umehara, T., and Horikoshi, M. (2002). Chromosomal gradient of histone acetylation established by Sas2p and Sir2p functions as a shield against gene silencing. Nat Genet *32*, 370-377.

Kouzarides, T. (2007). Chromatin modifications and their function. Cell *128*, 693-705.

Leatherman, J.L., and Dinardo, S. (2010). Germline self-renewal requires cyst stem cells and stat regulates niche adhesion in Drosophila testes. Nature cell biology *12*, 806-811.

Lifton, R.P., Goldberg, M.L., Karp, R.W., and Hogness, D.S. (1978). The organization of the histone genes in Drosophila melanogaster: functional and evolutionary implications. Cold Spring Harb Symp Quant Biol *42 Pt 2*, 1047-1051.

Lin, H., Yue, L., and Spradling, A.C. (1994). The Drosophila fusome, a germline-specific organelle, contains membrane skeletal proteins and functions in cyst formation. Development *120*, 947-956.

Luger, K., Mader, A.W., Richmond, R.K., Sargent, D.F., and Richmond, T.J. (1997). Crystal structure of the nucleosome core particle at 2.8 A resolution. Nature *389*, 251-260.

Marzluff, W.F., Gongidi, P., Woods, K.R., Jin, J., and Maltais, L.J. (2002). The human and mouse replication-dependent histone genes. Genomics *80*, 487-498.

Masumoto, H., Hawke, D., Kobayashi, R., and Verreault, A. (2005). A role for cell-cycle-regulated histone H3 lysine 56 acetylation in the DNA damage response. Nature *436*, 294-298.

Matsuo, Y., and Yamazaki, T. (1989). tRNA derived insertion element in histone gene repeating unit of Drosophila melanogaster. Nucleic Acids Res *17*, 225-238.

McKay, D.J., Klusza, S., Penke, T.J., Meers, M.P., Curry, K.P., McDaniel, S.L., Malek, P.Y., Cooper, S.W., Tatomer, D.C., Lieb, J.D*., et al.* (2015). Interrogating the function of metazoan histones using engineered gene clusters. Dev Cell *32*, 373-386.

Morgan, B.A., Mittman, B.A., and Smith, M.M. (1991). The highly conserved N-terminal domains of histones H3 and H4 are required for normal cell cycle progression. Mol Cell Biol *11*, 4111-4120.

Mu, X., Yan, S., Fu, C., and Wei, A. (2015). The Histone Acetyltransferase MOF Promotes Induces Generation of Pluripotent Stem Cells. Cell Reprogram.

Mugnier, N., Gueguen, L., Vieira, C., and Biemont, C. (2008). The heterochromatic copies of the LTR retrotransposons as a record of the genomic events that have shaped the Drosophila melanogaster genome. Gene *411*, 87-93.

Nakanishi, S., Sanderson, B.W., Delventhal, K.M., Bradford, W.D., Staehling-Hampton, K., and Shilatifard, A. (2008). A comprehensive library of histone mutants identifies nucleosomal residues required for H3K4 methylation. Nat Struct Mol Biol *15*, 881-888.

Nakayama, J., Rice, J.C., Strahl, B.D., Allis, C.D., and Grewal, S.I. (2001). Role of histone H3 lysine 9 methylation in epigenetic control of heterochromatin assembly. Science *292*, 110-113.

Ng, H.H., Feng, Q., Wang, H., Erdjument-Bromage, H., Tempst, P., Zhang, Y., and Struhl, K. (2002). Lysine methylation within the globular domain of histone H3 by Dot1 is important for telomeric silencing and Sir protein association. Genes Dev *16*, 1518-1527.

Pengelly, A.R., Copur, O., Jackle, H., Herzig, A., and Muller, J. (2013). A histone mutant reproduces the phenotype caused by loss of histone-modifying factor Polycomb. Science *339*, 698-699.

Prabhakaran, M., and Kelley, R.L. (2010). A new strategy for isolating genes controlling dosage compensation in Drosophila using a simple epigenetic mosaic eye phenotype. BMC Biol *8*, 80.

Raja, S.J., Charapitsa, I., Conrad, T., Vaquerizas, J.M., Gebhardt, P., Holz, H., Kadlec, J., Fraterman, S., Luscombe, N.M., and Akhtar, A. (2010). The nonspecific lethal complex is a transcriptional regulator in Drosophila. Mol Cell *38*, 827-841.

Reid, R.J., Gonzalez-Barrera, S., Sunjevaric, I., Alvaro, D., Ciccone, S., Wagner, M., and Rothstein, R. (2011). Selective ploidy abInterplay Between Histone H3 Lysine 56 Deacetylation and Chromatin Modifiers in Response to DNA Damagelation, a high-throughput plasmid transfer protocol, identifies new genes affecting topoisomerase I-induced DNA damage. Genome Res *21*, 477-486.

Robinson, P.J., An, W., Routh, A., Martino, F., Chapman, L., Roeder, R.G., and Rhodes, D. (2008). 30 nm chromatin fibre decompaction requires both H4-K16 acetylation and linker histone eviction. J Mol Biol *381*, 816-825.

Rothbart, S.B., and Strahl, B.D. (2014). Interpreting the language of histone and DNA modifications. Biochim Biophys Acta *1839*, 627-643.

Ruohola, H., Bremer, K.A., Baker, D., Swedlow, J.R., Jan, L.Y., and Jan, Y.N. (1991). Role of neurogenic genes in establishment of follicle cell fate and oocyte polarity during oogenesis in Drosophila. Cell *66*, 433-449.

Ryder, E., Blows, F., Ashburner, M., Bautista-Llacer, R., Coulson, D., Drummond, J., Webster, J., Gubb, D., Gunton, N., Johnson, G.*, et al.* (2004). The DrosDel collection: a set of P-element insertions for generating custom chromosomal aberrations in Drosophila melanogaster. Genetics *167*, 797-813.

Shogren-Knaak, M., Ishii, H., Sun, J.M., Pazin, M.J., Davie, J.R., and Peterson, C.L. (2006). Histone H4-K16 acetylation controls chromatin structure and protein interactions. Science *311*, 844-847.

Simoneau, A., Delgoshaie, N., Celic, I., Dai, J., Abshiru, N., Costantino, S., Thibault, P., Boeke, J.D., Verreault, A., and Wurtele, H. (2015). Interplay between histone H3 lysine 56 deacetylation and chromatin modifiers in response to DNA damage. Genetics *200*, 185-205.

Smith, E.R., Pannuti, A., Gu, W., Steurnagel, A., Cook, R.G., Allis, C.D., and Lucchesi, J.C. (2000). The drosophila MSL complex acetylates histone H4 at lysine 16, a chromatin modification linked to dosage compensation. Mol Cell Biol *20*, 312-318.

Strahl, B. D. and C. D. Allis (2000). "The language of covalent histone modifications." Nature **403**(6765): 41-45.

Suka, N., Luo, K., and Grunstein, M. (2002). Sir2p and Sas2p opposingly regulate acetylation of yeast histone H4 lysine16 and spreading of heterochromatin. Nat Genet *32*, 378-383.

Tessarz, P., and Kouzarides, T. (2014). Histone core modifications regulating nucleosome structure and dynamics. Nat Rev Mol Cell Biol *15*, 703-708.

Tulina, N., and Matunis, E. (2001). Control of stem cell self-renewal in Drosophila spermatogenesis by JAK-STAT signaling. Science *294*, 2546-2549.

Van Holde, K.E. (1989). Chromatin (New York: Springer-Verlag).

van Leeuwen, F., Gafken, P.R., and Gottschling, D.E. (2002). Dot1p modulates silencing in yeast by methylation of the nucleosome core. Cell *109*, 745-756.

Wolffe, A.P. (2001). Transcriptional regulation in the context of chromatin structure. Essays Biochem *37*, 45-57.

Wurtele, H., Kaiser, G.S., Bacal, J., St-Hilaire, E., Lee, E.H., Tsao, S., Dorn, J., Maddox, P., Lisby, M., Pasero, P.*, et al.* (2012). Histone H3 lysine 56 acetylation and the response to DNA replication fork damage. Mol Cell Biol *32*, 154-172.

Wurtele, H., and Verreault, A. (2006). Histone post-translational modifications and the response to DNA double-strand breaks. Curr Opin Cell Biol *18*, 137-144.

Xie, H.B., and Golic, K.G. (2004). Gene deletions by ends-in targeting in Drosophila melanogaster. Genetics *168*, 1477-1489.

Xu, F., Zhang, K., and Grunstein, M. (2005). Acetylation in histone H3 globular domain regulates gene expression in yeast. Cell *121*, 375-385.

Xue, Z., Ren, M., Wu, M., Dai, J., Rong, Y.S., and Gao, G. (2014). Efficient gene knock-out and knock-in with transgenic Cas9 in Drosophila. G3 (Bethesda) *4*, 925-929.

Ye, J., Ai, X., Eugeni, E.E., Zhang, L., Carpenter, L.R., Jelinek, M.A., Freitas, M.A., and Parthun, M.R. (2005). Histone H4 lysine 91 acetylation a core domain modification associated with chromatin assembly. Mol Cell *18*, 123-130.

Yu, Z., Ren, M., Wang, Z., Zhang, B., Rong, Y.S., Jiao, R., and Gao, G. (2013). Highly efficient genome modifications mediated by CRISPR/Cas9 in Drosophila. Genetics *195*, 289-291.

Yung, P.Y., Stuetzer, A., Fischle, W., Martinez, A.M., and Cavalli, G. (2015). Histone H3 Serine 28 Is Essential for Efficient Polycomb-Mediated Gene Repression in Drosophila. Cell Rep *11*, 1437-1445.

Figure Legends

Figure 3.1 Schematic representation of the histone deletion and complementation procedure

(A) The clustered regularly interspaced short palindromic repeats (CRISPR) associated with protein-9 nuclease (CRISPR/Cas9) mediated gene targeting method was used to introduce phage attachment (*attP*) and flippase recognition target (*FRT*) sites into chromosome 2 on either side of the histone gene cluster. Mediated by the endonuclease activity of Cas9, a DNA double strand break was introduced at the left side of the histone cluster, and a synthetic oligonucleotide donor containing *attP*, *FRT* and homologous arms was simultaneously integrated into the genome through homologous recombination (HR). A similar strategy was used to introduce *attP* and *FRT* sites at the right side of the histone cluster in another set of embryos. A circular plasmid containing the *attP-FRT-3×P3RFP* cassette was integrated into the genome in a manner resulting in the duplication of the *attP-FRT-3×P3RFP* cassette. Flies containing the integrated sites were crossed together to place these two engineered chromosomes in trans to one another, and the resulting progeny were heat-shocked to induce flipase activity (*hs-FLP*) and cause chromosomal rearrangements. One possible rearrangement, between the left side *FRT* in one chromosome and the proximal right side *FRT* in the other chromosome, resulted in a deletion of the entire histone gene cluster. The locations of four primers are indicated. **(B)** PCR analysis with P1 and R1 primers (top panel) was used to validate the left side of the histone deletion chromosome (His^{D}) and revealed two bands, which indicates the duplication of the attP-FRT-3P3RFP cassette. w^{1118} flies were used as a control. P2 and

R2 primers (bottom panel) were used to validate the right side of the histone deletion chromosome.

(C) Immunostaining of control and histone null mutant embryos with H3S28ph antisera (red) and DAPI (blue). No H3S28ph signal was detected in His^{D} or His^{C} embryos. w^{1118} and 20 His-GUs transgenic embryos were used as controls.

Figure 3.2 Low histone dosage affects the fertility of rescued adults

(A) Histogram of rescue tests for flies containing different numbers of wild-type His-GUs. Different numbers of histone units were reintroduced into histone null mutants to rescue the lethal phenotype. 5 or 6 copies of the histone unit fail to rescue the histone null mutants. The number of rescued flies observed for flies with 8 copies of His-GUs was 5% that of wild-type (WT). The rescue ratio increased with increasing histone copy number. 20 copies of His-GUs rescued the lethal phenotype to nearly 100%. Error bars represent standard deviation (SD).

(B) Western blot of histone H2B in 12 His-GUs, 16 His-GUs, 20 His-GUs, 24 His-GUs, His^{D}, His^{C}, or wild-type (WT) virgin adult flies.

(C, D) Plot of fertility tests of 12 His-GUs, 16 His-GUs, 20 His-GUs, 24 His-GUs, His^{D}, or wild-type (WT) adult male (C) or female (D) flies. The fertility test was done by counting the number of surviving adult progeny produced by male or female flies of the given genotype. Each point represents a vial of flies. Severe fertility defects were observed in low histone copy rescued adult females: 12 His-GUs and 16 His-GUs females produced very few progeny. Female fertility was restored in flies with 20 His-GUs. The fertility of rescued males was similar to that of wild-type males. The horizontal

bar indicates the average number of adult progeny produced by flies of the given genotype. Error bar represents standard error of the mean (SEM).

(E, F) Testes (E) and ovaries (F) were classified by their morphology into three categories, as shown in the top panels: wild-type (WT), moderate defect, and severe defect. The diagram below shows the number of adults of the given genotype that had testes (E) or ovaries (F) in each category. Severe developmental defects were observed in low histone dosage rescued ovaries and testes.

Figure 3.3 Low histone dosage affects testis and ovary development

(A) Illustration (top left) of a wild-type *Drosophila* germarium and egg chamber (modified from Ma et al., 2014). GSCs (dark red) reside in a germline niche and divide asymmetrically to form cystoblasts, which develop into 16-cell cysts surrounded by follicle cells (green). The cyst cells then bud from the germarium as individual egg chambers. As the egg chambers continue to grow, they move further to the posterior and form a chain of egg chambers connected by stalk cells (blue). The remaining panels are confocal images of ovaries from adult flies carrying different copy numbers of histones stained with anti-Vasa (red), DAPI (blue), anti-Zfh1 (green; somatic cells), and anti-Hts/1B1 and anti-Arm (white or green; fusomes and somatic cell membranes). Ovaries from 24 His-GUs rescued adults appear wild-type. Some of the ovaries in 20 His-GUs rescued adults show mild budding problems (solid arrowhead). All the ovaries in 10, 12, and 16 His-GUs rescued adults have severe budding problems and lack either mid-stage egg chambers or egg chambers at all stages. The GSCs in mutant germaria (for example, see 16 His-GUs) appear normal (open arrowhead). Scale bar, 20 μm.

(B) Illustration of a wild-type *Drosophila* testis (modified from Li et al., 2014). Non-dividing hub cells (yellow) are surrounded by germline stem cells (GSCs, dark red) and cyst stem cells (CySCs, dark green). GSCs with round fusomes (red) divide asymmetrically and produce differentiated spermatogonia (green) with branched fusomes. Testes in 20 His-GUs rescued male flies have similar numbers of GSCs as wild type testes and apear normal. Low copy number (<= 16) rescued testes have significantly smaller hubs and fewer GSCs. *** P-value < 0.0005; **** P-value < 0.00005. Testes from adult flies carrying different copy number of histones stained with anti-Vasa (red), DAPI (blue), and anti-Hts/1B1 and anti-Arm (green; fusomes and somatic cell membranes). Scale bar, 20 μm.

(C) Comparison of RNA-seq data from 12 His-GUs, 20 His-GUs, or wild-type testes or ovaries shows that the expression levels of many genes in 12 His-GUs ovaries are significantly up-regulated from those in WT ovaries. The expression levels from 20 His-GUs ovaries and from 12 His-GUs or 16 His-GUs testes are similar to the transcripts from WT ovary or testis.

Figure 3.4 Systematic mutagenesis of *Drosophila* histone H3 and H4 modifiable residues

(A) Schematic representation of histone mutagenesis procedures. One copy of wild type His-GU was inserted into an entry vector containing flanking attL1 and attL2 sites. “Seven step” assembly was performed to insert 5 mutant His-GU copies into the pUAST integration vector. 1. Break the wild-type His-GUs into 3 parts and assemble them into pUC19 vectors respectively. 2. Perform PCR-based site-directed mutagenesis to

introduce the desired mutation. 3. Subclone the mutated histone genes back into the entry vector. 4. Increase the mutated His-GUs to two copies. 5. Increase the mutated His-GUs to three copies. 6. Subclone two copies of the mutated His-GUs into the pUAST-attR vector. 7. Transfer 3 copies of mutated His-GUs to the pUAST integration vector via the Gateway assembly method.

(B) SalI assay indicates all histone genes in homozygous H4K8A mutants arise from the transgenic histone rescue locus. Heterozygous mutants shows a partial digestion pattern, indicating that the PCR product came from both transgenic mutant and wild type His-GUs. Quantitative analysis shows that the undigested DNA amount is 8.3 fold higher than the digested DNA amount, indicating that the histone copy number in the wild type chromosome is 83.

(C) Sequence confirmation of the H4K8A mutant. Primers are specific to mutant amplicons and are verified by sequencing.

(D) Western blot shows loss of H4K8Ac signal in homozygous H4K8A mutant flies.

Figure S3.1 Schematic representation of the histone gene cluster in *Drosophila melanogaster*

Drosophila histone genes form a gene cluster on the left arm of chromosome II, which contains around hundreds of His-GUs. Each His-GU contains a single copy of the five canonical histone genes, His1, His2A, His2B, His3 and His4.

Figure S3.2 Characterization of histone null flies rescued with different number of His-GUs

(A) Western blot of Histones H3 and H4 in wild type (w^{1118}) and different number of His-GUs rescued virgin adult flies. All of the rescued flies have no significant difference in protein levels compared to wild type.

(B) Polytene chromosomes staining of different number of His-GUs rescued flies. The polytene chromosomes were stained with DAPI (blue) and HP1 (red). No significant differences were observed among different histone copy rescued flies.

Figure S3.3 Morphologic observation of different number of His-GUs rescued fly adults

Male and female fly adults observed under the stereoscope. No significant differences were observed among wild-type and different number of His-GUs rescued flies.

Figure S3.4 Ovary and testis morphology of different number of His-GUs rescued flies

(A) Dissected ovaries from different number of His-GUs rescued flies. 8 His-GUs, 12 His-GUs and 16 His-GUs flies cannot produce normal eggs. Ovaries from 20 His-GUs flies are morphologically indistinguishable from wild-type ovaries.

(B) Testes from different histone dosage rescued flies are morphologically indistinguishable from wild-type testes.

Figure S3.5 Histone construct double integration verification

(A) Illustration of the attB-attP recombination scheme for integrating two 5 His-GUs containing constructs into the genome. A series of primers designed for PCR verification of attB-attP double recombination, for upstream attB-attP recombination, WZO195 / RFP-140R positive and WZO162 / RFP-140R negative indicates correct integration of histone mutant construct. For downstream attB-attP recombination, WZO268 / WZO195 positive and WZO268 / RFP-140R negative indicates correct integration of histone mutant construct.

(B) PCR verification for only upstream attB-attP recombination, only downstream attB-attP recombination, double attB-attP recombination and no attB-attP recombination negative control.

(C) attB-attP recombination discrimination by eye color. Eyes in wild type flies are white; eyes in single attB-attP recombination are yellow or orange, eyes in double attB-attP recombination flies are red.

(D) Histone mutant constructs double integration verification. PCR based attB-attP double integration method (described as A and B) was used to verify each histone mutant in the library,

Figure S3.6 SalI assay for all homozygous histone mutants

Transgenic histone mutants contain an additional SalI restriction enzyme site between histone H2A and H4, which can be used to distinguish transgenic histone genes from endogenous histone genes (Figure 3.4B). All of the mutants in this library contained the SalI site, allowing us to completely digest the SalI containing amplicons into two equal length fragments, indicating that they are homozygous for the transgenic histone mutants.

Figure S3.7 Viability statistics for all viable histone mutants

10 His-GUs^{mutant}/CyO was self crossed, 1/3 progenies were 10 His-GUs^{mutant} /10 His-GUs^{mutant}(20 His-GUs^{mutant}) according to Mendel's first law. The number of 20 His-GUs^{mutant} adults and total offspring was determined, and the ratio of the number of 20 His-GUs^{mutant} adults/(the number of total offspring *1/3) was used to represent the rescue ratio on y-axis. Different histone mutants are listed on the x-axis. The experiment was performed in triplicate. Error bars = SD (standard deviation).

Figure S3.8 Visible adult Morphological analysis of viable mutants

Mouth parts, antennae, eyes, legs, sex combs and wings were observed morphologically in rescued flies containing various numbers (8, 10, 12, 16, 20, 24, His^{D}, w^{1118}) of wild-type histone arrays (A) and 16 viable histone mutants (B). Only wings showed slight defects. The upper optical image in (C) shows a wild-type control wing with normal morphology, the middle two images show abnormal wings with ectopic veins (arrows) between the longitudinal wing veins L3 and L4. The lower image in (C) shows an abnormally shaped wing. The number of abormal wings and the total number of wings examined for each genotype, followed by the percentage of abnormal wings, is shown in A and B.

Figure S3.9 Morphological defects of ovaries and testes from viable histone mutant flies

20 His-GUs^{mutant} virgin females and males were collected and kept for 5 days before their ovaries or testes were dissected for observation. Ovaries (A) and testes (B) were

classified morphologically into three categories, as shown in the top panels: wild-type (WT, blue), moderate defect (green), and severe defect (red). The diagram below shows the number of adults of the given genotype that had ovaries (A) or testes (B) in each category.

Figure S3.10 Fertility test for all viable histone mutants

Fertility test of 20 His-GUs^{mutant} , adult male (A), or female (B) flies (x-axis). This test was done by counting the number of surviving adult progeny (y-axis) produced by male or female flies of the given genotype. Each point represents a vial of fly. The horizontal bar indicates the average number of adult progeny produced by flies of a given genotype. Error bars represent standard error of the mean (SEM). Severe fertility defects were observed in females of 20 His-GUs^{H3T3A}, 20 His-GUs^{H3R17A}, 20 His-GUs^{H3K23A}, 20 His-GUs^{H3K56A}, 20 His-GUs^{H4R3A}, 20 His-GUs^{H4K16A}, 20 His-GUs^{H4R23A}, 20 His-GUs^{H4R92A} mutant genotype. The only male mutant genotype with a detectable fertility defect was the 20 His-GUs^{H3R17A} mutant, which showed 31.6% (below 50%) fertility compared to 20 His-GUs^{WT}.

Figure S3.11 Identification of the lethal phases of adult lethal histone mutants

For adult lethal mutants, 10 His-GUs^{mutant}/ *CyO, P{ActGFP}MR1* flies were self-crossed, no first instar larvae lacking green fluorescent protein(GFP) expression were found in histone mutant H3K4A, H3R26A, H3K27A, H3Y41A, H4Y88A, H4K91A, hundreds of first instar larvae were observed (A). This indicated these six mutants were dead at the embryonic stage. For adult lethal histone mutants which were alive as first instar larvae, 150 GFP-positive first instar larvae (blue) and 150 GFP-negative first instar larvae (blue)

were collected and tracked on apple juice plates until adulthood. For each histone mutant, the number of progeny at 2nd instar larval (red), 3rd instar larval (green), pupal (purple), and adult (cyan) stages were counted and normalized to the number of first instar larvae. 20 His-GUs^{H3K37A} and 20 His-GUs^{H3T45A} died primarily at the first instar stage (C). 20 His-GUs^{H3K9A} died primarily as 3th instar larvae (C). 20 His-GUs^{H3R2A}, 20 His-GUsH^{3T6A}, 20 His-GUs^{H3R8A}, 20 His-GUs^{H3S10A}, 20 His-GUs^{H3S28A}, 20 His-GUs^{H3K36A}, 20 His-GUs^{H4K79A} and 20 His-GUs^{H4K12A} died at the pupal stage (C). For larval or pupal lethal histone mutants, hundreds of adults were observed, and no homozygous adults were found (B).

Figure S3.12 DNA-damage response screening for all viable histone mutants

Roaming 3rd instar larvae were picked and randomly divided in equal number into control and irradiation groups. The latter received 10 mJ/cm^2 UV irradiation (A) in a UV stratalinker 2400 (Stratagene) or 30Gy X-ray(B) in RS 2000 (Rad Source Technologies, Inc). Larvae were subsequently maintained in standard food for 9 days before the eclosed pharate adults were counted. The elosion ratio was caculated as the following: Ratio= E (eclosed pharates number in UV group) / C (eclosed pharates number in control group) x 100. The results represent at least three independent experiments. ** = $p<0.01$, * = $0.01 \leqq p<0.05$. P values determined using Student's T test.

Figure S3.13 Gene silencing defect screening of modifiable H3 and H4 mutant library

RT-qPCR was performed to test whether histone modification affects gene silencing. A natural transposable element (copia) was used as a target gene. Four histone mutants

(H3K9A, H3K23A, H3K56A and H4R23A) strongly expressed copia transcripts relative to control flies). Analysis of the expression of additional transposable elements in H3K9A (B) and H3K56A (C) flies showed non-universal gene silencing defects in these two mutants. Three biological replicates were performed for all samples. Error bar represents standard deviation.

Table 3.1 Phenotypic analysis of flies baring mutations on modified histone H3 and H4 residues

Mutant Allele	Fertility[a]		Abnormal morphology[b]	DNA damage sensitivity[c]		Gene silencing defects[d]
	♂	♀		UV	X-Ray	
H3T3A	++	sterile	-	nt	nt	+
H3R17A	+	sterile	wing	nt	nt	nt
H3K18A	++	++	-	++	++	-
H3K23A	++	+	-	nt	nt	+++
H3K56A	++	sterile	-	+++	+++	+++
H3K64A	++	++	-	+	+	-
H4T1A	++	++	-	++	+++	-
H4R3A	++	+	-	+	++	-
H4K5A	++	+++	-	nt	nt	-
H4K8A	+++	+++	-	++	++	-
H4K16A	*	sterile	wing	nt	nt	-
H4K20A	nt	nt	-	nt	nt	nt
H4R23A	+++	+	-	++	nt	++
H4Y51A	++	+++	-	+	++	-
H4K77A	+++	++	-	++	nt	-
H4R92A	++	+	-	+	nt	-

[a] Fertility was represented as ratio of the number of progenies between mutant and wild type when crossing with a wild type counterpart. +++ >80%; ++ 30%--80%; + ≦30%; nt not tested

[b] The examined morphologies include eye, wing, mouth part, antenna, Leg, sex comb, wing. The abnormality of wing is illustrated in Fig. S9. – no obvious changes of morphology

[c] Three instar larvae were treated with 100 J/cm^2 of UVB (230 nM) or X-ray irradiation (30 Gy). +++ <50%; ++ 50-75%; + ≧75%

[d] Gene silencing was measured by RT-PCR with primers specific to Copia retrotransposon. – no changes compared to wild type. + Low expression; ++ Medium expression; +++ Strong expressionLimited male (<1/1000 viable).

Figure 3.1

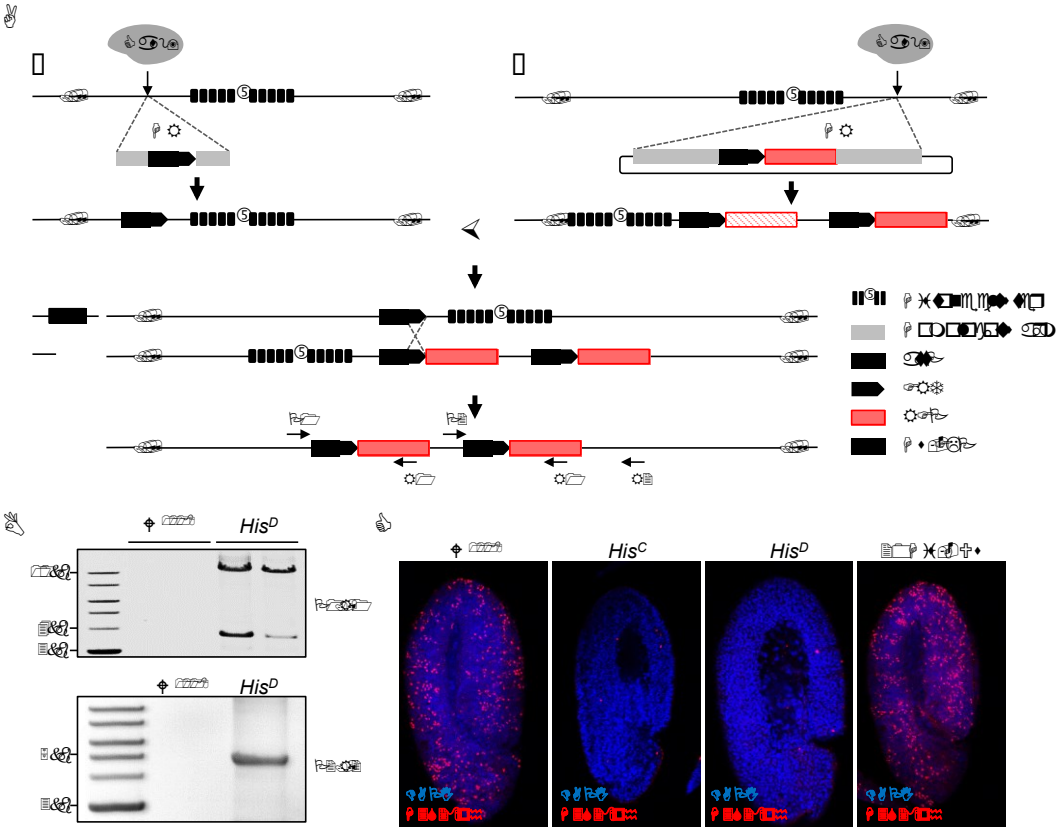

Figure 3.2

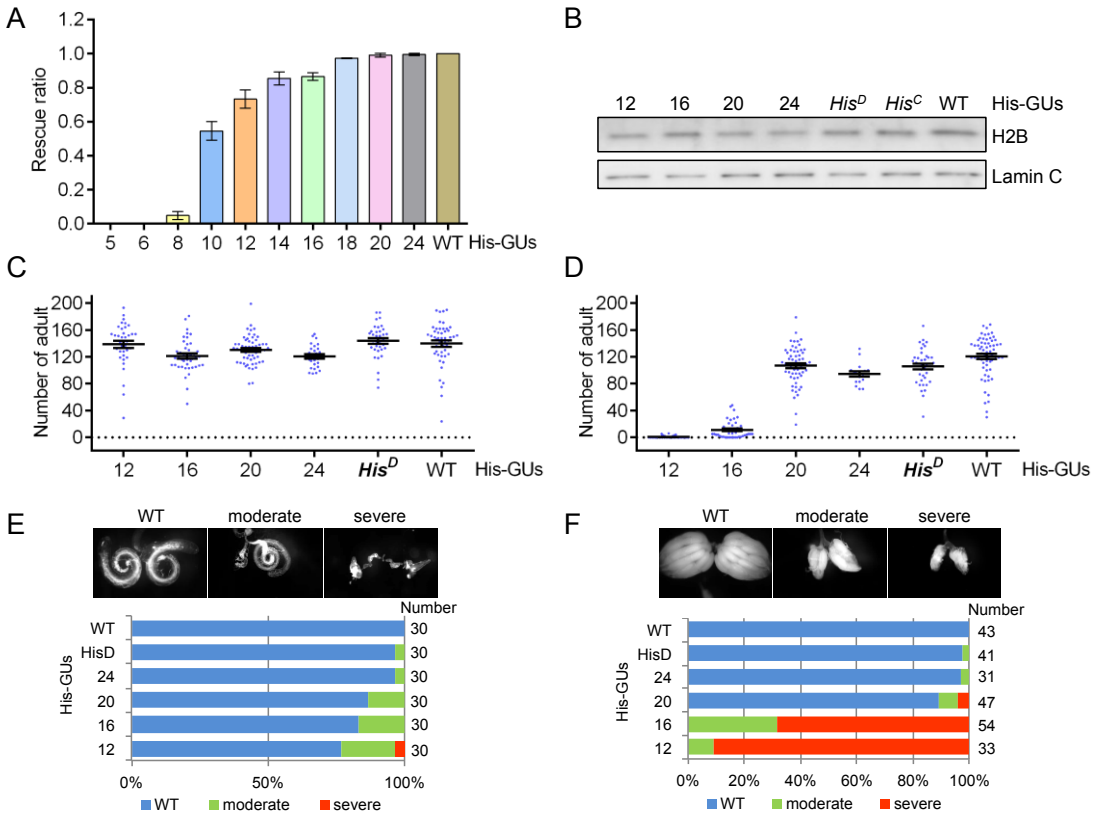
A
Rescue ratio
1.2
1.0
0.8
0.6
0.4
0.2
0.0
5 6 8 10 12 14 16 18 20 24 WT His-GUs
B
12 16 20 24 HisD HisC WT His-GUs
H2B
Lamin C
C
Number of adult
200
160
120
80
40
0
12 16 20 24 HisD WT His-GUs
D
Number of adult
200
160
120
80
40
0
12 16 20 24 HisD WT His-GUs
E
WT moderate severe
Number
His-GUs
WT 30
HisD 30
24 30
20 30
16 30
12 30
0% 50% 100%
WT moderate severe
F
WT moderate severe
Number
His-GUs
WT 43
HisD 41
24 31
20 47
16 54
12 33
0% 20% 40% 60% 80% 100%
WT moderate severe

Figure 3.3

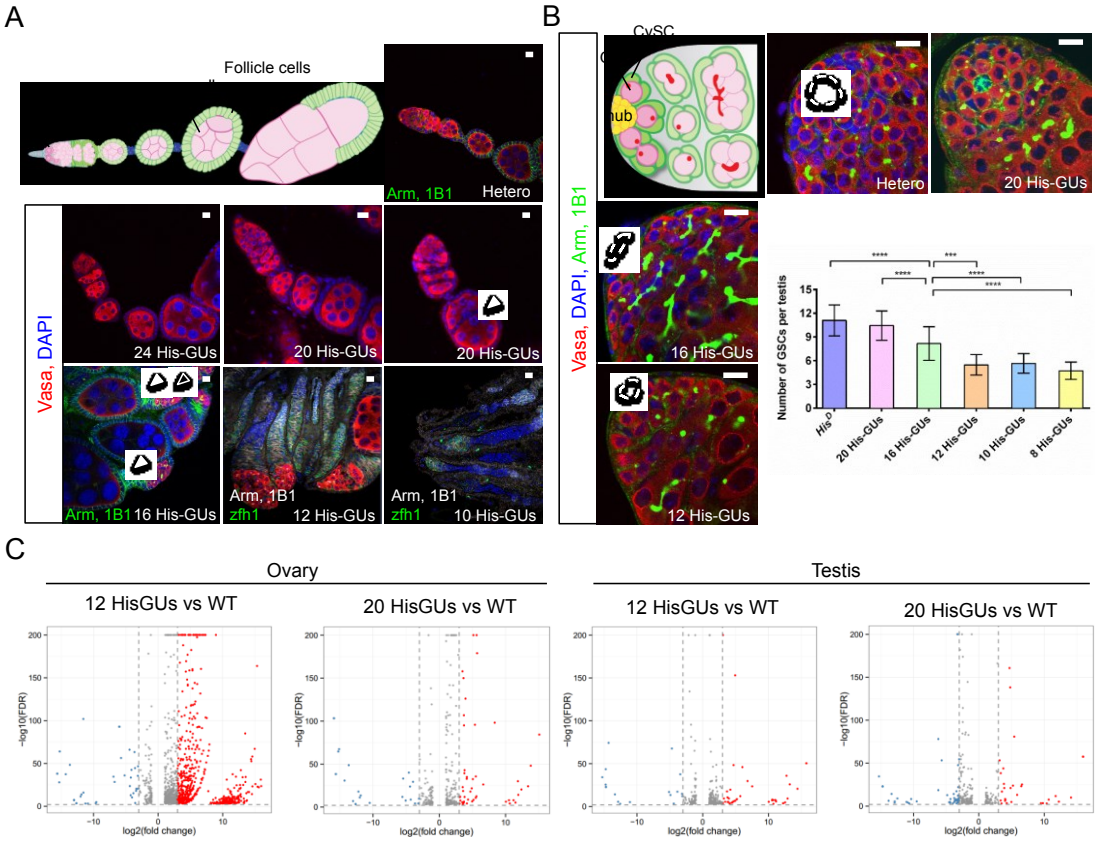
A
Follicle cells
Arm, 1B1
Hetero
Vasa, DAPI
24 His-GUs
20 His-GUs
20 His-GUs
Arm, 1B1 16 His-GUs
Arm, 1B1 zfh1 12 His-GUs
Arm, 1B1 zfh1 10 His-GUs
B
CySC
Hub
Hetero
20 His-GUs
Vasa, DAPI, Arm, 1B1
16 His-GUs
12 His-GUs
Number of GSCs per testis
His-
20 His-GUs
16 His-GUs
12 His-GUs
10 His-GUs
8 His-GUs
C
Ovary
Testis
12 HisGUs vs WT
20 HisGUs vs WT
12 HisGUs vs WT
20 HisGUs vs WT
-log10(FDR)
log2(fold change)

Figure 3.4

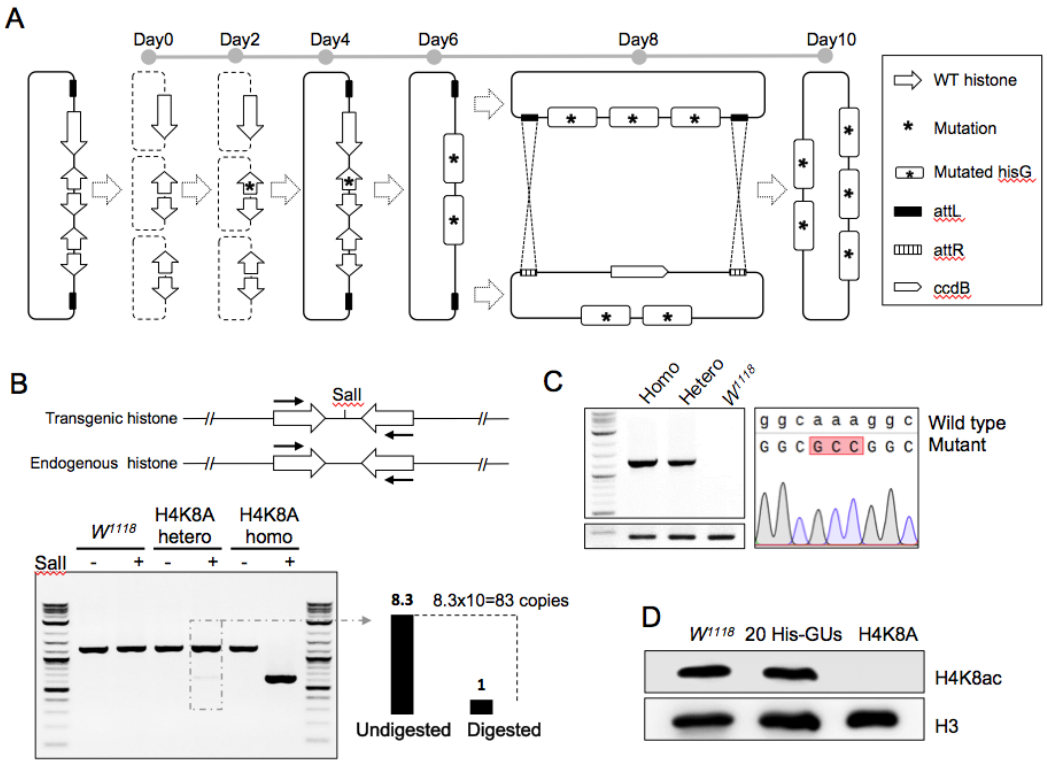
A
Day0
Day2
Day4
Day6
Day8
Day10
WT histone
Mutation
Mutated hisG
attL
attR
ccdB
B
Transgenic histone
Endogenous histone
SalI
W1118
H4K8A hetero
H4K8A homo
SalI
8.3
8.3x10=83 copies
1
Undigested
Digested
C
Homo
Hetero
W1118
g g c a a g g c
G G C G C C G G C
Wild type
Mutant
D
W1118
20 His-GUs
H4K8A
H4K8ac
H3

Figure S3.1

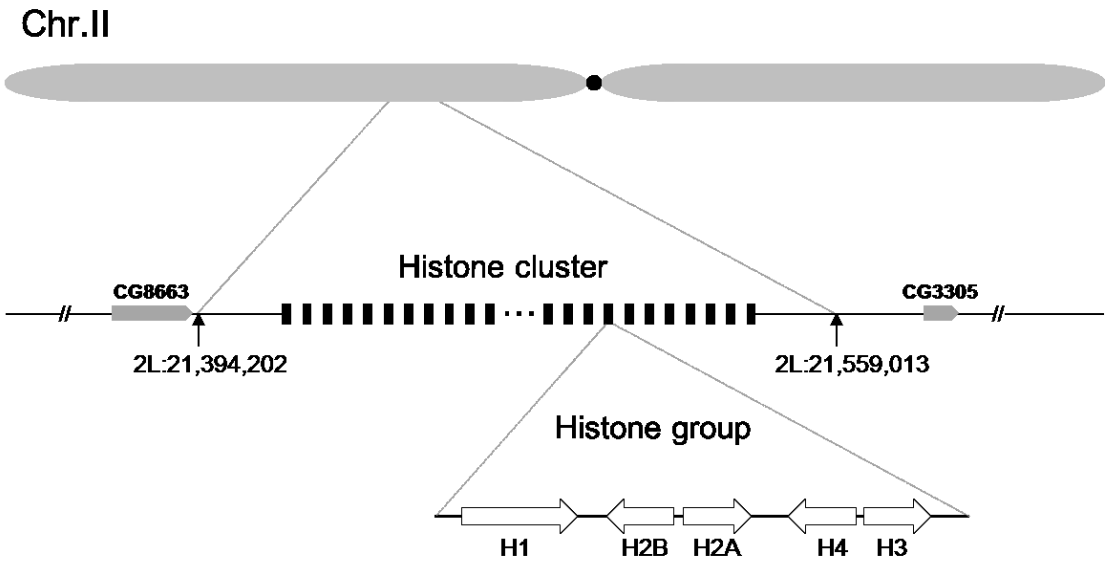
Chr.II
Histone cluster
CG8663
CG3305
2L:21,394,202
2L:21,559,013
Histone group
H1
H2B
H2A
H4
H3

Figure S3.2

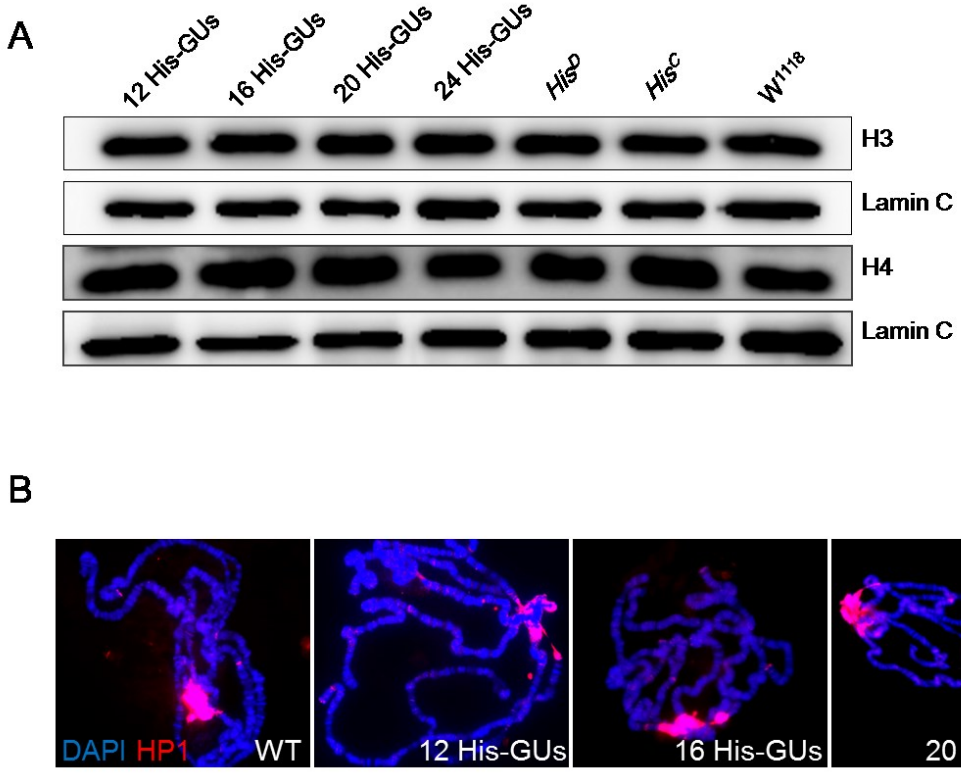
A
12 His-GUs
16 His-GUs
20 His-GUs
24 His-GUs
His^D
His^C
W^1118
H3
Lamin C
H4
Lamin C
B
DAPI HP1
WT
12 His-GUs
16 His-GUs
20 His-GUs

Figure S3.3

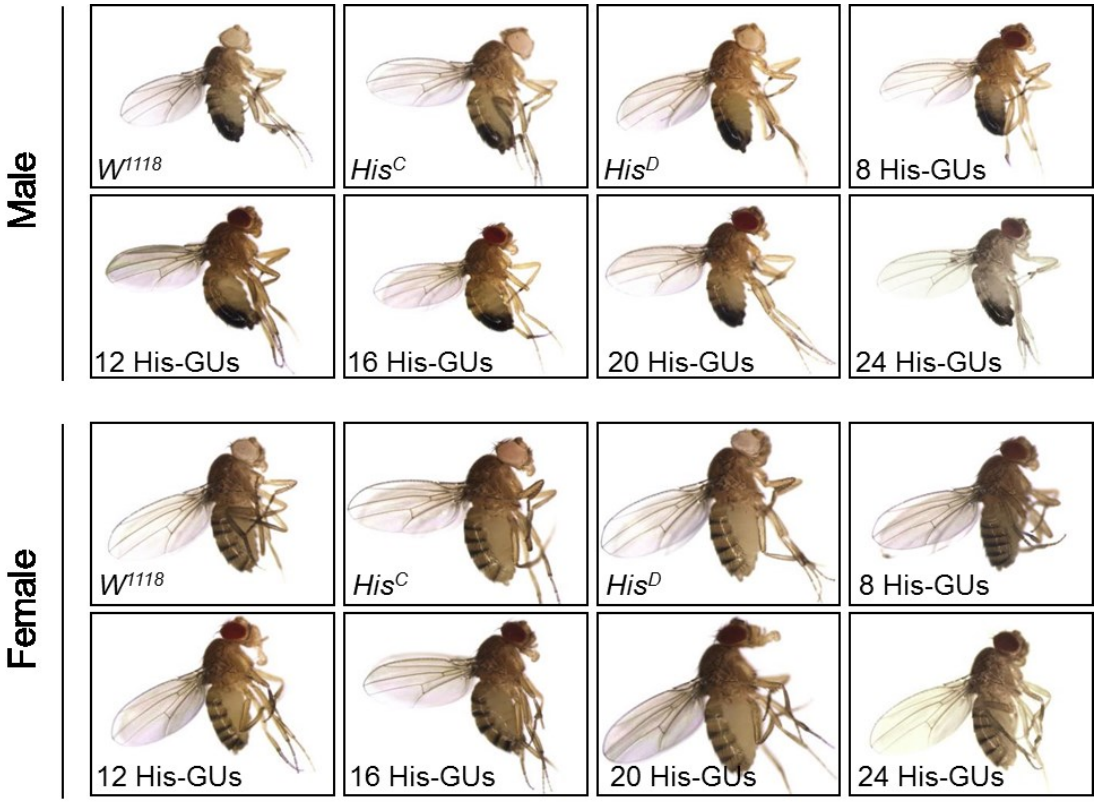
Male
W1118
HisC
HisD
8 His-GUs
12 His-GUs
16 His-GUs
20 His-GUs
24 His-GUs
Female
W1118
HisC
HisD
8 His-GUs
12 His-GUs
16 His-GUs
20 His-GUs
24 His-GUs

Figure S3.4

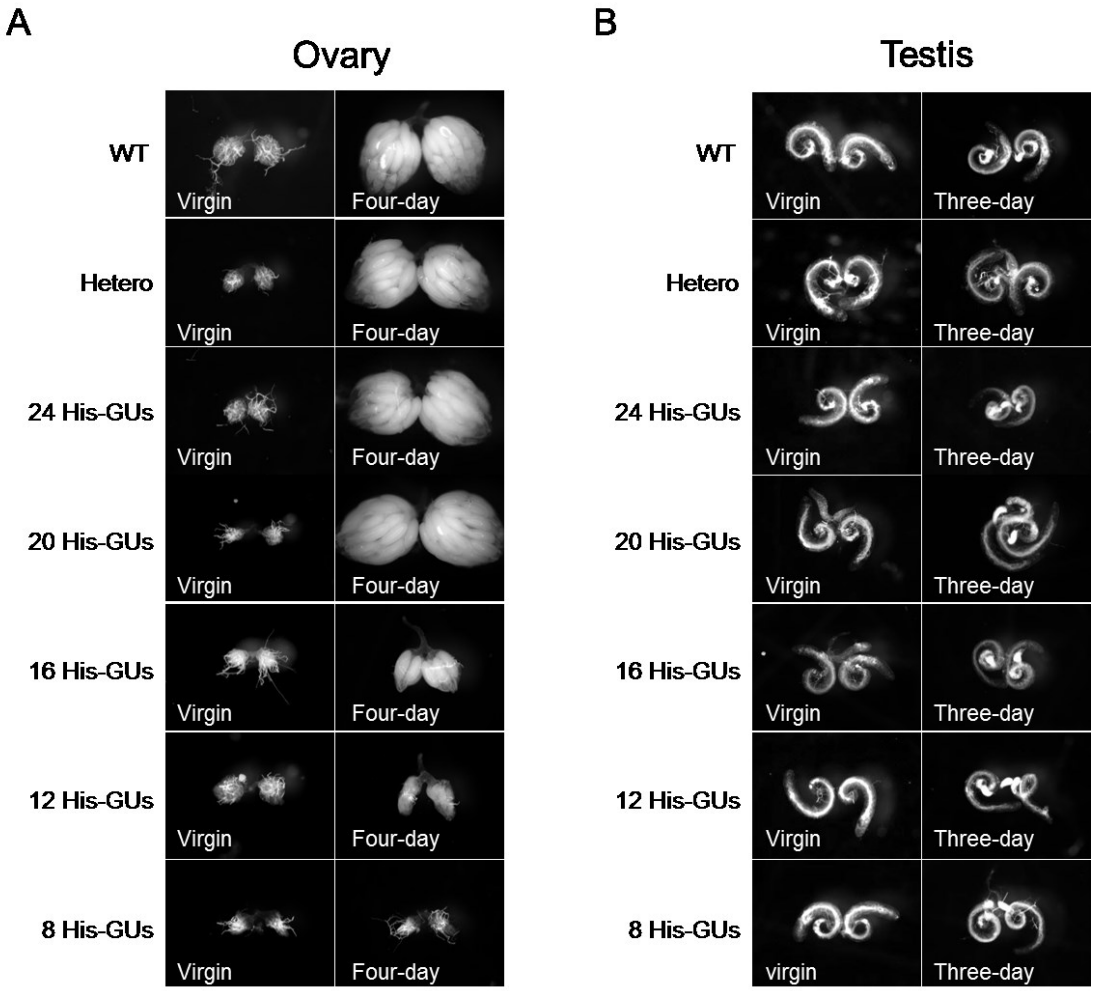
A
Ovary
WT
Hetero
24 His-GUs
20 His-GUs
16 His-GUs
12 His-GUs
8 His-GUs
Virgin
Four-day
B
Testis
WT
Hetero
24 His-GUs
20 His-GUs
16 His-GUs
12 His-GUs
8 His-GUs
Virgin
virgin
Three-day

Figure S3.5

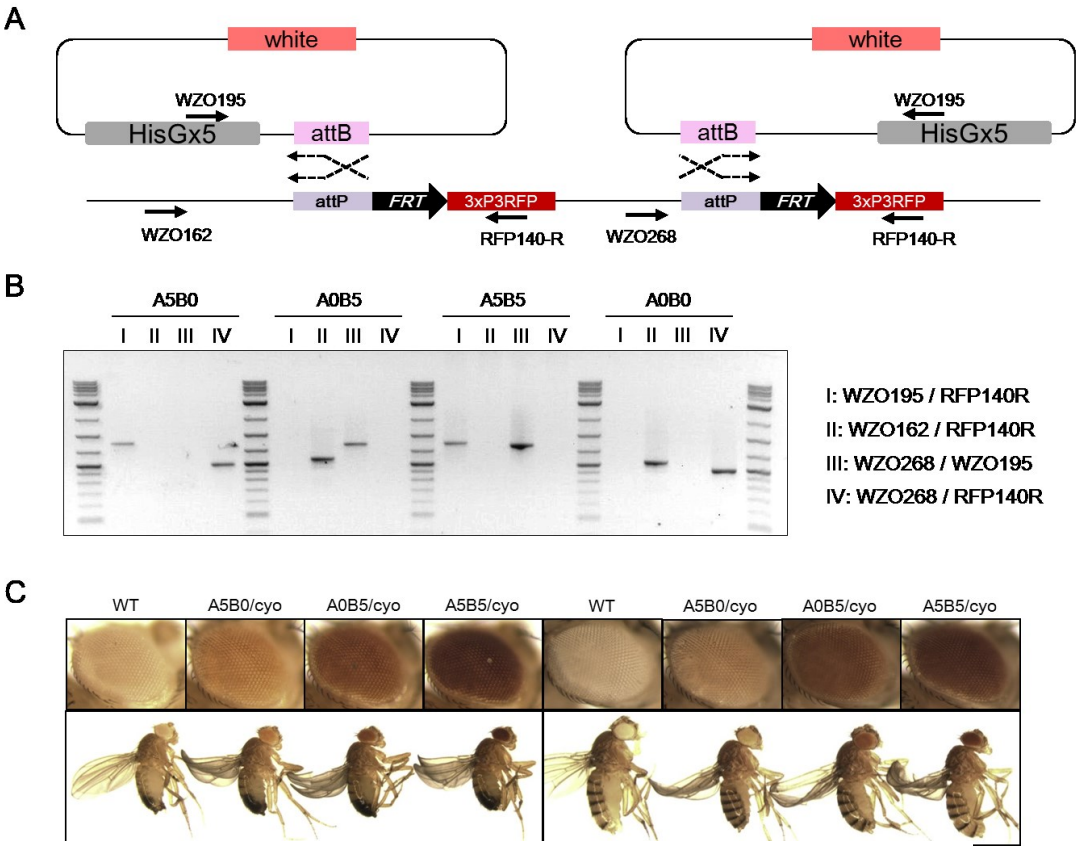
A
white
WZO195
HisGx5
attB
attP
FRT
3xP3RFP
WZO162
RFP140-R
WZO268
B
A5B0
A0B5
A5B5
A0B0
I II III IV
I: WZO195 / RFP140R
II: WZO162 / RFP140R
III: WZO268 / WZO195
IV: WZO268 / RFP140R
C
WT
A5B0/cyo
A0B5/cyo
A5B5/cyo
D
H3T3A
H3K4A
H3T6A
H3R8A
H3K9A
H3S10A
H3R17A
H4K18A
H4K23A
H4R26A
H4K27A
H3S28A
H3K36A
H4T45A
H3K56A
H3K64A
H3K79A
H4T1A
H4R3A
H4K5A
H4K8A
H4K12A
H4K16A
H4R23A
H4Y51A
H4K77A
H4Y88A
H4K91A
H4R92A

Figure S3.6

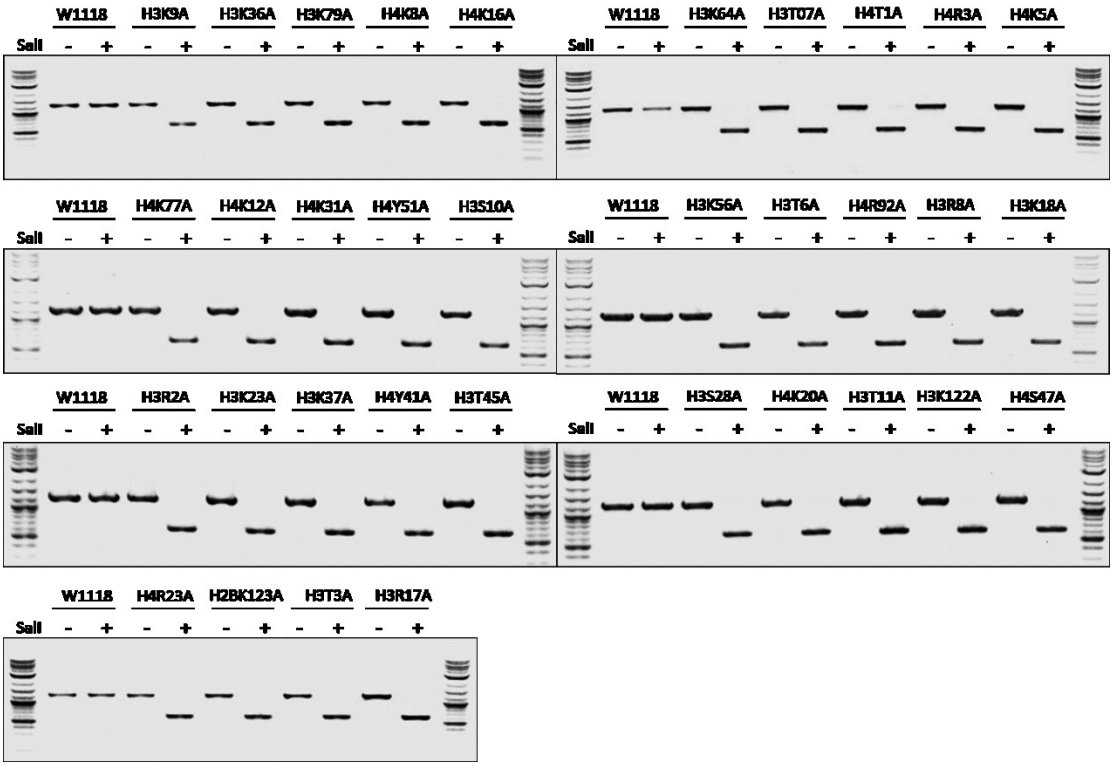
W1118
H3K9A
H3K36A
H3K79A
H4K8A
H4K16A
SalI
W1118
H3K64A
H3T07A
H4T1A
H4R3A
H4K5A
SalI
W1118
H4K77A
H4K12A
H4K31A
H4Y51A
H3S10A
SalI
W1118
H3K56A
H3T6A
H4R92A
H3R8A
H3K18A
SalI
W1118
H3R2A
H3K23A
H3K37A
H4Y41A
H3T45A
SalI
W1118
H3S28A
H4K20A
H3T11A
H3K122A
H4S47A
SalI
W1118
H4R23A
H2BK123A
H3T3A
H3R17A
SalI

Figure S3.7

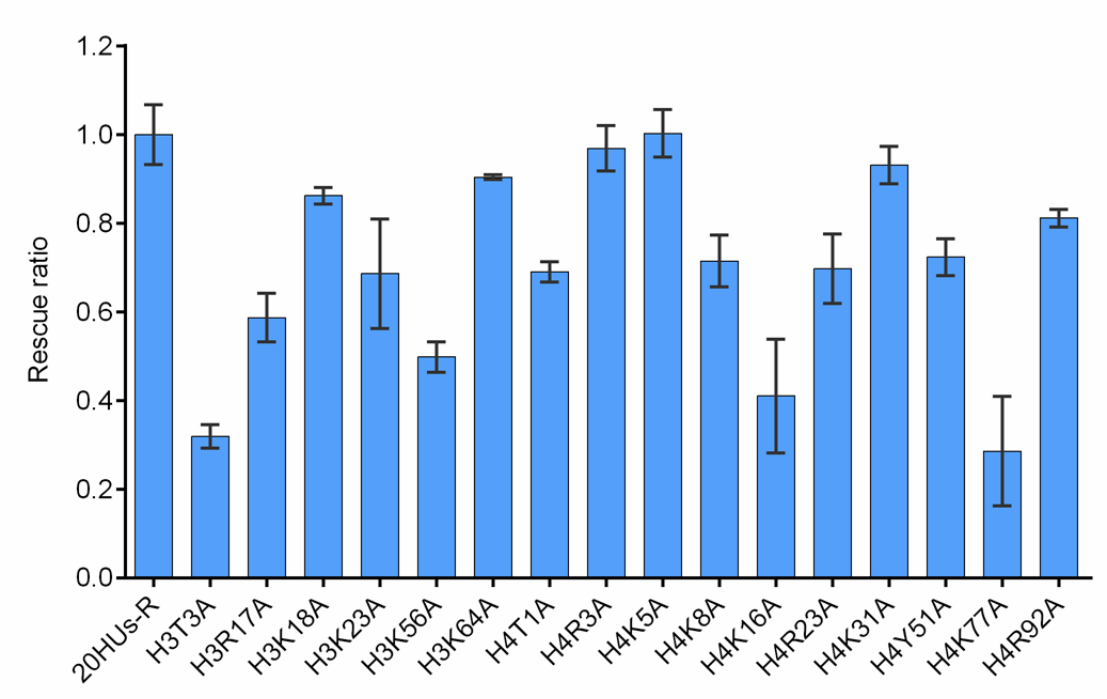
Rescue ratio
1.2
1.0
0.8
0.6
0.4
0.2
0.0
20HUs-R
H3T3A
H3R17A
H3K18A
H3K23A
H3K56A
H3K64A
H4T1A
H4R3A
H4K5A
H4K8A
H4K16A
H4R23A
H4K31A
H4Y51A
H4K77A
H4R92A

Figure S3.8

mutant	Wing defect
W1118	0/60
His-del	0/60
24HisC-R	0/60
20HisC-R	0/60
16HisC-R	0/60
12HisC-R	2/63, 3.2%
10HisC-R	5/48, 10.4%
8HisC-R	0/5

mutant	Wing defect
H3T3A	2/69, 2.3%
H3R17A	2/7, 28.6%
H3K18A	6/60, 10%
H3K23A	4/61, 6.7%
H3K56A	1/70, 1.4%
H3K64A	0/68
H4T1A	0/60
H4R3A	0/76
H4K5	0/14
H4K8A	1/60, 1.7%
H4K16	14/42, 33.3%
H4R23A	0/34
H4K31A	0/60
H4Y51A	0/62
H4K77A	3/63, 4.8%
H4R92A	2/67, 33.0%

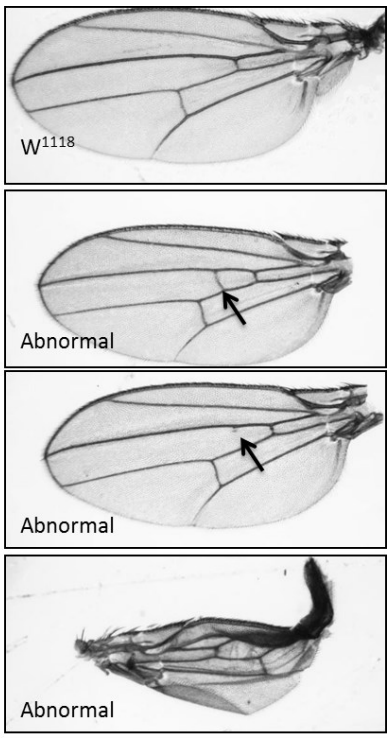

Figure S3.9

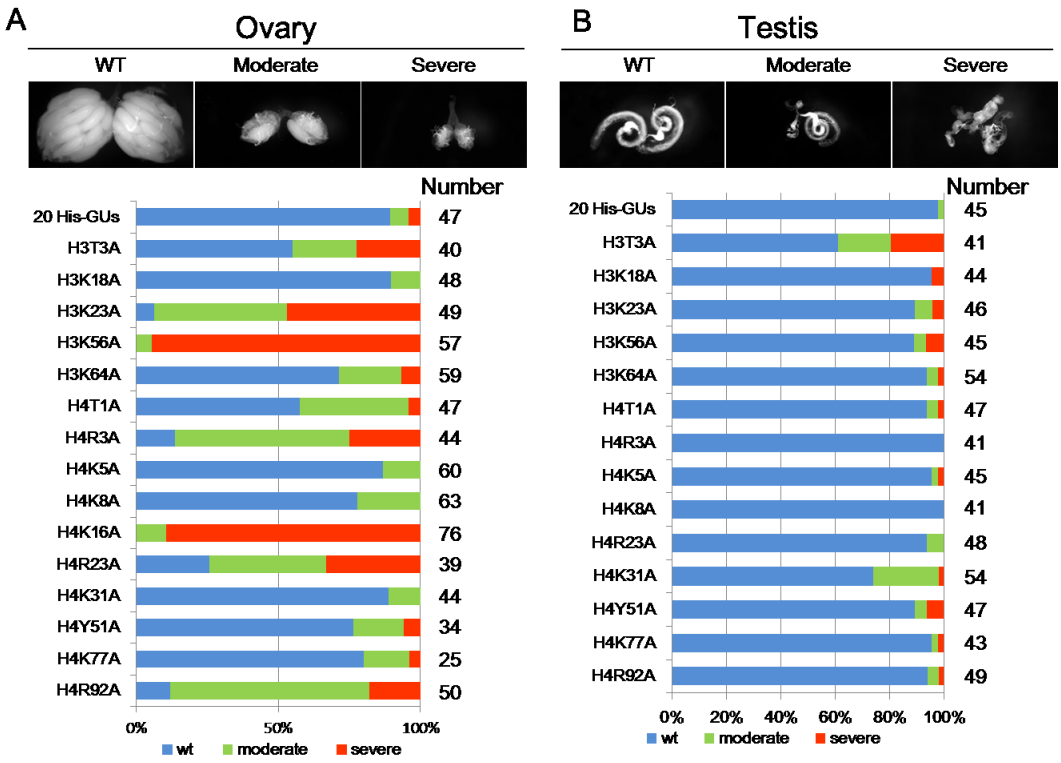
A
Ovary
WT
Moderate
Severe
Number
20 His-GUs 47
H3T3A 40
H3K18A 48
H3K23A 49
H3K56A 57
H3K64A 59
H4T1A 47
H4R3A 44
H4K5A 60
H4K8A 63
H4K16A 76
H4R23A 39
H4K31A 44
H4Y51A 34
H4K77A 25
H4R92A 50
0% 50% 100%
wt moderate severe
B
Testis
WT
Moderate
Severe
Number
20 His-GUs 45
H3T3A 41
H3K18A 44
H3K23A 46
H3K56A 45
H3K64A 54
H4T1A 47
H4R3A 41
H4K5A 45
H4K8A 41
H4R23A 48
H4K31A 54
H4Y51A 47
H4K77A 43
H4R92A 49
0% 20% 40% 60% 80% 100%
wt moderate severe

Figure S3.10

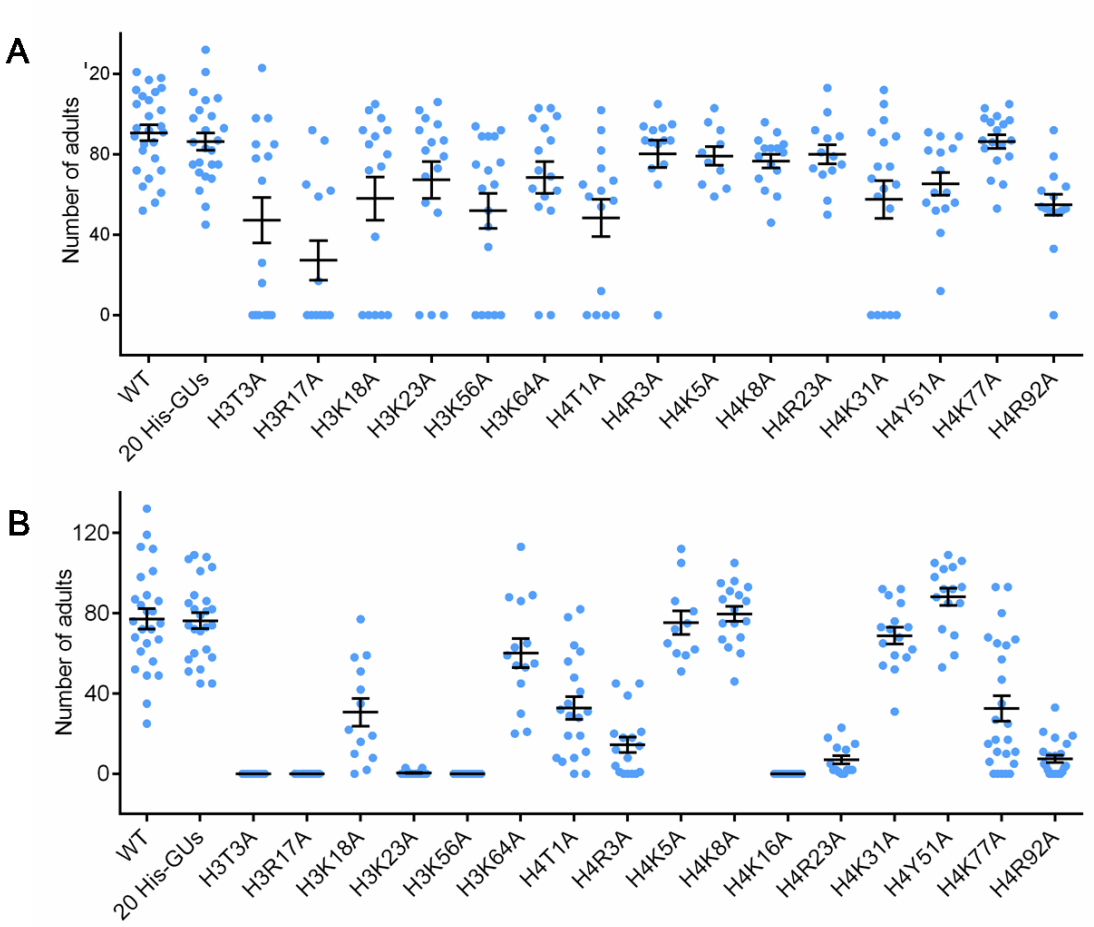
A
Number of adults
120
80
40
0
WT
20 His-GUs
H3T3A
H3R17A
H3K18A
H3K23A
H3K56A
H3K64A
H4T1A
H4R3A
H4K5A
H4K8A
H4R23A
H4K31A
H4Y51A
H4K77A
H4R92A
B
Number of adults
120
80
40
0
WT
20 His-GUs
H3T3A
H3R17A
H3K18A
H3K23A
H3K56A
H3K64A
H4T1A
H4R3A
H4K5A
H4K8A
H4K16A
H4R23A
H4K31A
H4Y51A
H4K77A
H4R92A

Figure S3.11

A

Viability	Mutants	1st larva Homozygote/total	Adult homozygote /total
Embryonic lethal	H3K4A	0/326	0/990
	H3R26A	0/263	0/123
	H3K27A	0/290	0/570
	H3Y41A	0/302	0/118
	H4Y88A	0/332	0/471
	H4K91A	0/368	0/380

B

Viability	mutant	Adult homozygote/total
Larval lethal	H3K9A	0/404
	H3K37A	0/1018
	H3T45A	0/1356
Pupa lethal	H3R2A	0/236
	H3T6A	0/2771
	H3R8A	0/2501
	H3S10A	0/577
	H3S28A	0/830
	H3K36A	0/804
	H3K79A	0/887
	H4K12A	0/3303

C

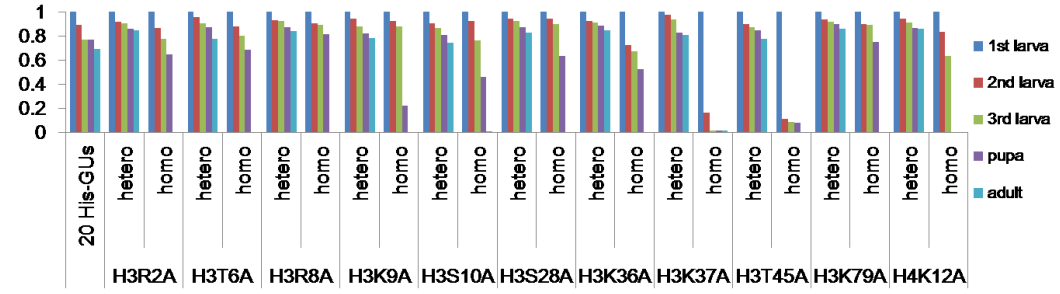

Figure S3.12

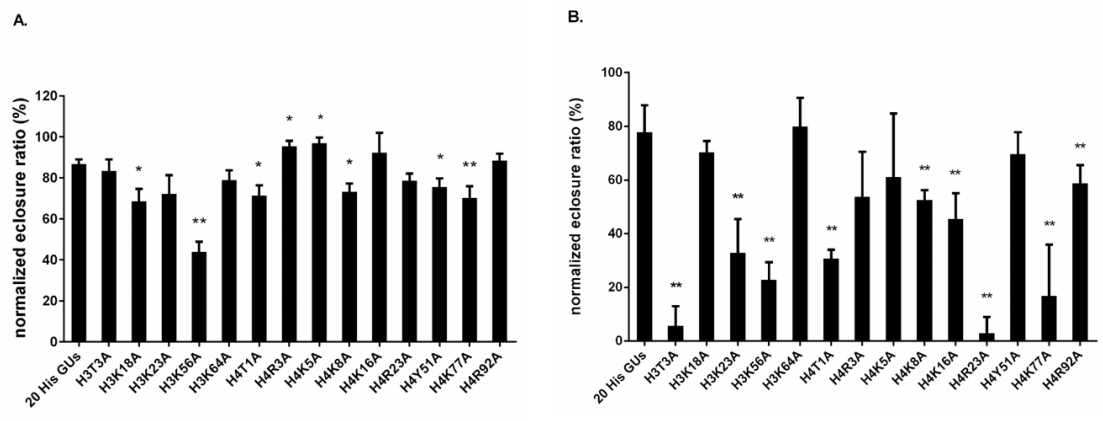
A.
normalized eclosure ratio (%)
120
100
80
60
40
20
0
20 His GUs
H3T3A
H3K18A
H3K23A
H3K56A
H3K64A
H4T1A
H4R3A
H4K5A
H4K8A
H4K16A
H4R23A
H4Y51A
H4K77A
H4R92A
B.
normalized eclosure ratio (%)
100
80
60
40
20
0
20 His GUs
H3T3A
H3K18A
H3K23A
H3K56A
H3K64A
H4T1A
H4R3A
H4K5A
H4K8A
H4K16A
H4R23A
H4Y51A
H4K77A
H4R92A

Figure S3.13

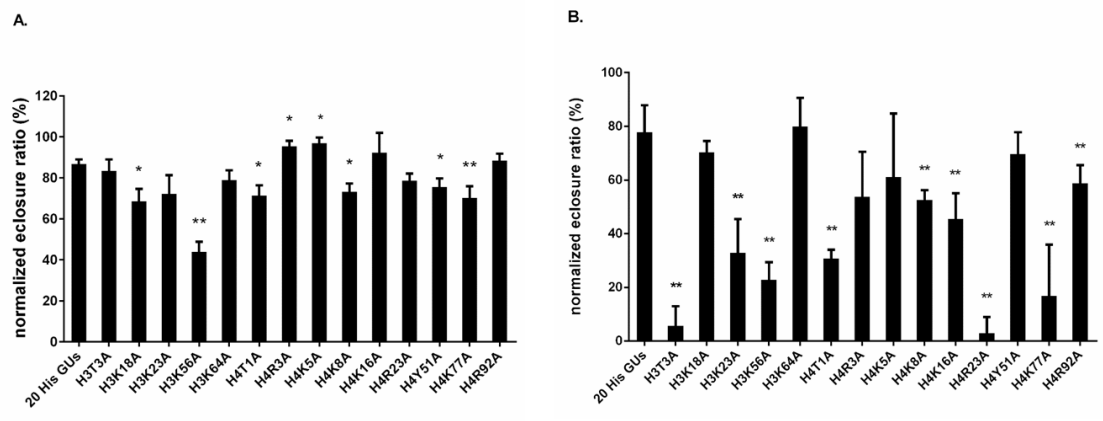
A.
normalized eclosure ratio (%)
120
100
80
60
40
20
0
20 His GUs
H3T3A
H3K18A
H3K23A
H3K56A
H3K64A
H4T1A
H4R3A
H4K5A
H4K8A
H4K16A
H4R23A
H4Y51A
H4K77A
H4R92A
B.
normalized eclosure ratio (%)
100
80
60
40
20
0
20 His GUs
H3T3A
H3K18A
H3K23A
H3K56A
H3K64A
H4T1A
H4R3A
H4K5A
H4K8A
H4K16A
H4R23A
H4Y51A
H4K77A
H4R92A

Chapter 4

Cell-type specific transcriptional profiling within the adult *Drosophila* ovary and testis

Summary

Cell-type specific gene expression profiles can help to better understand the complex regulatory role of niches in maintaining stem cells. The Brand lab recently developed Targeted DamID (TaDa), which permits genome-wide binding profiling of DNA-binding or chromatin-binding proteins without cell isolation. Specifically, they successfully performed TaDa to approximate cell-type specific transcription profiles by fusing *DNA adenine methyltransferase* with *RNA Polymerase II* (*Pol II*). By expressing this Dam-Pol II fusion protein under temporal and spatial control using the *Drosophila* Gal4-UAS system, Pol II binding sites can be determined for subsets of cells within an intact organism. Here, we established conditions that enable the use of TaDa in the adult *Drosophila* testis and ovary. We performed TaDa in different somatic cell types within these tissues, including hub cells or CySC lineage in the testis and escort cells and follicle cells in the ovary. By using cell-type specific Gal4 drivers to briefly express the methyltransferase, and then isolating and sequencing genomic DNA based on methylated GATC sites, we identified thousands of candidate sex-specific genes, including genes likely to be specifically expressed in subsets of cells within each gonad. This sets the stage for many future studies of stem cells and their associated niche cells in both the *Drosophila* testis and ovary.

Introduction

Adult stem cell fate is regulated locally, systemically and epigenetically. Stem cells are located in specific environments, called niches. To understand the complex regulatory role of niches in maintaining stem cells, conventional *in vivo* approaches, including gene-specific knock down of candidate regulatory factors, are often performed. These studies implicate several different signaling pathways as regulators of stem cell fate in many different niches. However, a full understanding of stem cell regulation is still limited due to technical barriers. *Drosophila melanogaster* gonads are powerful systems to study the molecular mechanisms regulating stem cell maintenance and differentiation. Extensive global gene expression profiling studies using techniques including RNA sequencing (RNA-seq) and microarray analysis, have been applied to identify genes involved in stem cell maintenance and differentiation in the fly gonads (Andrews, Bouffard et al. 2000, Gan, Chepelev et al. 2010). However, these methods are restricted in that they only reveal the transcriptome of the whole gonad, which contains a heterogeneous mixture of germline and somatic cells at multiple stages of differentiation. Obtaining transcriptional profiles from distinct cell types and stages is much more valuable, but is a more challenging goal.

In order to obtain a cell-type specific transcriptome, cell isolation is typically necessary. Cell separation can be achieved using fluorescent activated cell sorting (FACS) or laser capture microdissection (LCM), and transcriptional profiling can be derived using RNA-seq (Fu, Spence et al. 1999, Neira and Azen 2002). However, cell isolation is technically challenging in *Drosophila* testes and ovaries as cells adhere to one another, and can lead to a mixed population of cells upon purification. One can also

examine transcription profiles using targeted expression of RNA-binding or ribosomal-binding proteins within a subset of cells. The RNA associated with these proteins can be isolated after immunoprecipitation of RNA-protein complexes, and subsequent sequence analysis reveals the transcriptome of the cells of interest (Roy, Stuart et al. 2002, Miller, Robinson et al. 2009, Thomas, Lee et al. 2012). However, these kinds of approaches are unable to provide the genome-wide binding profile of chromatin binding or transcription factors.

Several years ago, the van Steensel lab invented the technique of Dam identification (DamID) based on the enzyme DNA adenine methyltransferase, which methylates adenines in the sequence GATC (Figure 4.1A) (van Steensel and Henikoff 2000, van Steensel, Delrow et al. 2001). Dam is a protein found in *Escherichia coli* and absent in most eukaryotes. Therefore, methylation of adenine is not found in most eukaryotic organisms, including *S. pombe*, *C.elegans*, *D. melanogaster*, mouse and human. DamID takes advantage of this difference in methylation status by fusing a protein of interest (typically a chromatin binding protein or transcription factor) to Dam. Upon fusion protein expression in either cultured cells or intact organisms, Dam is targeted to the regions within the genome where the protein of interest normally binds. This results in local methylation of adenines (Figure 4.1B). The methylation marks can then be identified by specific methylation-sensitive restriction enzyme digestion, followed by PCR amplification and high-throughput sequencing (Figure 4.1C). DamID is similar to chromatin immunoprecipitation (ChIP) in that they can both provide protein-DNA binding profiles. Side by side comparisons have been performed in the *Drosophila* larval nervous system and the two methods result in comparable protein binding profiles

(Greil, Moorman et al. 2006, Aughey and Southall 2015). Even though the resolution of DamID (approximately 200 bps in fly, which is determined by the median spacing between GATC fragments) is poorer than the resolution for ChIP, which is typically less than 50 bps, DamID has several advantages over ChIP. DamID does not require ChIP-grade antisera. It also has been suggested that DamID works particularly well for proteins that interact transiently with their target DNA sequences since irreversible Dam methylation occurs even during a brief protein-DNA interaction. Moreover, cell-type specific chromatin binding patterns can easily be achieved by restricting the expression of Dam-fusion protein to specific cell types, thereby circumventing the need to purify or sort cell types from a tissue. This is particularly important when studying stem cells and their niches, because these cells usually represent a very small subset of the cells within the tissue they regenerate.

Based on the reasons above, the Brand lab developed targeted DamID (TaDa) to study the genome-wide binding profile of a Dam-fusion protein under both spatial and temporal control (Southall, Gold et al. 2013). They took advantage of the GAL4-UAS system to obtain binding profiles from specific cell types in vivo without cell isolation. Specifically, they fused *Dam* with *RNA polymerase II* (*Pol II*). They chose Pol II because this critical eukaryotic enzyme, catalyzes the synthesis of RNA from DNA template (Sugaya, Vigneron et al. 2000), and the Pol II occupancy profile can be used to predict actively transcribed genes (Min, Waterfall et al. 2011). The method is very sensitive and works with fewer than, possibly far fewer than, 10,000 cells (Southall, Gold et al. 2013).

The temporal control of this system is a very important aspect because high levels of Dam-fusion protein expression can cause nonspecific DNA methylation that is toxic to

the cells and the organism (van Steensel and Henikoff 2000). Therefore, in order to attenuate Dam-fusion protein expression, the Brand lab generated transgenic fly lines where the open reading frame (ORF) of Dam is located downstream of a full length *mCherry* ORF (Figure 1.4D). Separating the Dam ORF from the UAS construct dampens its expression such that it can only be expressed at a low frequency through ribosome re-initiation in induced cells. Therefore, translation of Dam is null in uninduced cells and sufficiently low in induced cells (at levels undetectable by immunostaining or by western blotting), limiting toxicity. Furthermore, with this construct, almost no DNA methylation is observed in the absence of Gal4. Using TaDa, the Brand lab successfully identified genes involved in neural stem cell regulation according to endogenous Pol II occupancy profile in neuroepithelium or in neuroblasts (Southall, Gold et al. 2013). Here, we adapt the TaDa technique for use in the *Drosophila* testis and ovary, and obtain cell-type specific gene expression data from subsets of cells in these tissues.

Results

Optimizing TaDa for the *Drosophila* testis and ovary

In order to obtain cell-type specific transcription profiles from subsets of cells within the *Drosophila* testis and ovary, several different GAL4 drivers were used. We focused on drivers specifically expressed in the hub cells, early germline cells and early CySC lineage cells in the testis. In the ovary, an early germline driver, and two early somatic cell drivers (expressed in escort cells and follicle cells) were used. We also performed TaDa on testes and ovaries using a ubiquitous driver in order to compare TaDa data to RNA seq data from whole testes or ovaries processed in parallel (Table 4.1). The expression patterns of each driver was confirmed by crossing flies carrying each driver to flies bearing UAS reporter constructs expressing visible markers including nuclear (nGFP), cytoplasmic GFP (cGFP) or membrane GFP (mGFP) (Figure 4.2A-E).

An important consideration regarding DamID is that in addition to binding the sites in the genome that are preferred targets of the Dam-fusion protein, diffusion of the Dam-fusion protein within the nucleus also causes considerable non-specific background methylation, especially in the "open" regions of chromatin where genes are actively transcribed. Consistent with this idea, we observed methylated genomic fragments in samples collected from testes where either Dam or Dam-Pol II were expressed, but not in wild-type testes (Figure 4.2F). In all of our TaDa experiments, we prepared the samples where an unfused Dam protein was processed in parallel to correct for the non-targeted background methylation caused by variation in chromatin accessibility.

As mentioned above, since excessive GATC methylation is toxic to flies, and also can saturate methylation levels non-specifically (van Steensel and Henikoff 2000), it is important to use the lowest possible level of Dam expression in order to obtain detectable but unsaturated methylation patterns. To optimize TaDa conditions for the *Drosophila* testis and ovary, we induced the expression of Dam or Dam-Pol II fusion proteins at different temperatures for varying lengths of time. We first confirmed that DNA methylation is not induced at 18°C to ensure that methylation is not occurring during development (Figure 4.2F). We next induced Dam-Pol II expression at either 29°C or 31°C for 1 to 3 days. We found that expression at 29°C for 24 hours is sufficient to induce considerable levels of methylation (Figure 4.2F). This was also the induction paradigm used previously by the Brand lab (Southall, Gold et al. 2013). Therefore, we used expression for 24 hours at 29°C as our working condition for the rest of our experiments.

Dam-Polymerase II occupancy from TaDa can predict cell-type transcription profiles in adult Drosophila gonads

We then analyzed the sequencing data using a DamID pipeline developed by the Brand lab (Marshall and Brand 2015). With this pipeline, we were able to identify genes significantly bound by Dam-Pol II. To validate our data, we first compared Dam-Pol II occupancy in the euchromatin and heterochromatin obtained from whole female or male flies expressing a ubiquitous driver (tub-Gal4, Figure 4.2A). Using the right arm of the third chromosome in the *Drosophila* genome (3R) as an example, we found that Dam-Pol II is more likely to methylate DNA in the euchromatic regions of 3R, relative to the

heterochromatic regions (Figure 4.3A, B). This is consistent with the hypothesis that heterochromatin, being a more tightly packed form of DNA, is less accessible to transcription factors or other proteins including Dam-Pol II. In general, heterochromatic genes are transcriptionally silenced. In contrast, euchromatic DNA is less tightly packed and therefore is accessible for Dam-Pol II to bind and is a better substrate for methylation A previous study found that only 20% of the transcripts from the gonad were sex-biased (10% of the transcripts are male specific; 11% of the transcripts are female specific) (Parisi, Nuttall et al. 2003). Therefore, we expect the Dam-Pol II binding profiles from whole female and male adult flies to look similar. This is what is observed in our data (Figure 4.3A, B). Moreover, Dam-Pol II occupancy patterns from different biological replicates of the same genotype processed at different times are similar to each other (for example, Dam-Pol II occupancy on chromosome 3R in cells expressing tub-Gal4 in females, Figure 4.3A, B). We compared the similarity between different samples by looking at the percentage of genes that are or are not expressed in all the samples of the same genotype. The two samples from female flies expressing tub-Gal4 share 90.5% similarity. Together, we discovered 5,732 genes expressed in female flies with false discovery rate (FDR) smaller than 0.05. This suggests that TaDa will be an appropriate tool to generate robust and reproducible estimates of the transcriptional profile of cells within the ovary and testis.

Given that TaDa appeared to be performing as expected in the whole flies, based on Dam-Pol II occupancy in cells expressing the global driver tub-Gal4, we next looked at cell-type specific Dam-Pol II occupancy profile from testes or ovaries, focusing on the hub cells and the CySC lineage from testes and the escort cells and follicle cells from

ovaries (Table 1). We looked at 5 different loci. The first was *Yolk protein1* (*Yp1*), which is highly transcribed in follicle cells in the ovary but not in the testis (Logan, Garabedian et al. 1989, Ma, Wawersik et al. 2014). Here, we found that the *Yp1* locus is significantly bound by Dam-Pol II in the somatic cells of the ovary but not the testis (Figure 4.4A). In contrast, the positive control *Glyceraldehyde-3-Phosphate Dehydrogenase* (*GAPDH*), a housekeeping gene expressed in all the cell types, has high Dam-Pol II occupancy in all of the cell types we examined (Figure 4.4A). We also examined our dataset for 'negative controls' - genes for which transcripts were previously shown to be undetectable in the cell types of interest. For example, transcripts from the *sungrazer* (*sunz*) loci are detectable in spermatids but not in the somatic cells in the testis (Barreau, Benson et al. 2008). As expected, Dam-Pol II occupancy within the *sunz* locus in both hub cells and CySC lineage cells in the testis was undetectable (Figure 4.4B). This suggests that TaDa behaves as expected for the very few individual genes where we can compare Dam-Pol II occupancy to known mRNA expression patterns. Therefore, we then moved on to get a more general idea of which genes might be expressed in a cell-type specific or sex-specific manner. Comparing TaDa data collected from whole male or female flies expressing the globally expressed driver tub-Gal4 revealed 1800 female-specific genes and 758 male-specific genes. If we focus on the cell types that express the c587 Gal4 driver in both sexes, we identify 1079 female-specific genes and 2777 male-specific genes. Learning that TaDa is able to identity sex-specific genes, we then moved on to cell-type specific genes expressed in the testis or ovary. According to RNA in situ hybridization, *unpaired* (*os*) expression is highly enriched in the hub cells of the testis and in polar cells within the ovary (Tulina and Matunis 2001, McGregor, Xi et al. 2002),

Consistent with our TaDa data, Dam-Pol II occupies the *upd* locus in hub cells within the testis, but not in the cells in the CySC lineage. Similarly, the *upd* locus is not occupied by Dam-Pol II in ovarian follicle cells and escort cells (Figure 4.5A). In contrast, Dam-Pol II only binds *traffic jam* (*Tj*) in the CySC lineage in the testis or escort cells and follicle cells in the ovary (Figure 4.5B). This is also consistent with the expression pattern of *Tj* in both sexes (Ma, Wawersik et al. 2014). We conclude that cell-type-specific differences in RNA Pol II occupancy can recapitulate previously known differences in gene expression in subsets of cells within the *Drosophila* testis and ovary.

We then looked at the Dam-Pol II binding profile in the cells driven by either Tj-Gal4 or c587-Gal4 in the ovary. Since Tj-Gal4 and c587-Gal4 are expressed in the same cell types in the ovary, except that Tj-Gal4 has broader follicle cell expression pattern (Table 1), we expect the binding profile of Dam-Pol II to be similar in these two cell types. We found that out of 16,428 genes we looked at, Tj-Gal4 and c587-Gal4 have 79.1% similarity in Dam-Pol II occupancy. We also discovered 3,460 genes that may be expressed specifically in the hub cells and 2,391 in the CySC lineage in the testis (comparing TaDa results from E132-Gal4 with TaDa results from c587-Gal4). The data obtained from TaDa will help us better understand the stem cell niches in the testis or ovary.

Discussion

TaDa is a highly sensitive technique that allows the identification of cell-type-specific DNA binding profiles of chromatin binding or DNA binding proteins (Southall, Gold et al. 2013). In *Drosophila*, we can take advantage of the powerful GAL4-UAS system and drive expression of Dam fusion protein in subsets of cells within intact tissues. Specifically, when Dam is fused to Pol II, it enables indirect transcriptome analysis in a cell-specific fashion. Performing TaDa in different cell types in either testes or ovaries, we were able to identify hundreds of sex-specific genes and niche factors. Comparing known RNA in situ data or protein expression data to that obtained for putative targets discovered in the TaDa analysis suggests this approach will be useful, and should be expanded upon in the future.

Currently, we can identify genes that are likely to be expressed specifically in the hub cells or CySC lineage in the testis and in the escort cells and the follicle stem cells and their early progeny in the ovary. Verification of additional genes on these lists by comparing them to RNA-seq data where available is an important next step. In the future, we can use additional cell-type specific Gal4 drivers to get a deeper understanding of these stem cell niches. For example, we can compare Dam-Pol II occupancy in the late germline to that in the early germline to obtain genes expressed in the GSCs. We can also identify CySC-specific genes by substracting genes specifically found in the late cyst cells from genes expressed throughout the CySC lineage. Another advantage of TaDa is that this technique will also be able to track gene expression changes in specific cell types in response to environmental change or upon disruption of certain genes. For example, our lab previously found that the transcriptional repressor and JAK-STAT target

Chronologically inappropriate morphogenesis (*chinmo*) is required for somatic stem cell maintenance and promotes the male fate of these cells, which connects niche signaling to stem cell maintenance and sex maintenance (Flaherty, Salis et al. 2010, Ma, Wawersik et al. 2014). Since sex maintenance is also conserved and is a rare example of stem cell transdifferentiation in vivo, we are interested in pursuing the underlying mechanisms. TaDa would be an excellent technique to help identify genes expressed in wild-type versus $chinmo^{ST}$ CySCs and early cyst cells). To obtain the gene expression profile of CySCs and their early progeny we can express *UAS-Dam-Pol II* specifically in these cells under the control of *c587- Gal4*. We can then compare expression profiles in the wild type cells to the mutant cells to identify candidate *chinmo* targets. This will provide a comprehensive picture of the circuitry regulating adult stem cell sex identity.

Overall, TaDa is a sensitive and powerful technique, which allows us to quickly and easily identify genes specifically expressed in certain cell types or specific sexes. These data will provide the foundation for future studies to uncover the genes required for stem cell function, sex maintenance and many other biological processes.

Experimental Procedures

Fly stocks and cultures for DamID

Fly stocks were raised at 25˚C on standard molasses/yeast medium unless otherwise indicated. *UAS-LT3-NDam* and *UAS-LT3-NDam-RpII215* (Southall, Gold et al. 2013) were crossed to GAL4 lines containing $GAL80^{ts}$, including E132-Gal4, c587-Gal4, tj-Gal4, nanos-Gal4, tub-Gal4 (from C. Thummel) and reared at 18°C (restrictive temperature). 0-3 day old flies were shifted to 29°C (permissive temperature) for 24 hr before dissection. Around 200 ovaries or 300-400 testes were dissected for each biological replicate. Genomic DNA was extracted and methylated DNA was digested, ligated to adaptors, amplified. Libraries were then prepared and sent for high-throughput sequencing as described (Southall, Gold et al. 2013).

DamID analysis

Data from each biological replicate were analyzed separately. Log2 ratio files were generated (Dam-Pol II over Dam-only) and median normalized; false discovery rate (FDR) was used to identify genes with significantly Pol II occupancy (Marshall and Brand 2015).

Immunofluorescence microscopy

Testes or ovaries were dissected, fixed, and stained as described previously (Matunis 1997). The following antibodies were used: rabbit anti-Vasa (d-260) (Santa Cruz Biotechnology, 1:400); chicken anti-GFP (Abcam, 1:10,000). Alexa fluor-conjugated secondary IgG (H+L) antibodies were diluted at 1:200 for 568 and 1:400 for 488

conjugates. Secondary antisera were: goat anti-rabbit 568, goat anti-chicken 488 (Molecular Probes/Invitrogen). DNA was stained with 4,6-diamidino-2-phenylindole (DAPI; Sigma) at 1 ug/ml. Fixed testes were mounted in Vectashield (Vector Labs) for imaging. Confocal images were obtained with a Zeiss LSM 5 Pascal.

References

Andrews, J., G. G. Bouffard, C. Cheadle, J. N. Lu, K. G. Becker and B. Oliver (2000). "Gene discovery using computational and microarray analysis of transcription in the Drosophila melanogaster testis." Genome Research **10**(12): 2030-2043.

Aughey, G. N. and T. D. Southall (2015). "Dam it's good! DamID profiling of protein-DNA interactions." Wiley Interdiscip Rev Dev Biol.

Barreau, C., E. Benson, E. Gudmannsdottir, F. Newton and H. White-Cooper (2008). "Post-meiotic transcription in Drosophila testes." Development **135**(11): 1897-1902.

Flaherty, M. S., P. Salis, C. J. Evans, L. A. Ekas, A. Marouf, J. Zavadil, U. Banerjee and E. A. Bach (2010). "chinmo is a functional effector of the JAK/STAT pathway that regulates eye development, tumor formation, and stem cell self-renewal in Drosophila." Dev Cell **18**(4): 556-568.

Fu, A. Y., C. Spence, A. Scherer, F. H. Arnold and S. R. Quake (1999). "A microfabricated fluorescence-activated cell sorter." Nat Biotechnol **17**(11): 1109-1111.

Gan, Q., I. Chepelev, G. Wei, L. Tarayrah, K. Cui, K. Zhao and X. Chen (2010). "Dynamic regulation of alternative splicing and chromatin structure in Drosophila gonads revealed by RNA-seq." Cell Res **20**(7): 763-783.

Greil, F., C. Moorman and B. van Steensel (2006). "DamID: Mapping of in vivo protein-genome interactions using tethered DNA adenine methyltransferase." DNA Microarrays Part A: Array Platforms and Wet-Bench Protocols **410**: 342-359.

Logan, S. K., M. J. Garabedian and P. C. Wensink (1989). "DNA Regions That Regulate the Ovarian Transcriptional Specificity of Drosophila Yolk Protein Genes." Genes & Development **3**(9): 1453-1461.

Ma, Q., M. Wawersik and E. L. Matunis (2014). "The Jak-STAT target Chinmo prevents sex transformation of adult stem cells in the Drosophila testis niche." Dev Cell **31**(4): 474-486.

Marshall, O. J. and A. H. Brand (2015). "damidseq_pipeline: an automated pipeline for processing DamID sequencing datasets." Bioinformatics **31**(20): 3371-3373.

Matunis, E. (1997). "punt and schnurri regulate a somatically derived signal that restricts proliferation of committed progenitors in the germline." Development **124**: 4383-4391.

McGregor, J. R., R. Xi and D. A. Harrison (2002). "JAK signaling is somatically required for follicle cell differentiation in Drosophila." Development **129**(3): 705-717.

Miller, M. R., K. J. Robinson, M. D. Cleary and C. Q. Doe (2009). "TU-tagging: cell type-specific RNA isolation from intact complex tissues." Nat Methods **6**(6): 439-441.

Min, I. M., J. J. Waterfall, L. J. Core, R. J. Munroe, J. Schimenti and J. T. Lis (2011). "Regulating RNA polymerase pausing and transcription elongation in embryonic stem cells." Genes Dev **25**(7): 742-754.

Neira, M. and E. Azen (2002). "Gene discovery with laser capture microscopy." Methods Enzymol **356**: 282-289.

Parisi, M., R. Nuttall, D. Naiman, G. Bouffard, J. Malley, J. Andrews, S. Eastman and B. Oliver (2003). "Paucity of genes on the Drosophila X chromosome showing male-biased expression." Science **299**(5607): 697-700.

Roy, P. J., J. M. Stuart, J. Lund and S. K. Kim (2002). "Chromosomal clustering of muscle-expressed genes in Caenorhabditis elegans." Nature **418**(6901): 975-979.

Southall, T. D., K. S. Gold, B. Egger, C. M. Davidson, E. E. Caygill, O. J. Marshall and A. H. Brand (2013). "Cell-type-specific profiling of gene expression and chromatin binding without cell isolation: assaying RNA Pol II occupancy in neural stem cells." Dev Cell **26**(1): 101-112.

Sugaya, K., M. Vigneron and P. R. Cook (2000). "Mammalian cell lines expressing functional RNA polymerase II tagged with the green fluorescent protein." J Cell Sci **113 (Pt 15)**: 2679-2683.

Thomas, A., P. J. Lee, J. E. Dalton, K. J. Nomie, L. Stoica, M. Costa-Mattioli, P. Chang, S. Nuzhdin, M. N. Arbeitman and H. A. Dierick (2012). "A versatile method for cell-specific profiling of translated mRNAs in Drosophila." PLoS One **7**(7): e40276.

Tulina, N. and E. Matunis (2001). "Control of stem cell self-renewal in Drosophila spermatogenesis by JAK-STAT signaling." Science **294**(5551): 2546-2549.

van Steensel, B., J. Delrow and S. Henikoff (2001). "Chromatin profiling using targeted DNA adenine methyltransferase." Nat Genet **27**(3): 304-308.

van Steensel, B. and S. Henikoff (2000). "Identification of in vivo DNA targets of chromatin proteins using tethered dam methyltransferase." Nat Biotechnol **18**(4): 424-428.

Figure Legends

Figure 4.1 TaDa can yield cell-type-specific protein DNA binding profiles.

(A) Prokaryotic protein DNA adenine methyltransferase methylates adenine in the sequence GATC. **(B)** Principle of DamID. Dam fused with a DNA-binding or chromatin binding protein (RNA polymerase II in our experiment) can specifically methylate DNA close to where the protein of interest binds. **(C)** Flowchart illustrating the DamID technique. Genomic DNA is digested by a specific methylation-sensitive restriction enzyme and then PCR amplified, followed by genomic DNA preparation and high-throughput sequencing. **(D)** Illustration of the TaDa method (modified from Figure 1A in Southall, Gold et al. 2013). Expression of Dam-fusion protein is under temporal and spatial control of the Gal4-UAS system. An additional *mCherry* ORF is inserted upstream of Dam-Pol II to reduce expression levels of the fusion protein so that there will be no methylation when Gal4 is not present, and to minimize the level of nonspecific methylation when Gal4 is introduced.

Figure 4.2 Analysis of TaDa working conditions in the *Drosophila* testis and ovary.

(A)-(E) Expression patterns of different Gal4 lines in adult gonads. Cytoplasmic GFP (cGFP), nuclear GFP (nGFP), or membrane-targeted GFP (mGFP) are driven by the globally expressed driver *tubP-Gal4* **(A, A')**, the somatic cell drivers *c587-Gal4* **(B, B')** or *Tj-Gal4* **(C, C')**, the germline driver *nanos-Gal4* **(D, D')** or hub driver *E132-Gal4* **(E)**. Testes (A, B, C, D, E) and ovaries (A', B', C', D') from newly eclosed flies are stained with DAPI (blue), anti-Vasa (red), and anti-GFP (green). **(F)** DamID in GSCs and spermatogonia (lane 3) produces DNA fragments of the expected size. Control flies not

expressing Dam (lane 1) yield no fragments, while flies expressing Dam alone (lane 2) yield some background fragments as expected. **(G)** Methylation is barely detectable at 18°C. Expression of Dam or Dam fusion protein at 29°C or 31°C results in considerable amounts of methylation.

Figure 4.3 Metagene profile for Dam-Pol II across a heterochromatin or euchromatin region.

Dam-Pol II has low occupancy in a heterochromatic region **(A)** but high occupancy in an euchromatic region of chromosome 3R **(B)**. y-axis is log2 ratio files (Dam-Pol II over Dam-only) and median normalized.

Figure 4.4 TaDa recapitulates sex-specific gene expression in the fly ovary and testis.

(A) RT-PCR analysis shows that *Yp1* RNA is found in the ovary but not testis (Ma, Wawersik et al. 2014). We found that Dam-Pol II only binds to *Yp1* in cells from the ovary. As a positive control, Dam-Pol II has high occupancy on housekeeping gene *GAPDH* in all the cell types (bottom panel, male and female). **(B)** Dam-Pol II occupancy on negative control *sunz*. Dam-Pol II does not methylate the *sunz* locus in the hub cells or CySC lineage which is consistent with the RNA in situ of *sunz* showing that *sunz* is only expressed in the spermatids (Barreau, Benson et al. 2008).

Figure 4.5 TaDa recapitulates cell type-specific gene expression in the fly ovary and testis.

(A) According to RNA in situ, *os* is only expressed in the polar cells in the ovary and hub cells in the testis (Tulina and Matunis 2001, McGregor, Xi et al. 2002). Consistent with this, we only observe significant Dam-Pol II occupancy on the *os* locus in the cells expressing the hub driver *E132-Gal4*. **(B)** *c587-Gal4* and *Tj-Gal4* are expressed in the somatic cells in the testis and ovary but not in the hub cells. Consistent with this, we observe high occupancy of Dam-Pol II in CySC lineage cells but not hub cells in the testis and in escort and follicle cells in the ovary with these drivers.

Table 4.1. Cell type-specific expression patterns in young wild type testes or ovary (Full genotypes are listed below the table)		
Cell Type	**Tissue**	**Gal4 driver**
early germline	testis	nanos-Gal4
early germline	ovary	
CySCs and early cyst cells	testis	c587-Gal4
escort cells, FSCs, early follicle cells	ovary	
CySCs, early cyst cells and some later cyst cells	testis	Tj-Gal4
escort cells, FSCs, early follicle cells, late follicle cells	ovary	
hub	testis	E132-Gal4
all cells	testis	tubulin-Gal4
all somatic cells (UASt drives dam constructs)	ovary	

Figure 4.1

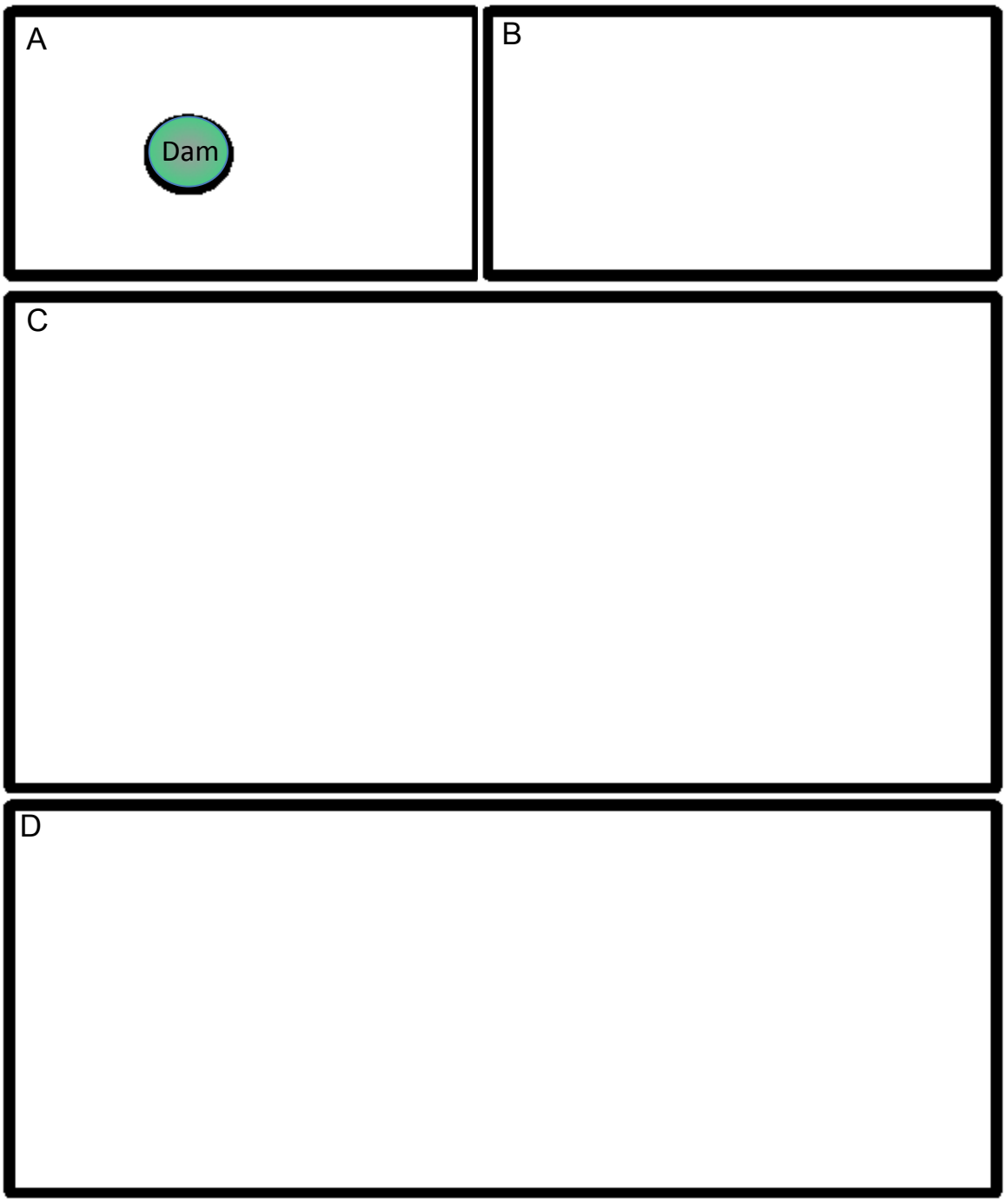

Figure 4.2

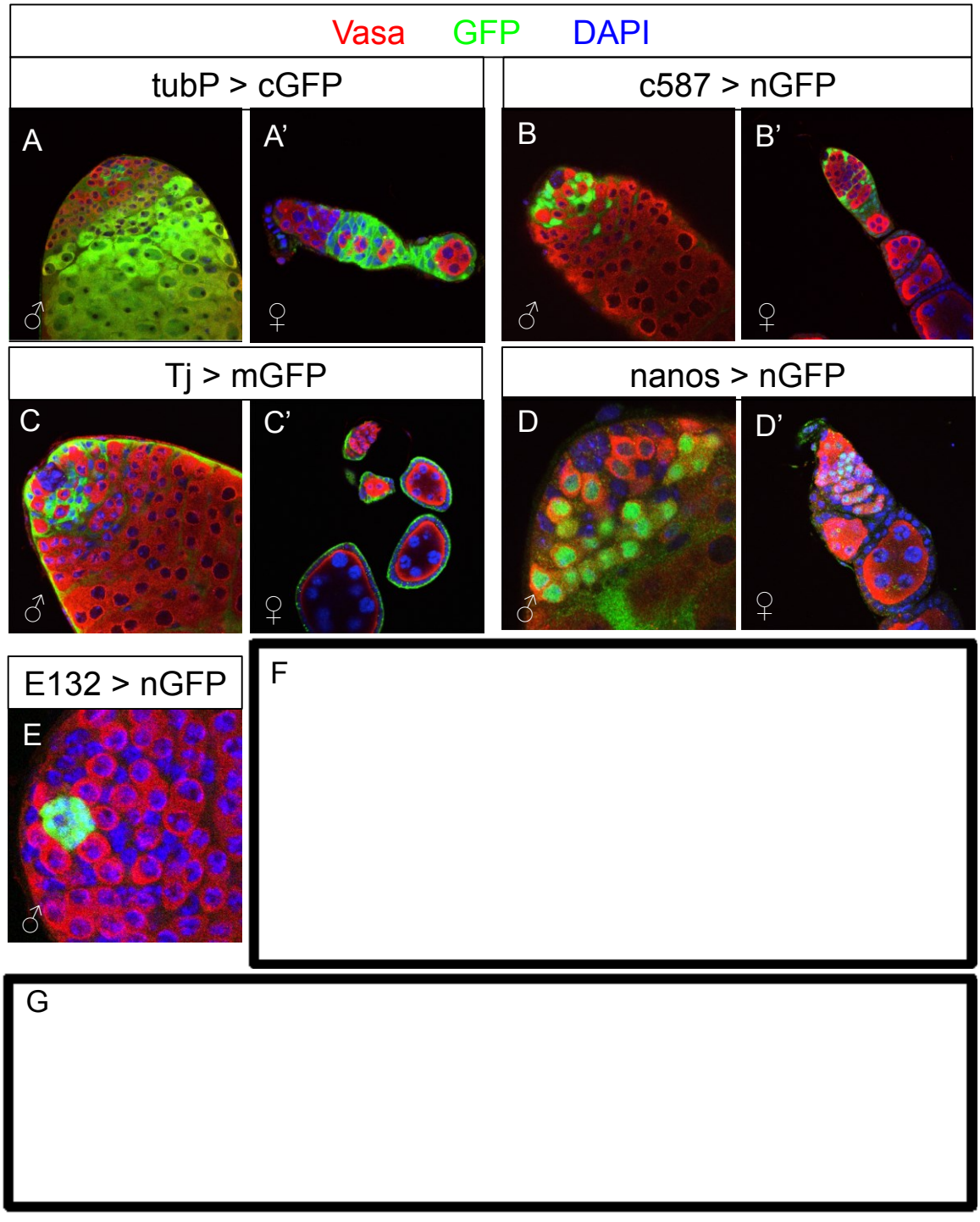
Vasa GFP DAPI
tubP > cGFP
c587 > nGFP
A
A'
B
B'
Tj > mGFP
nanos > nGFP
C
C'
D
D'
E132 > nGFP
E
F
G

Figure 4.3

A

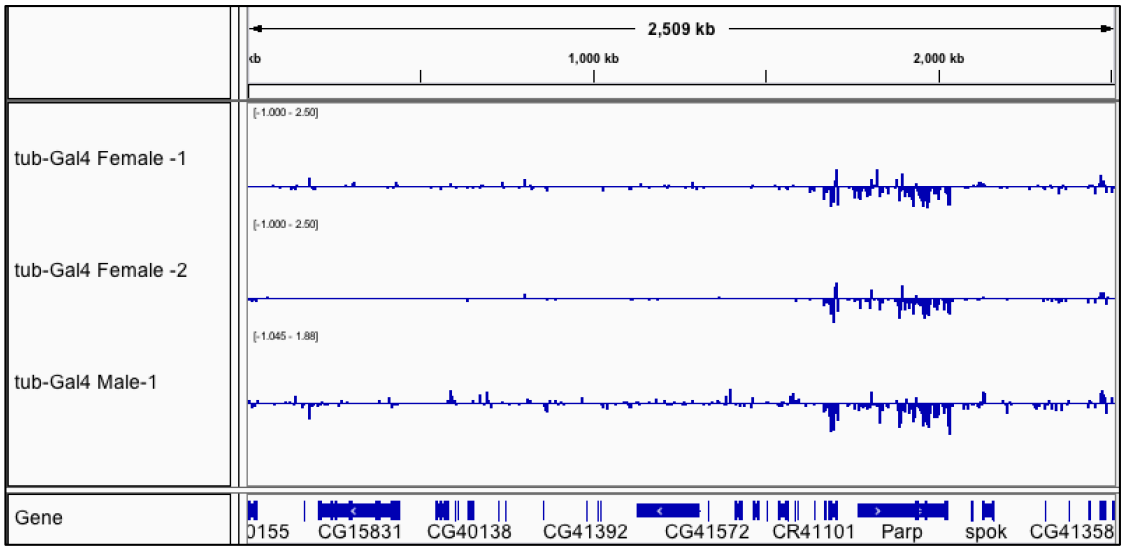
3R Heterochromatin
2,509 kb
1,000 kb
2,000 kb
tub-Gal4 Female -1
tub-Gal4 Female -2
tub-Gal4 Male-1
Gene
CG15831
CG40138
CG41392
CG41572
CR41101
Parp
spok
CG41358

B

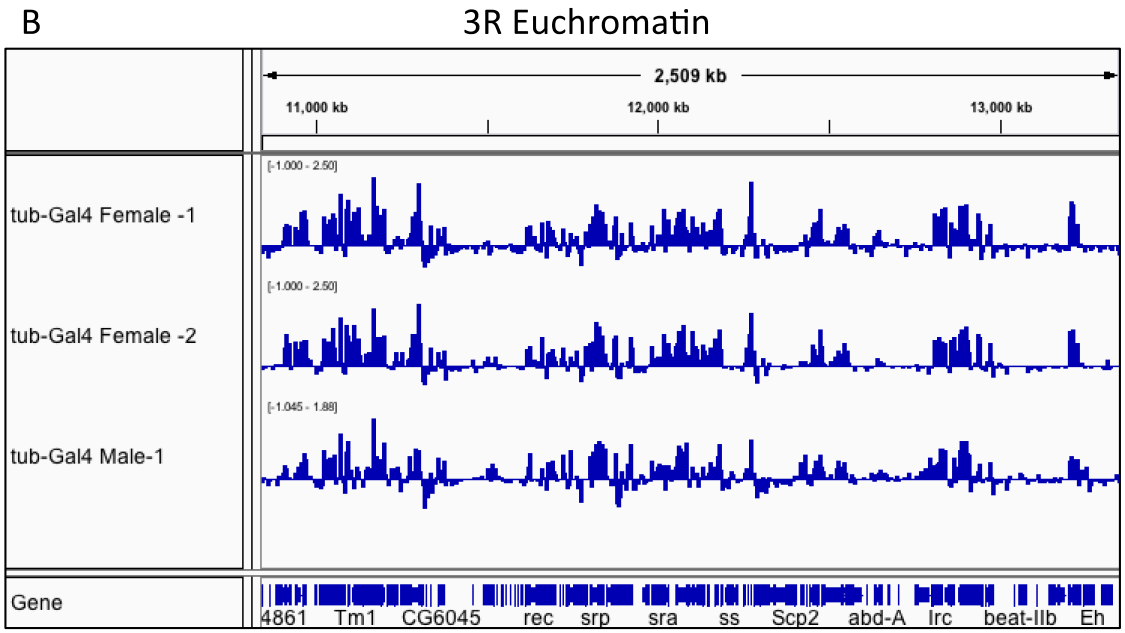
3R Euchromatin
2,509 kb
11,000 kb
12,000 kb
13,000 kb
tub-Gal4 Female -1
tub-Gal4 Female -2
tub-Gal4 Male-1
Gene
Tm1
CG6045
rec
srp
sra
ss
Scp2
abd-A
Irc
beat-IIb
Eh

Figure 4.4

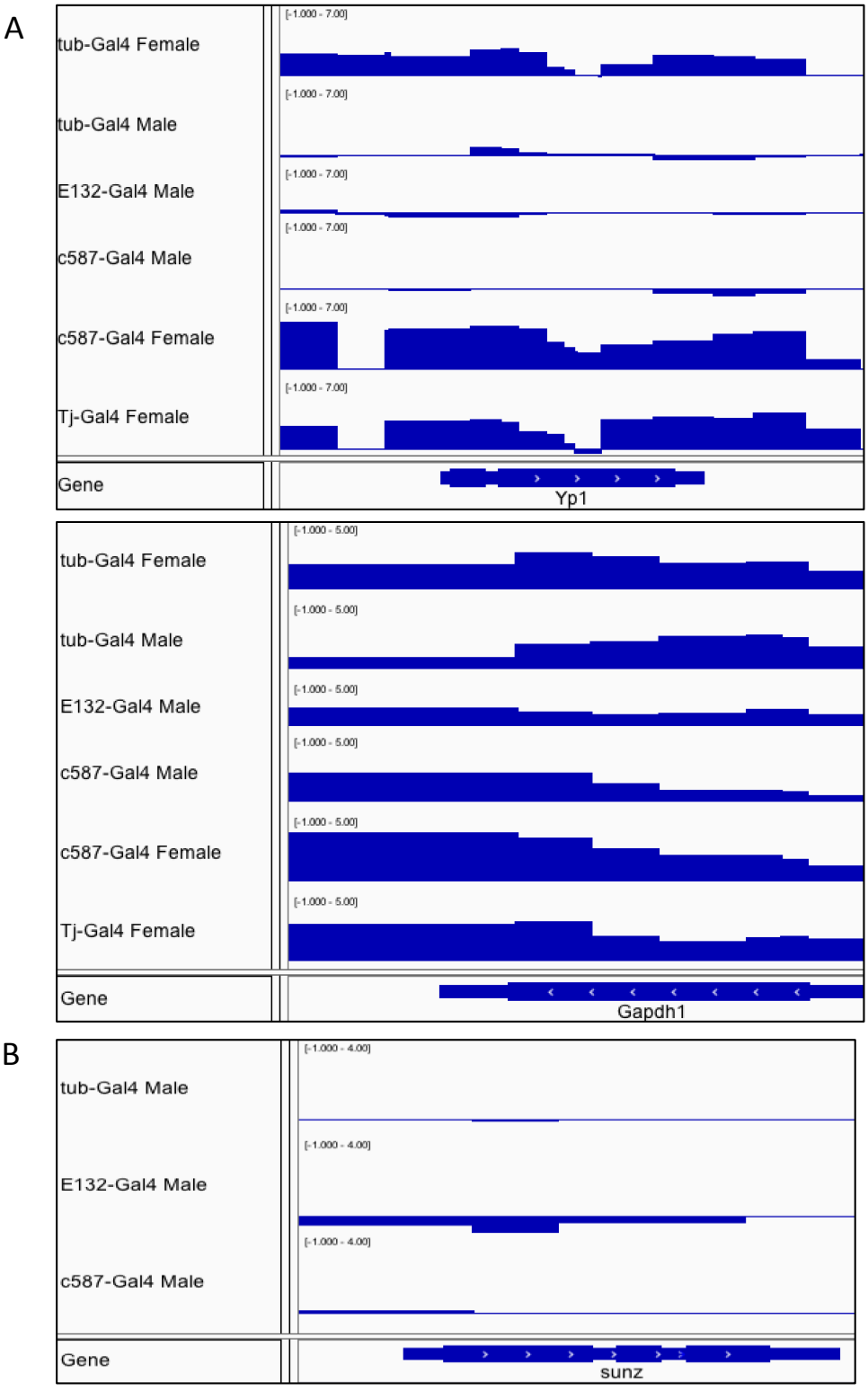
A
tub-Gal4 Female
tub-Gal4 Male
E132-Gal4 Male
c587-Gal4 Male
c587-Gal4 Female
Tj-Gal4 Female
Gene
Yp1
tub-Gal4 Female
tub-Gal4 Male
E132-Gal4 Male
c587-Gal4 Male
c587-Gal4 Female
Tj-Gal4 Female
Gene
Gapdh1
B
tub-Gal4 Male
E132-Gal4 Male
c587-Gal4 Male
Gene
sunz

Figure 4.5

A

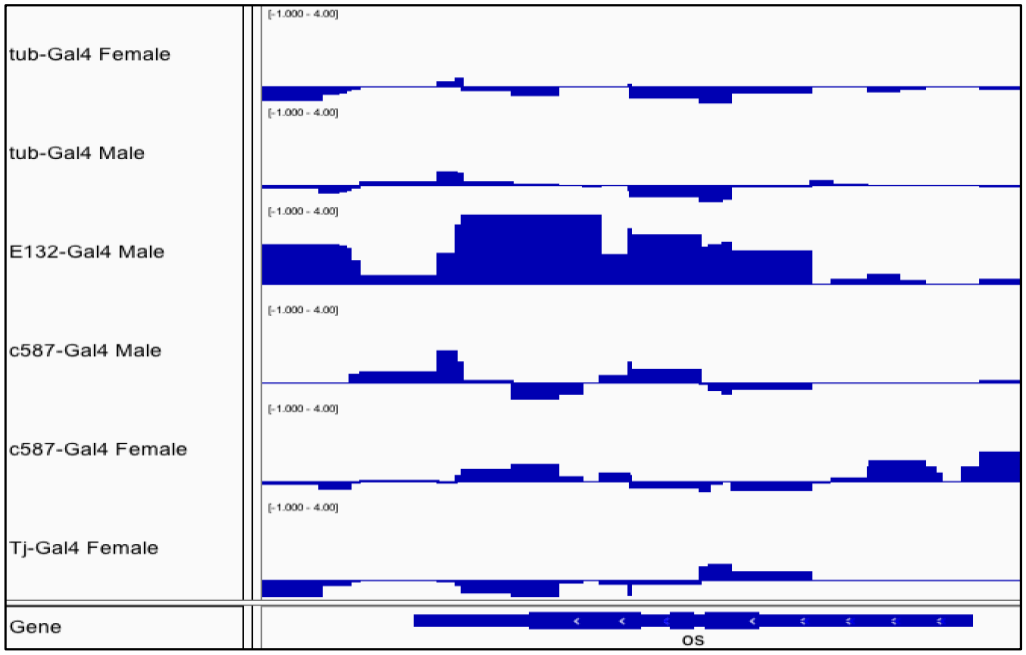
tub-Gal4 Female
tub-Gal4 Male
E132-Gal4 Male
c587-Gal4 Male
c587-Gal4 Female
Tj-Gal4 Female
Gene
os

B

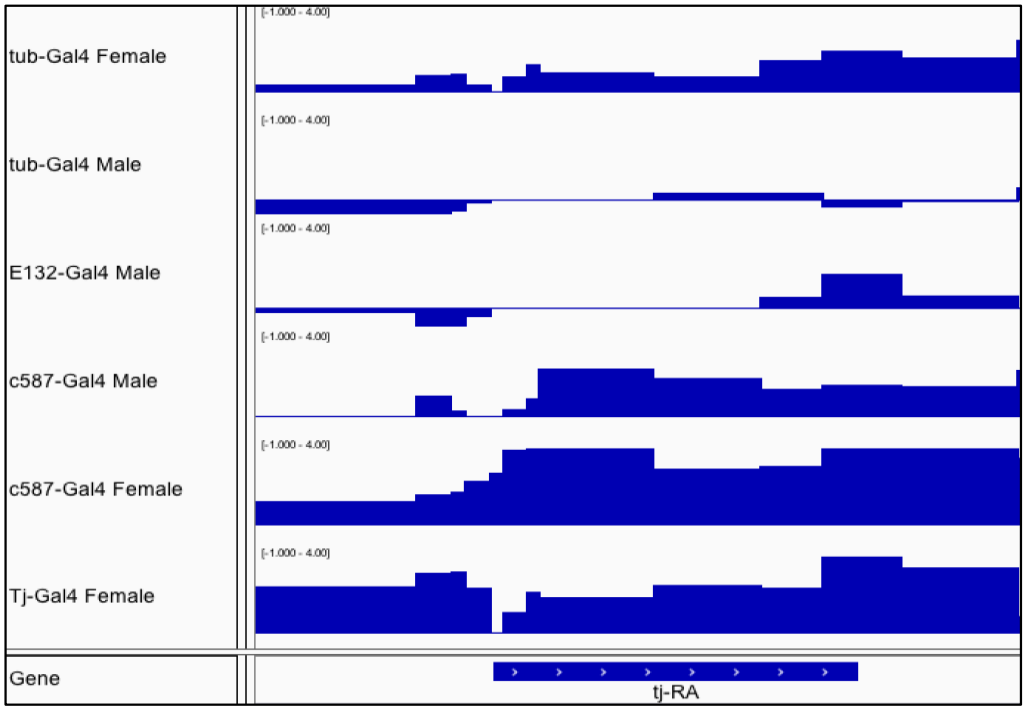
tub-Gal4 Female
tub-Gal4 Male
E132-Gal4 Male
c587-Gal4 Male
c587-Gal4 Female
Tj-Gal4 Female
Gene
tj-RA

Yijie Li
725 N Wolfe St, Hunterian G1, Baltimore, MD, 21205

yli86@jhmi.edu

Education

2015	Ph.D.	Biochemistry, Cellular and Molecular Biology	Johns Hopkins University School of Medicine
2015	M.S.	Computer Science	Johns Hopkins University
2009	B.S.	Chemistry	Peking University, China
2009	B.S.	Biological Science	Peking University, China

Honors and Awards

2007	"Top 10 Student Journals" of Peking University
2007	National Science Foundation of China (The Fostering Talents of Basic Science Award, JO630421)
2007	Research grant from President Foundation
2008	Starlight International Media Scholarship of Excellent Academic Performance

Research Experience

2010-Present **Graduate student**, Laboratory of Erika Matunis, Department of Cell Biology, Johns Hopkins University School of Medicine

My graduate research has focused on understanding the local, systemic and epigenetic signals that regulate stem cell fate in the Drosophila testis and ovary stem cell niche.

I have worked on three projects:

- Regulation of stem cell maintenance by steroid hormones (published)
- Probing the function of histone in *Drosophila* with a systematic library of histone H3 and H4 mutants (in preparation)
- Studying the cell-type specific transcription profile in Drosophila testis or ovary stem cell niche using TaDa (in preparation)

2008-2009 **Undergraduate research fellow**, Laboratory of Luhua Lai, State Key Laboratory of Molecular Dynamics and Stable Structure, Institute of Physical Chemistry, CCME, Peking University

- Study how different solution conditions, such as pH and salt concentration,

influence fibril structure, morphology and aggregation.

2007-2008 **Undergraduate research fellow**, Laboratory of Qi Ouyang, Department of Physics, Peking University
- Used synthetic biology to construct a genetic circuit in yeast, which used Activation-Induced DNA-Cytosine Deaminase to induce mutations and direct the evolution of proteins.

Publications

Li Y, Ma Q**,** Cherry CM, Matunis E. (2014) Steroid signaling promotes stem cell maintenance in the Drosophila Testis. ***Developmental Biology*** 394: 129-141.

Selected Poster Presentations

2014 Ecdysone Regulation of Stem Cell Maintenance in the Drosophila Testis Niche Keystone Symposia on Stem Cells and Reprogramming, 2014, Olympic Valley, CA

2013 Ecdysone Regulation of Stem Cell Maintenance in the Drosophila Testis Niche 54th Annual Drosophila Research Conference, Washington DC

2012 Ecdysone Regulation of Stem Cell Maintenance in the Drosophila Testis Niche 53rd Annual Drosophila Research Conference, Chicago, IL

Teaching, Work and Leadership Experience

2012-2013 **Tutor,** Genetics, Graduate student course at Johns Hopkins University School of Medicine

2008 **Team Leader,** Peking iGEM (International Genetically Engineered Machine competition) team

2006-2007 **Advertising Chair**, Student Association of CCME, Peking University

2005-2006 **Vice Advertising Chair**, Office of Jingwu Association, Peking University